TEXTILE RESEARCH JOURNAL

VOLUME XXVIII January 1958 NUMBER 1

PUBLICATION OF
TEXTILE RESEARCH INSTITUTE

Publications Department: P. O. Box 625, Princeton, N. J.

TEXTILE RESEARCH JOURNAL

VOL. XXVIII, No. 1 JANUARY 1958

IN THIS ISSUE

MECHANICS OF ELASTIC PERFORMANCE OF TEXTILE MATERIALS. *PART XIII:* TORQUE DEVELOPMENT IN YARN SYSTEMS: SINGLES YARN. Milton M. Platt, William G. Klein, and Walter J. Hamburger . . 1

NOVEL MERCERIZING TECHNIQUE TO ESTABLISH "TRUE" LENGTH OF COTTON YARN. Charles F. Goldthwait and Alton L. Murphy . . 15

CHARGE TRANSFER UPON CONTACT BETWEEN METALS AND INSULATORS. D. O. Van Ostenburg and D. J. Montgomery 22

PENETRATION AND SUPERCONTRACTION OF KERATIN FIBERS BY LITHIUM BROMIDE SOLUTIONS. A. R. Haly and June Griffith . . 32

COMPRESSIONAL AND ABSORPTIVE BEHAVIOR OF BULK FIBER SYSTEMS. Irvin M. Gottlieb, Helmut Wakeham, and Hester M. Virgin . 41

Industrial Section

SOME DYNAMOMETRIC APPLICATIONS OF AN ELECTRONIC INTEGRATOR-DIFFERENTIATOR. J. Grignet and F. Monfort 47

PHYSICAL PROPERTIES OF CHEMICALLY MODIFIED COTTONS. *PART IV:* EFFECTS OF PARTIAL CARBOXYMETHYLATION. James N. Grant, Allan W. McDonald, and Geraldine C. Humphreys 60

CARBONIZING INVESTIGATIONS. W. G. Crewther and T. A. Pressley

PART IV: INDUSTRIAL CARBONIZING TRIALS TO ASSESS THE PROTECTION OF WOOL BY SURFACE ACTIVE AGENTS ADDED TO THE WOOL 67

PART V: THE EFFECT OF WATER CONTENT ON THE ACTION OF SULFURIC ACID ON WOOL: THE SIGNIFICANCE OF TESTS FOR DAMAGE 73

RHOVYL-POLYVINYL CHLORIDE FIBERS. L. Hochstaedter 78

Letters to the Editor

ACTIVATION ANALYSIS OF FIBROUS MATERIALS. Otto Teszler and Henry A. Rutherford 86

IP-4 CHART COMPUTER. J. P. Parker and C. M. Rice 87

SOME HISTORICAL EVIDENCE RELATIVE TO THE ASSESSMENT OF WOOL FIBER DIAMETER. F. Bryant 88

MODIFIED VIBRASCOPE TECHNIQUE. G. F. Bush 89

CORTICAL DIFFERENCES IN BURMESE WOOL. W. R. Lang 90

A RAPID APPROXIMATION FOR STANDARD DEVIATION AND COEFFICIENT OF VARIATION. James H. Burkhalter 91

BOOK REVIEWS 93

Editor: Julian S. Jacobs *Production Editor:* Candida Frenking

Associate Editors

H. J. Ball — W. J. Hamburger — Harold P. Lundgren
Earl E. Berkley — Milton Harris — H. Mark
Henry Eyring — K. L. Hertel — E. R. Schwarz

TEXTILE RESEARCH JOURNAL, published monthly at Prince and Lemon Streets, Lancaster, Pa., is devoted to the interest of research in textile and allied industries. It is published by Textile Research Institute.

Entered as second-class matter, April 27, 1945, at the post office at Lancaster, Pa., under the Act of August 24, 1912. Accepted for mailing at special rate of postage provided for in paragraph (d-2), Section 34.40, P. L. & R. of 1948, authorized May 9, 1950.

Manuscripts and communications should be sent to the Publications Department, P.O. Box 625, Princeton, N. J.

Subscription rates: $20.00 per year; additional for postage, 50 cents to Canada, $1.00 to all other countries. Single copies, $2.00 each.

Contents copyrighted © 1958 by Textile Research Institute. Advertising rates supplied on request.

TEXTILE RESEARCH JOURNAL

VOL. XXVIII, No. 1 JANUARY 1958

Mechanics of Elastic Performance of Textile Materials

Part XIII: Torque Development in Yarn Systems: Singles Yarn

Milton M. Platt, William G. Klein, and Walter J. Hamburger

Fabric Research Laboratories, Inc., Dedham, Massachusetts

Abstract

This paper is the first of a series which will deal with torque in textile systems. It is concerned principally with the analysis of torque developed in twisted singles yarns as created by (a) fiber bending, (b) fiber torsion, and (c) bending and torsion in combination. Equations are developed, using elastic theory, relating singles yarn torque to fiber elastic properties, fiber geometry, and singles yarn structure. Extension and application of the theory presented herein to torque in higher order textile structure, e.g., plied yarns and fabrics, will appear in subsequent publications.

Introduction

In the development of a rational system of applied mechanics of textile yarns, at least two types of loading conditions must be considered. The first of these, the reaction of the yarn to externally applied stresses and strains, usually treats the twisted structure as in a state of zero internal stress or strain prior to external force application. In other words, the mechanics of stress response is developed by supposing the helical configuration to have been achieved by an essentially stressless process, such as molding. Successful theoretical approaches based on such assumptions have been developed both for tensile load application to singles and plied yarns [5, 6, 7, 8, 9], and also for the bending of singles yarns [1]. In both instances no stresses or strains of formation were considered, the sole effect of the processes of manufacture having been assumed to be the creation of a geometric structure which, when idealized to a system of perfect helices, could be studied for its stress response.

The present paper also deals with such an idealized geometry, but is concerned solely with the development of a quantitative theory of torsional stress of formation of the singles yarn. Future publications, the basic work for which has already been completed, will extend the theory to plied yarns. For this present work, the only stresses which will be considered in any detail are those which involve fiber bending and fiber torsion. The effects of tensile stresses imposed during spinning or throwing will be neglected, although it is recognized that in practice they may, under certain conditions, be dominant in affecting the magnitude of yarn torque. Additionally, yarn torque may be developed by applying a tensile stress to a twisted singles yarn which would otherwise not exhibit any residual torque or torsional rotative tendencies.

This latter case also will not be considered in detail herein. Thus, the specific problem which will be treated in detail is the development of torques created by the process of twisting singles yarn and the dependence thereof on fiber size, yarn size, yarn twist, fiber bending rigidity, and fiber torsional rigidity.

That the practical problem of torque in yarns is of importance can hardly be questioned if it be considered that the following undoubtedly incomplete list of yarn and fabric characteristics depends upon yarn torque in whole or in part: singles yarn wildness; plied yarn balance; knit goods curling tendencies; woven goods skew, spiral, and curling tendencies; fabric drape; fabric crease resistance; the production of novelty effects in fabrics (e.g., pebble or pucker), etc. That the theoretical problem is of interest follows not only from the practical values which could be achieved thereby, but also, as will be indicated in the formal analysis and the discussion pertaining thereto, in the clarification of the question of fiber torque and the geometric conditions under which it can or cannot exist.

Analysis of Yarn Torque

The general approach which will be used in the analysis will be:

1. To express quantitatively the pertinent geometric parameters of the fiber, produced by yarn construction, in terms of known geometric parameters of the yarn. The fiber geometric parameters will be its curvature and its torsion. The yarn parameters will be helix angle, turns of twist per unit length, and radius.

2. Having by (1) delineated the pertinent fiber geometry produced by yarn construction, the state of internal fiber bending and torsion strain will be quantitatively established for the assumed idealized yarn geometry.

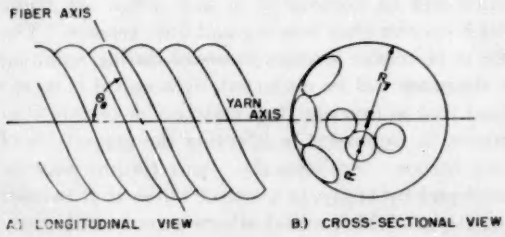

Fig. 1

3. From the classical theories of bending and twist of homogeneous elastic rods, the internal fiber bending moments and torsional couples required to maintain the internal fiber curvature and torsion will be analyzed.

4. These internal fiber bending moments and torsional couples finally will be related to the resultant yarn torque necessary to hold them in equilibrium, which is the yarn torque necessary to twist the yarn originally, assuming no time effects; i.e., no stress relaxation.

Throughout this work, the word "torsion" is used in the sense of twisting deformation or strain, while "torsional couple" or torque refers to the twisting moment acting on the cross section of a member.

Yarn Geometry and Fiber Bending

The yarn geometry which will be considered herein is idealized to the extent of assuming:

1. The fibers are assumed circular in cross section, with their diameters negligibly small compared to the yarn diameter.

2. The center line of each fiber forms a perfect cylindrical helix about the yarn center line.

3. The fibers fall into a rotationally symmetric array in cross-sectional view.

4. The yarn is uniform along its length and its cross-sectional outline is circular.

Nothing has been assumed about the twist of the individual fibers as they lie in the yarn. The gross geometry represented by the foregoing set of assumptions is given in Figure 1. Here a yarn, whose radius is R_y, is shown twisted to a surface helix angle θ_s. The radius to the center line of any fiber is shown as R, so that $R_y > R > 0$. Yarn twist per unit length T_y, yarn radii R, and helix angles θ are related, for the case of the perfect helix, as follows:

$$\begin{aligned} \tan\theta &= 2\pi T_y R \\ \tan\theta_s &= 2\pi T_y R_y \end{aligned} \qquad (1)$$

A moment's reflection will indicate that each fiber, as it lies in the helical configuration corresponding to the foregoing geometry, has a definite curvature. This curvature, designated as $1/\rho$ where ρ is the corresponding radius of curvature, is classically defined as the rate of change in the direction of the curve with respect to its length, or

$$1/\rho = d\phi/ds \qquad (2)$$

where $d\phi$ is the angle between two tangents to the curve at points separated by an arc length ds.

From the differential geometry of space curves [12], the curvature $\frac{d\phi}{ds}$ is also expressible as

$$\frac{1}{\rho} = \frac{d\phi}{ds} = \sqrt{\left(\frac{d^2X}{ds^2}\right)^2 + \left(\frac{d^2Y}{ds^2}\right)^2 + \left(\frac{d^2Z}{ds^2}\right)^2}$$

where X, Y, and Z are the cartesian coordinates of any point on the curve.

When the parametric equations for the helix are used,

$$\begin{aligned} X &= R\cos\delta \\ Y &= R\sin\delta \\ Z &= \frac{\delta}{2\pi T_y} \end{aligned} \qquad (3)$$

where δ is the cylindrical coordinate of the fiber center line corresponding to cross-sectional angle of rotation, one obtains for the curvature, following the indicated differentiations and algebraic manipulations:

$$\frac{1}{\rho} = \frac{\sin^2\theta}{R}$$

$$\sin^2\theta = \frac{4\pi^2 T_y^2 R^2}{1 + 4\pi^2 T_y^2 R^2} \qquad (4)$$

Thus, in terms of fiber radial position R and yarn twist T_y, the curvature of any fiber may be expressed as:

$$\frac{1}{\rho} = \frac{4\pi^2 T_y^2 R}{1 + 4\pi^2 T_y^2 R^2} \qquad (5)$$

Study of Equation 5 will indicate that (1) the fiber or fibers close to the yarn center have, for the idealized geometry, almost zero curvature, and (2) for a given yarn twist T_y, fiber curvature increases with increasing distance of the fiber from the yarn center R until a helix angle of 45° is reached. Since such a high helix angle is rarely encountered in practice, it can be concluded reasonably that curva-

Glossary

D_y = yarn denier.
D_f = fiber denier.
E_f = fiber modulus of elasticity in bending.
G = modulus of elasticity in torsion of a rod.
G_f = modulus of elasticity in torsion of a fiber.
I_f = moment of inertia of the fiber cross section.
I_p = polar moment of inertia of cross section of circular rod or fiber.
K = effective torsional inertia of a rod of any cross section.
K_f = value of K for a single fiber.
l = length of a rod of circular cross section.
M_B = bending moment acting in the plane of bending of any fiber.
M_{BA} = component of M_B which produces torque about the yarn axis.
M_{BT} = total yarn torque due to bending of all the fibers of the yarn.
M_T = internal torque acting on each fiber; torque applied to a circular rod.
M_{TA} = component of M_T which produces torque about the yarn axis.
M_{TT} = total yarn torque due to torsion of all the fibers of the yarn.
M_S = total yarn torque due to fiber bending and fiber torsion combined.
N_f = total number of fibers in a cross section of a yarn.
p = packing factor of a yarn.
R = radial distance from fiber center line to yarn center line; helix radius of fiber center line.
R_f = radius of a fiber.
R_r = radius of a circular rod.
R_y = radius of a yarn; radius of a bundle.
r_f = radial distance from fiber center line to any point in the fiber cross section.
r_r = radius to any point of a circular rod.
T = turns per unit length of surface generator in a twisted rod.
T_f = effective twist of a fiber as it lies in the yarn.
T_{f_0} = pretwist in fibers so as to result in zero effective twist as they lie in twisted yarn.
T_{f_s} = twist of straightened fiber which exhibits no torsional strain as it lies in the yarn.
T_y = yarn twist, turns per unit length; twist of a bundle of fibers; twist of a cylindrical helix.
ds = differential element of arc length.
α = cross-sectional coordinate (with respect to the center of the fiber) locating the generator.
β = total angular rotation (in radians) of the loaded end of a twisted circular rod.
γ = shearing strain of the circular rod at a point of radius r_r.
δ = parametric angle in the equation of the helix.
θ = helix angle of any fiber in the yarn.
θ_f = angle between external surface generator of a fiber and center line of fiber after twist has been inserted.
θ_r = helix angle of a deformed surface generator of a circular twisted rod.
θ_s or θ_y = angle between center line of surface fiber and center line of yarn.
ν = Poisson's ratio for fibers.
ρ = radius of curvature of center line of any fiber in the yarn.
$\frac{1}{\rho}$ = curvature of center line of any fiber in the yarn.
σ = fiber density.
τ = radius of torsion of center line of any fiber in the yarn.
$\frac{1}{\tau}$ = torsion of center line of any fiber in the yarn.
$d\varphi$ = angle between two tangents to a curve at two points separated by arc length ds.
$d\psi$ = angle between two binormals to a curve at two points separated by arc length ds.
ω = ratio of torsional to flexural rigidity of a fiber.

ture increases with increasing distance from the yarn center.

The existence of the curvatures given by Equation 5 indicates that each fiber, the axis of which prior to yarn twisting was in a straight line, must have been deformed through the action of a bending moment. A constant bending moment applied to the ends of an initially straight rod will cause it to deform into an arc of constant radius of curvature, the radius of curvature being inversely proportional, for a linearly elastic material, to the bending moment, and directly proportional to the bending rigidity EI, of the rod, in the plane of bending.

Unfortunately, textile fibers are not linearly elastic materials. However, most fibers, when subjected to very low strains, exhibit approximately constant moduli. Since the bending strains usually encountered in spinning are of relatively low magnitude, linear elasticity will be assumed in the following work. It is believed that the errors resulting from this assumption will be small. Under such circumstances, it follows that M_B, the bending moment acting in the plane of bending of each fiber as it lies in the twisted singles yarn, can be related to the geometry of the yarn as follows:

$$M_B = \frac{E_f I_f}{\rho} = E_f I_f \frac{4\pi^2 T_y^2 R}{1 + 4\pi^2 T_y^2 R^2} \qquad (6)$$

where E_f and I_f are respectively the modulus of elasticity of the fiber in bending and moment of inertia of the cross section of the fiber in the plane of bending. Pictorially, the direction of the internal bending moment acting on the fiber so as to hold it in the bent state can be seen readily from Figure 2. The plane of bending is the plane containing (a) the tangent to the helical curve traced by the fiber center line and (b) the radial line from the center of the yarn to the center line of the fiber. This plane continually rotates in space in passing from point to point along the axis of any fiber. However, the normal to this plane always is inclined to the yarn axis at the angle $(90° - \theta)$. For ease in handling, the vector representation for couples will be used. Thus, in Figure 2, the straight line M_B is the vector representation for the bending moment. This vector is always oriented in the direction of the normal to the plane of bending (normal to the plane of principal curvature) and its sense in the direction governed by the right hand screw rule. Such a vector representation not only simplifies drawings but also the process of resolution and composition of rotative loads, such as couples.

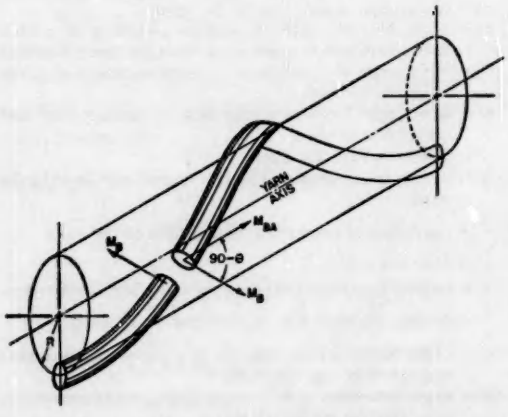

Fig. 2. Representation of internal fiber bending moment, M_B.

The component of the M_B vector parallel to the yarn axis represents a rotative couple about the yarn axis center; in other words, a contribution to yarn torque. Thus, if M_{BA} is the axial (to the yarn) component of the internal bending moment acting on any fiber necessary to hold the fiber in its bent state as it lies in the yarn, then

$$M_{BA} = M_B \sin\theta = \frac{E_f I_f}{R}\left[\frac{4\pi^2 T_y^2 R^2}{1 + 4\pi^2 T_y^2 R^2}\right]^{3/2} \qquad (7)$$

For an annular element of yarn cross-sectional area dR in thickness and of $2\pi R$ units of length in circumference, the number of fibers which would be enclosed (dN_f) is given by

$$dN_f = \frac{N_f}{\pi R_y^2} \cdot 2\pi R\, dR \cos\theta \qquad (8)$$

where N_f is the total number of fibers in the yarn cross section. The factor $\cos\theta$ is introduced into Equation 8 since the oblique fiber cross section presented by those fibers which are inclined by the angle θ to the yarn axis limits the number of fibers which can be packed into the available space prescribed by the ideal geometry. Under such circumstances, the contribution from bending of all fibers in the annular element of area to yarn torque

(dM_{BT}) is determined from $dM_{BT} = M_{BA}\,dN_f$, or

$$dM_{BT} = \frac{N_f}{\pi R_y^2} \cdot E_f I_f 2\pi \left[\frac{4\pi^2 T_y^2 R^2}{1 + 4\pi^2 T_y^2 R^2}\right]^{3/2} \times \frac{dR}{(1 + 4\pi^2 T_y^2 R^2)^{1/2}} = \frac{N_f E_f I_f}{\pi R_y^2}\, 2\pi \frac{8\pi^3 T_y^3 R^3}{(1 + 4\pi^2 T_y^2 R^2)^2}\, dR \qquad (9)$$

The total yarn torque available from fiber bending, then, is merely the total integral of Equation 9:

$$M_{BT} = \frac{N_f E_f I_f}{\pi R_y^2} \int_0^{R_y} 2\pi \frac{8\pi^3 T_y^3 R^3}{(1 + 4\pi^2 T_y^2 R^2)^2}\, dR = \frac{N_f E_f I_f}{R_y} \left[\frac{\log_e \sec \theta_s - \sin^2 \theta_s}{\tan \theta_s}\right] \qquad (10)$$

Prior to examination of Equation 10, it should be observed that, from symmetry, the vector sum of all components $(M_B \cos \theta)$ of the M_B vectors acting over the entire yarn cross section and which are perpendicular to the yarn axis, produces a zero resultant, whether the yarn be twisted "S" or "Z." Nevertheless, considering each fiber as a structural element, it is clear that the bending moment components $(M_B \cos \theta)$ if not externally resisted, would cause each unrestrained fiber end to move outward radially from the yarn center. As will be shown in a subsequent paper, the resultant torque acting on a plied yarn theoretically may be balanced by geometric means; i.e., through proper selection of singles and plied yarn constructions. However, the use of such methods does not, in general, remove the individual fiber bending components corresponding to $M_B \cos \theta$. Thus, if a geometrically balanced plied yarn is cut, the unrestrained components will cause the cut end to increase in bulk; i.e., to broom or brush out. This will be evidenced both within the singles (i.e., fibers will tend to move out from each singles yarn center) and also among the singles (i.e., each singles will tend to move radially outward from the plied yarn center).

Reference to Equation 10 will show that the yarn torque due to fiber bending is:

1. Directly proportional to the number of fibers in the yarn, inversely proportional to the yarn radius, and directly proportional to the bending rigidity $(E_f I_f)$ of a fiber. The net result of such variations is given by Equation 12.

2. A function of the yarn surface helix angle θ_s. The form of this latter function is not clearly delineated by Equation 10; Figure 3 dimensionlessly plots $M_{BT} \Big/ \frac{N_f E_f I_f}{R_y}$ versus yarn surface helix angle, θ_s.

The large plot of Figure 3 shows the result over an extremely wide range of yarn surface helix angles; i.e., from 0° to 60°. As indicated earlier herein, singles yarn surface helix angles rarely exceed 45° for conventional yarns. The large range shown is merely to indicate the overall trend and to indicate the rapid rise of yarn torque due to fiber bending as yarn surface helix angle increases. Moreover, and as will be discussed later in detail, as helix angles rise, the ratio of maximum possible yarn torque resulting from fiber *torsion* to yarn torque arising from fiber *bending* tends to diminish; numerical values of M_{BT} over an extreme helix angle range will simplify the discussion pertaining thereto.

For facility in understanding relative magnitudes, it should be observed that the trigonometric portion of Equation 10, when $\theta_s < 30°$, approximates simply as $\frac{\theta_s^3}{2}$; i.e.,

$$M_{BT} \Big/ \frac{N_f E_f I_f}{R_y} = \frac{\theta_s^3}{2}; \quad 0 < \theta_s < \frac{\pi}{6} \qquad (11)$$

where θ_s is now in radians. This would indicate yarn torque due to fiber bending to be approximately proportional to the cube of the yarn surface helix angle, if R_y is constant.

Regarding fiber properties and yarn size, it is clear that M_{BT} is proportional, for a given yarn surface helix angle, to the product $N_f E_f I_f / R_y$. Now, assuming a given fiber type; i.e., constant fiber modulus E_f, the quantity $N_f I_f / R_y$ may be examined as follows:

1. N_f, the total number of fibers in the yarn,

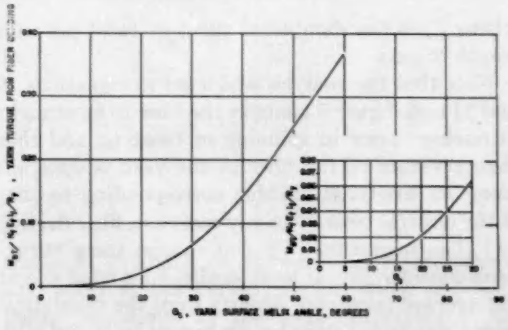

Fig. 3. Yarn torque due to fiber bending vs. yarn surface helix angle.

may be taken to be proportional to the yarn denier/fiber denier = D_y/D_f.

2. I_f, the moment of inertia of the fiber cross section, may be taken to be proportional to the fourth power of a linear dimension of its cross section, or, in other words, proportional to the square of the fiber cross sectional area; i.e., proportional to the square of the ratio of fiber denier to fiber density, D_f^2/σ^2. Note that this neglects fiber cross-sectional shape.

3. The yarn radius, R_y, may be taken as proportional to the square root of the ratio of the yarn denier, D_y, to the product of fiber density times packing factor, p, of the yarn; i.e., $R_y \propto \sqrt{\frac{D_y}{p\sigma}}$.

Thus, the factor $N_f I_f / R_y$ may be taken as

$$\frac{N_f I_f}{R_y} \propto \frac{D_y}{D_f} \cdot \frac{D_f^2}{\sigma^2} \sqrt{\frac{\sigma p}{D_y}}$$

$$\propto D_f \sqrt{D_y} \frac{\sqrt{p}}{\sigma^{3/2}} \qquad (12)$$

Equation 12 indicates that if yarn denier, D_y, is kept constant, minimum yarn torque from fiber bending will occur when the filament denier is least; i.e., by the use of a large number of fine fibers, a result which might be intuitively predicted from the formal analysis. Similarly, yarn torque due to fiber bending will increase as the square root of yarn denier, if fiber denier and yarn surface helix angle are maintained constant.

However, where packing factor, p, and fiber density, σ, are varied, the analysis of yarn torques resulting from fiber bending should consider the effects on θ_s occasioned by such variations, since θ_s varies as follows for small angles:

$$\theta_s \approx \tan \theta_s = 2\pi T_y R_y \qquad (13)$$

where T_y is the number of turns of twist per unit length of yarn.

Note that the analysis which led to Equations 10 and 11 and Figure 3 assumes the fiber to be straight (stressless) prior to spinning or twisting, and that the curvature of the fiber in the yarn is constant along its length at a value corresponding to that of the circular helix. In any real case, fiber darting [9] (i.e., migration [4]) can change these curvatures considerably, at least locally. To what extent the average curvature departs from the theoretical over a significant yarn length cannot be stated with certainty at this time. However, it is felt that large departures do not occur for any significant gauge length and, moreover, the results for the idealized geometry offer, at the very least, the approximate torque magnitude due to fiber curvature as well as its sensitivity to changes in yarn construction. Experimental work beyond the scope of the present paper would be required for a complete evaluation of the practical accuracy of the analysis and its results. However, as will appear in a later publication, the results, when extended to plied yarns, seem to indicate correctly with surprisingly excellent precision those geometric conditions usually found for torque balance in practice; i.e., for the construction of a nonwild plied yarn.

Yarn Geometry and Fiber Torsion

General. Textile research workers have been plagued with the question as to whether or not fibers as they are twisted into yarns truly develop torsion about their own axes, and hence whether or not internal fiber torsional couples exist. The unequivocal answer to this question can be forthcoming only by careful examination of fibers as they lie in yarns, guided by the following:

1. The method of spinning or twisting the yarn.
2. Any experimental data on torque-twist relationships of a spun yarn, the form of which relationships might determine the extent of fiber torsion.
3. Knowledge of the intrinsic mechanical properties of fibers in torsion, determined by testing fibers, and their surface frictional characteristics in yarns to establish the limits, if any, of the extent of fiber torsion which could possibly occur, if at all, when a yarn is spun.

With respect to (3) above (the magnitude of fiber torsion which could possibly occur), Guthrie et al. [3] have determined torsional rigidities of a variety of fibers using a torsional pendulum. Assuming frictional coefficients of the order of 1/3 and fiber pressures likely to occur within spun yarn, they indicate that slippage without any appreciable fiber torsion being developed will occur at the nontwisted end of a fiber gripped in a yarn when the other nongripped end is twisted. They thus conclude that "the torsional rigidities of all fibers considered are high enough to prevent twisting of the fibers. . . ." In certain cases they were unable to observe any actual fiber torsional strain using a low power microscope.

Others, chiefly Schwarz [10], Woods [13], and Chow [2] have discussed the question of fiber torsion in the case of singles yarns and singles yarn torsion in the case of plied yarns under the terminology of "tortuosity." This subject will be further discussed below in an attempt to (a) clarify its meaning in the present instance of fiber torsion and (b) to elucidate the *in situ* geometric conditions under which fiber torsion does and does not exist.

Classical torsion. In the classical illustration of torsion, a right circular cylinder is imagined clamped at one end, and the other end rotated by an externally applied torque, as in Figure 4. For this case it is shown that straight lines drawn originally on the surface of the cylinder parallel to its axis will be deformed into helices whose equilibrium geometries depend on the elastic rigidity of the rod and the magnitude of the applied torque, M_T, shown both in vector manner and also as a couple in Figure 4. For linearly elastic materials, the relationships among the several quantities shown on Figure 4 are as follows:

$$\text{(a)} \quad M_T = KG\frac{d\beta}{dl}$$

$$\text{(b)} \quad \frac{d\beta}{dl} = \beta/l = 2\pi T$$

$$\text{(c)} \quad \tan\theta_r = 2\pi T R_r$$

where G = modulus of elasticity of the rod in torsion = $E/2(1+\nu)$ for a classically linear material, E = modulus of elasticity in bending or tension for a classically linear material, ν = Poisson ratio, K = a factor based on shape and dimensions of the rod cross section, reflecting its "torsional inertia," = the polar moment of inertia for a circular cross section, I_p, β = total angular rotation, in radians, of the loaded end of the rod, R_r = radius of the rod, θ_r = helix angle of the deformed surface generator, and T = twist, in turns per inch, of the helix.

The foregoing relationships are derived using classical stress-strain relationships applicable in elastic theory. Basic to the derivation is the concept of internal shear strains and stresses developed in such a rod under the action of a twisting torque. Stated simply for the case under consideration, the shearing stresses are distributed across any cross section in such a manner that they are at every point directed perpendicular to the radius, r_r, to that point and of magnitude directly proportional to the radial distance. The shearing strains, then,

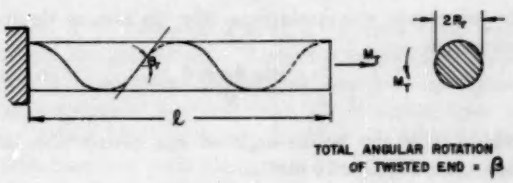

Fig. 4. Illustration of classical torsion.

by Hooke's Law, are linearly related to the stresses. For magnitudes of strains which are not limited to being small, the shearing strain, γ, is defined as the tangent of the change in angle of a generator on any cylinder concentric with the rod as a consequence of the torque; i.e., referring to Figure 4, shearing strain

$$\gamma = \tan\theta = 2\pi T r_r \qquad (14)$$

where r_r is the radius to *any* point in the rod cross section. Thus, the existence of shearing strains implies shearing stresses and therefore an applied torque to hold their resultant in equilibrium.

Fibers in a yarn. Returning now to the case of fibers spun or twisted into a yarn, classical mathematics, similar to that employed previously in this paper for curvature, defines the torsion of a space curve, such as a helix. The helix under investigation at the present is that formed by the center line of a fiber as it lies in a spun yarn. Torsion, $1/\tau$, is the rate of change of direction of the binormal to the helix with respect to its arc length, or

$$\frac{1}{\tau} = \frac{d\psi}{ds} \qquad (15)$$

where ψ is the angle between two binormals separated by an arc length ds.

From the differential geometry of space curves [12], the torsion is expressible as

$$\frac{1}{\tau} = \frac{d\psi}{ds} = -\rho^2 \begin{vmatrix} \frac{dX}{ds} & \frac{dY}{ds} & \frac{dZ}{ds} \\ \frac{d^2X}{ds^2} & \frac{d^2Y}{ds^2} & \frac{d^2Z}{ds^2} \\ \frac{d^3X}{ds^3} & \frac{d^3Y}{ds^3} & \frac{d^3Z}{ds^3} \end{vmatrix}$$

where X, Y, and Z are the cartesian coordinates of any point of the curve. Again, using the parametric equations for the helix (Equation 3) and performing the indicated differentiations followed

by algebraic manipulations, the torsion is determined as

$$\frac{1}{\tau} = \frac{\sin\theta\cos\theta}{R} \qquad (16)$$

where θ is the helix angle of the center line of fiber and R its helix radius.

Whether or not torsional strain in the classical sense and hence fiber torque accompanies such torsion depends solely upon how the twisting is carried out and the mechanical properties of the fibers. Illustrations will make this point clearer. Let us imagine a parallel bundle of rod-like fibers the external boundary of which bundle is kept circular. Let the bundle be clamped at both ends, and suppose one end to be rotated. Let it also be assumed that the lengths of the rods are adjusted so that no tensions are developed; i.e., we assume the idealized geometry. Refer to Figure 5, which illustrates the example, and, for definiteness, focus attention in Figure 5a at points A_1–A_5, selected so that for the imposed twist there will be a cross-sectional rotation of point A_5 to A'_5 of say a complete revolution, as shown in Figure 5b. Under the prescribed condition of twisting, all points A′ will appear on the yarn *external* surface, rotated in relation to their original positions. Further increases in twist will further rotate points A′, but in each case displaced points A will always appear external to the yarn surface. Similarly, for any given twist, a straight line connecting all points originally placed along a generator; i.e., parallel to the center line of the undistorted fiber, will always appear symmetrically placed with respect to the yarn center line, when viewed on cross section; e.g., points B'_1–B'_5 in Figure 5b. There will not, at least under external examination, be any *apparent* helical winding of the elements of the fiber around its own axis. However, if all fibers except one are cut and removed without further twisting of this remaining fiber, and the fiber straightened, again without twisting, it will be found that the original straight line along a generator is now helically wound about the fiber axis with a twist of $T_y \cos\theta$ turns per unit length, where T_y is the twist per unit length present in the bundle and θ is the helix angle corresponding to the inclination of the center line of the fiber before straightening out. This result is well known to most textile technologists, and is, in fact, used in the determination of the twist of singles in plied yarns.

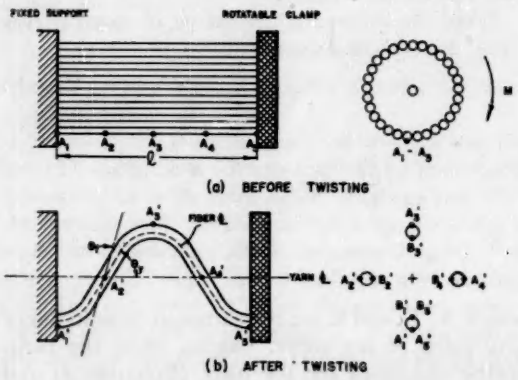

Fig. 5. Pure twisting.

However, a moment's reflection will indicate that twist arrived at by the process of straightening, as described, does not correctly yield the twist in the fiber as it lies in the yarn. Visualize the imaginary conditions of Figures 5a and 5b carried to the extreme of producing a 90° helix angle for the center line of the fiber. Under these extreme conditions, it is clear that there is absolutely no twist of the fiber about its own axis, only bending. Yet, the described straightening procedure will indicate a twist of 1 turn per circumference of the bundle, or a twist of $1/2\pi R_y$ turns per unit length. Thus, the straightening procedure is incorrect for the intended purpose.

It is thus clear from the foregoing that (a) in the process described by Figures 5a and 5b, there is no visual classical winding of surface generators about the fiber center line, and (b) straightening does not give a correct picture of *in situ* twist or torsion of the fiber.

Nothing has been said thus far as to whether or not torsional strains exist throughout the cross section of the fiber shown in Figure 5b. Reference to this figure will show two angles defined, θ_y and θ_f. The angle θ_y is the yarn surface helix angle; i.e., the angle between the center line of the fiber and the center line of the yarn. The angle θ_f is a local angle between the generator through A and the center line of the fiber after the bundle twist has been inserted. For circular fibers, the local torsional strain would equal tan θ_f. That such a torsional strain or angle of distortion exists becomes evident if it be realized that, for example, the generator (corresponding to points A_1–A_5) and the center line of the fiber (of which points A_1–A_5 are

a part) both wind helically around the yarn center with a twist N_y, although at different helix radii, namely, R_y for the fiber center line and $(R_y + R_f)$ for the external generator. Thus, the angle θ_y is given by

$$\tan \theta_y = 2\pi T_y R_y \tag{17}$$

and the angle $(\theta_f + \theta_y)$ is given by

$$\tan (\theta_f + \theta_y) = 2\pi T_y (R_y + R_f) \tag{18}$$

where R_y and R_f are yarn radius and fiber radius respectively. Then, from the identity

$$\tan (\theta_f + \theta_y) = \frac{\tan \theta_f + \tan \theta_y}{1 - \tan \theta_f \tan \theta_y} \tag{19}$$

one obtains

$$\tan \theta_f = \frac{\sin \theta_y \cos \theta_y R_f / R_y}{1 + \sin^2 \theta_y R_f / R_y} \tag{20}$$

For the points B_1–B_5 diametrically opposite to points A_1–A_5, the torsional strain $\tan \theta_f$ would be the same as that given by Equation 20, except that the term $\sin^2 \theta_y R_f / R_y$ would be subtracted from 1 rather than added. The points A and B are the only points the angular distortion for which can be easily computed as above without the use of complex differential geometry, since a line joining them is in the plane of principal curvature of the fiber axis. Chow [2] has carried through the general analysis for the case of singles twisted into plied yarns, which when applied to the present problem yields the following general equation:

$$\tan \theta_f = \frac{\sin \theta_y \cos \theta_y r_f / R}{1 - (r_f / R) \sin^2 \theta_y \cos \alpha} \tag{21}$$

where $\tan \theta_f$ is now the torsional strain for any generator and α is the cross-sectional coordinate which locates the generator; i.e., for points B, $\alpha = 0$ and for A, $\alpha = 180°$. In general terms, r_f in Equation 21 is the radial distance to *any* point in the fiber cross section from the fiber center line, while R is the radial distance from the fiber center line to the yarn center line.

Study of Equations 20 and 21 will indicate that the numerator is maximized when θ_y is 45°. The additive trigonometric term in the denominator is basically the effect of fiber curvature in stretching the outside or compressing the inside of the fiber in the bent state. For r_f/R or R_f/R_y, small compared to 1, this additive term is negligible, particularly when it be considered that it appears both positively and negatively. Thus, for further discussion it will be neglected, although if one were concerned with values of θ_f closer than 1% it would have to be taken into account. Neglect of the additive trigonometric term leads to the result that the torsional strain is constant at any given value of θ_y and R; i.e., it is rotationally symmetric about the fiber axis and varies linearly with distance from the fiber center.

Having obtained the torsional strain, $\tan \theta_f$, for a circular fiber, it is of interest to ascertain how much twist per unit length of fiber would be required to produce the same strain were the fiber axis straight. In this case, we must find T_f in the expression

$$\tan \theta_f = 2\pi R_f T_f \tag{22}$$

and by solving Equations 20 and 22 simultaneously there results

$$T_f = T_y \cos^2 \theta_y \tag{23}$$

which indicates that when fibers are twisted in accordance with the method of Figure 5, the "equivalent twist" of the fiber as it lies in the yarn is equal to the yarn twist, T_y, multiplied by the $\cos^2$ of the fiber center line helix angle. For the case of an imaginary yarn twisted to a 90° helix angle, Equation 23 would indicate zero *in situ* fiber twist, as would actually be the case.

As an incidental point, note that for the center fiber; i.e., $R = 0$, Equation 23 would yield a twist of T_y turns per unit length, and Equations 20 and 21 would yield $\tan \theta_f = 2\pi T_y R_f$, both of which results would be expected for straight fibers which are twisted. Note also that the theoretical mathematical torsion given by Equation 16 also applies to the yarn of Figure 5. Torsional strain, $\tan \theta_f$, at any distance r_f from the center of a circular fiber would be equal to the product of the torsion of Equation 16 and the distance r_f. Additionally, the tortuosity effect as employed in the literature can be seen to be the angular distortion effect produced by twisting, while tortuous twist is that amount of twist (turns per unit length) which would, when the element's axis is straight, produce the same angular distortion as the element receives from being twisted in the bundle. In the case of a singles yarn, tortuous twist is the "effective" fiber twist as it lies in the yarn. For plied yarn, tortuous twist is the "effective" change in single twist occurring as the

result of plying. Both cases assume the formation of the final structure, either twisting of singles or plying, to duplicate that shown in Figure 5.

In most practical yarns, it is extremely unlikely that one can observe the fiber torsional strain by microexamination of the outside of a yarn, unless highly precise techniques are employed. As an example, take a yarn composed of about 100 fibers with a surface helix angle as high as 45°. In this case, the angle θ_f between the center line of the outermost fiber and any external generator would, from Equation 20, be computed as

$$\tan \theta_f = \frac{\sqrt{2}}{2} \frac{\sqrt{2}}{2} \frac{R_f}{R_y} \Big/ 1 + \frac{R_f}{2R_y}$$

$$= \frac{1}{2} \frac{R_f}{R_y} \Big/ 1 + \frac{R_f}{2R_y}$$

For 100 fibers, and even assuming close hexagonal packing to the fibers so as to make R_y as small as possible, the approximate value of R_f/R_y would be 1/11. Thus, for the example

$$\tan \theta_f = \frac{\frac{1}{2} \times \frac{1}{11}}{1.05} = \frac{1}{23}$$

Therefore $\theta_f \approx 2.5°$. For 61 fibers in the cross section, the angle of torsion would be only 3.2°. Large angles of torsional strain are developed only when very small groups of fibers are twisted to high helix angles.

No statement is made at present as to whether fibers in actual yarn twisting can develop sufficient frictional force to produce the torsional stresses corresponding to the strains determined for Figure 5. Certainly, in spun yarns the possibility exists for fiber slippage to occur. The main point is that merely by observing the outside of a twisted yarn, not previously marked in some way, one could hardly make sufficiently precise measurements to detect the extent of *in situ* torsional fiber strain.

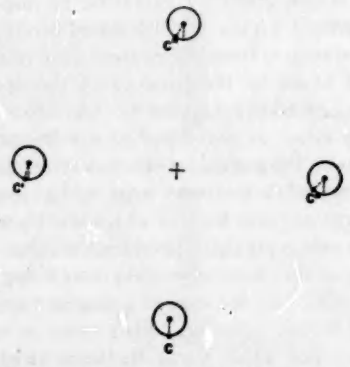

Fig. 6. Twisting with zero fiber torsion.

The minimum degree of fiber torsion which could exist in a yarn would be achieved if the fiber were pretwisted in a direction opposite to the subsequent yarn twist to an extent that the resultant tan θ_f would be equal to zero. Thus, if T_{f_0} represents the magnitude of this pretwisting in turns per unit length of fiber axis, then to achieve the torsionless state

$$T_{f_0} - T_y \cos^2 \theta_y = 0$$

or

$$T_{f_0} = T_y \cos^2 \theta_y \tag{24}$$

If, for a yarn so made, the cutting and subsequent straightening of a single fiber were carried out, the measured twist of the straightened fiber would be

$$T_{f_s} = T_{f_0} - T_y \cos \theta_y \tag{25}$$

where T_{f_s} and T_{f_0} represent turns of twist per unit length of fiber axis. This then, would mean that

$$T_{f_s} = T_y \cos^2 \theta_y - T_y \cos \theta_y$$
$$= -T_y \cos \theta_y (1 - \cos \theta_y) \tag{26}$$

and the straightened fiber would exhibit a torsion, albeit quite low. The resultant twist for this straightened fiber would be in the direction of the yarn twist; i.e., opposite to the direction of fiber twist inserted before spinning. Thus, as contrasted with Figure 5, the configuration of generators for zero fiber torsion would appear as shown in Figure 6. The angular rotation of generators per unit length of yarn, as for example, point C in Figure 5, would be, in this case, merely $2\pi T_y(1 - \cos \theta_y)$.

Yarn Torque Due to Fiber Torsion

Under conditions described by Figure 6, there would be no fiber torsional strain and hence no yarn torque due to fiber torque. The total yarn torque, for this case, would be governed entirely by fiber bending and would be determined by Equation 10 or Figure 3.

The situation is more complex for the other extreme case of yarn twisting described by Figure 5, and will now be analyzed. The idealized yarn geometry and linear elasticity are again assumed. The equivalent twist of the fibers as they lie in the

yarn, T_f, is given by the following equation:

$$T_f = T_y \cos^2 \theta_y \tag{27}$$

Thus, for the linear elasticity assumed for the fibers,

$$\begin{aligned} M_T &= K_f G_f 2\pi T_f \\ &= K_f G_f 2\pi T_y \cos^2 \theta_y \end{aligned} \tag{28}$$

where all terms are as previously defined and M_T is the internal torque acting on any fiber in order to hold it in equilibrium. Figure 7 illustrates the torque, M_T, using both the vector representation and the twisting couple. The component of fiber torque parallel to the yarn axis, M_{TA}, represents the fiber torque contribution to the yarn torque, or

$$\begin{aligned} M_{TA} &= M_T \cos \theta_y \\ &= K_f G_f 2\pi T_y \cos^3 \theta_y \end{aligned} \tag{29}$$

For the annular element of yarn cross-sectional area, $2\pi R\, dR$, in area units, there then results an element of yarn torque $dM_{TT} = M_{TA}\, dN_f$, or

$$dM_{TT} = \frac{N_f}{\pi R_y^2} K_f G_f 2\pi R\, dR \frac{\tan \theta_y \cos^4 \theta_y}{R} \tag{30}$$

which, after substitution for the various trigonometric terms, becomes

$$dM_{TT} = \frac{2N_f}{R_y^2} K_f G_f \frac{2\pi T_y R\, dR}{(1 + 4\pi^2 T_y^2 R^2)^2} \tag{31}$$

The integration of Equation 31 yields for total yarn torque, M_{TT}, due to fiber torsion

$$\begin{aligned} M_{TT} &= \frac{N_f K_f G_f}{R_y} \frac{\sin^2 \theta_s}{\tan \theta_s} \\ &= \frac{N_f K_f G_f}{R_y} (\sin \theta_s \cos \theta_s) \end{aligned} \tag{32}$$

where N_f is the number of fibers in the yarn cross section, $K_f G_f$ is the torsional rigidity of a single fiber, R_y is the yarn radius, and θ_s is the yarn surface helix angle.

Prior to examination of Equation 32, it should be observed that, from symmetry, the vector sum of all components ($M_T \sin \theta$) of the M_T vectors acting on the entire yarn cross section which are perpendicular to the yarn axis produces a zero resultant. Nevertheless, considering each fiber as a structural element, it is clear that the fiber torque components, $M_T \sin \theta$, if not externally resisted, would cause each unrestrained fiber end to tend to move inward radially toward the yarn center. This tendency would be resisted by the corresponding bending components, $M_B \cos \theta$, which were previously discussed. It can be shown that the components $M_B \cos \theta$ for any fiber act in an opposite sense to the components $M_T \sin \theta$ for that fiber, and that the ratio $\frac{M_T \sin \theta}{M_B \cos \theta}$ is independent of the fiber helix angle θ, the ratio depending only on the ratio of fiber torsional rigidity, KG, to fiber bending rigidity, EI. This ratio of rigidities, as will be seen from examination of existing experimental data reported herein, has been found to be less than unity. Thus, it can be concluded that the bending component will prevail, resulting in a brooming rather than a consolidating tendency.

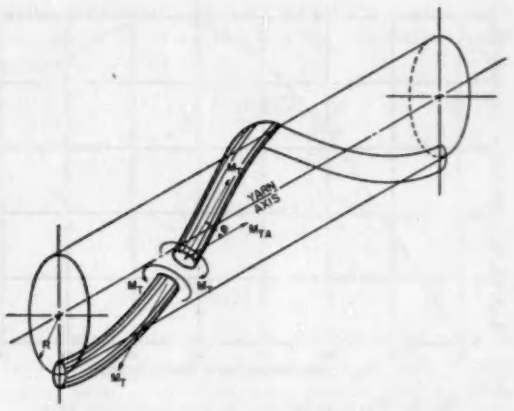

Fig. 7. Representation of internal fiber torsional couple.

Reference to Equation 32 will show that yarn torque due to fiber torsion is:

1. Directly proportional to the number of fibers in the yarn, inversely proportional to the yarn radius, and directly proportional to the torsional rigidity, $K_f G_f$, of a fiber. The net result of such variations is given by Equation 33.

2. A function of the yarn surface helix angle, θ_s. For small angles; i.e., yarn surface helix angles below about 30°, the form of the function is approximately linear with θ, as shown in Figure 8, which plots $M_{TT}/N_f K_f G_f/R_y$ vs. θ_s.

Although yarn torque from fiber torsion increases with increasing yarn twist, the rate of increase diminishes until a turning point is reached. The turning point at 45° is probably rarely achieved in practice since (a) few yarns are ever spun to such a high twist, and (b) probably distortions such as fiber buckling will occur, strongly violating the idealized geometry. Nevertheless, the rate of yarn

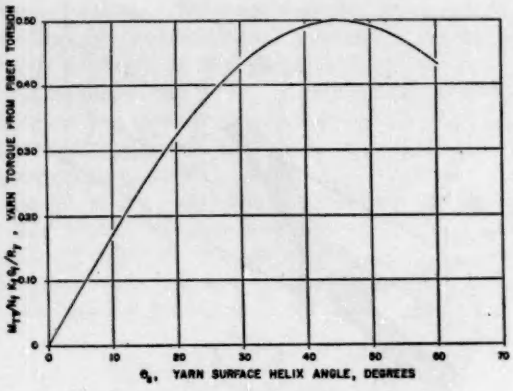

Fig. 8. Yarn torque due to fiber torsion vs. yarn surface helix angle.

torque increase should decrease. This is, of course, mainly the result of the fact that the ratio between effective fiber twist and yarn twist decreases with increasing yarn twist, due to the fact that the fiber axis, as it lies in the yarn, is not straight. Additionally, only components of fiber torque are manifested in yarn torque, and the greater the yarn twist the smaller the contribution of total fiber torque to yarn torque.

For a given surface yarn helix angle, yarn torque arising from fiber torque is directly proportional to $N_f K_f G_f / R_y$. For a given fiber type; i.e., constant torsional modulus, G_f, the analysis of the factor $N_f K_f / R_y$ yields essentially the same results as did the analysis of the factor $N_f I_f / R_y$ given previously for fiber bending, since usually K_f is proportional to the fourth power of a linear dimension of the fiber cross section. For a circular fiber cross section, K_f is merely the polar moment of inertia, $= 2I_f$. Thus, in general, the factor $\frac{N_f K_f}{R_y}$ may be taken as

$$\frac{N_f K_f}{R_y} \propto D_f \sqrt{D_y} \frac{\sqrt{p}}{\sigma^{3/2}} \tag{33}$$

where D_y is the yarn denier, D_f the filament denier, p the yarn packing factor, and σ the fiber density. The interpretation of Equation 33 and the limitations pertaining thereunto are precisely the same as given previously for Equation 12.

Combination of Fiber Bending and Fiber Torsion

Having analyzed, for the idealized case, the yarn torque resulting individually from fiber bending and extreme fiber torsion, it is now necessary to consider their resultant effect when present simultaneously; i.e., for a yarn spun to the idealized condition represented by Figure 5. For this case, total yarn torque, M_S, is merely the sum of the yarn torque from fiber bending, M_{BT}, plus the yarn torque from fiber torsion, M_{TT}, since the latter two torques are parallel and hence can be added algebraically. Thus

$$M_S = M_{BT} + M_{TT} \tag{34}$$

which, after substitution for the individual torques in terms of fiber and yarn characteristics, becomes

$$M_S = N_f E_f I_f / R_y \left[\frac{ln \sec^2 \theta_s - \sin^2 \theta_s}{\tan \theta_s} \right] + \frac{N_f K_f G_f}{R_y} \frac{\sin^2 \theta_s}{\tan \theta_s} \tag{35}$$

Now, letting the ratio $K_f G_f / E_f I_f$ be represented by the symbol ω, Equation 35 becomes

$$M_S = \frac{N_f E_f I_f}{R_y \tan \theta_s} [ln \sec^2 \theta_s + (\omega - 1) \sin^2 \theta_s] \tag{36}$$

Thus, solution of yarn torque in the general case requires a knowledge of ω, the ratio of torsional to flexural rigidity of the fiber. Recognizing that fibers differ in their cross-sectional shapes, but simultaneously lacking knowledge of the precise orientation of nonrotationally symmetrical cross-

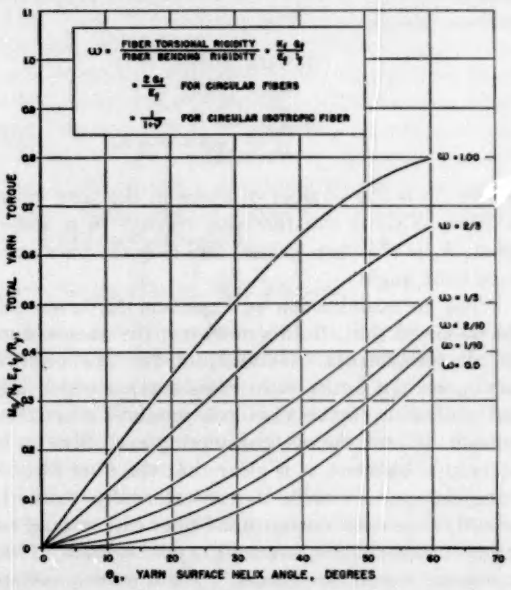

Fig. 9. Total yarn torque vs. yarn surface helix angle.

sectional shapes with reference to the plane of bending, the best that can be done theoretically is to treat the fibers as circular. Under such circumstances, $K_f/I_f = 2$, and ω can be taken as $2G_f/E_f$. To illustrate magnitude, the value of the ratio G_f/E_f for an isotropic material having a Poisson's ratio, ν, of 1/2 would be determined from $G_f = E_f/2(1 + \nu)$; $2G_f/E_f = 2/3$. Thus, for this example, $\omega = 2/3$. Figure 9 plots $M_S/N_f E_f I_f/R_y$ vs. θ_s for various assumed values of ω. The case $\omega = 0$ is equivalent to the case where fiber bending is the only contribution to yarn torque; i.e., the case where extreme fiber torsional strain exists, but where the fiber torsional rigidity = 0; hence there would be no fiber torque.

Several points worthy of note arise from examination of Figure 9. First, it will be observed that with increasing ratio of fiber torsional rigidity to bending rigidity, the initial portion of the curves becomes more nearly linear. Within this low twist region, yarn torque is critically dependent upon fiber torque; i.e., the ratio of total yarn torque to yarn torque arising from only fiber bending is very great, the specific ratio depending of course on the magnitude of ω. For higher yarn helix angles the ratio is not as great. This is more easily seen by considering, for any single fiber, the ratio of yarn torque contributed by fiber torsion to yarn torque contributed by fiber bending for a constant yarn geometry.

$$\frac{M_{TA}}{M_{BA}} = \frac{K_f G_f 2\pi T_y \cos^3\theta}{E_f I_f \dfrac{\sin^3\theta}{R_y}}$$

$$= \frac{K_f G_f \tan\theta \cos^3\theta}{E_f I_f \sin^3\theta}$$

$$= \frac{\omega}{\tan^2\theta} \qquad (37)$$

Thus, for constant ω, the smaller the helix angle of the fiber axis the greater the ratio of yarn torque due to fiber torsion to yarn torque due to fiber bending, and conversely.

Data have recently appeared in the literature on bending and torsional rigidities of fibers, both measured dynamically. However, the conditions of test in each case do not necessarily develop comparable time effects. Nonetheless, such data will help to establish the relative values of ω, the ratio of torsional to bending rigidity. Usually such ratios will be found to decrease as the degree of fiber orientation increases. Table I gives results found by Guthrie, Morton, and Oliver [3] for a variety of fibers, while Table II gives results for nylon and

TABLE I. Values of $K_f G_f$ and E_f/I_f for Various Fibers*

Fiber	Dynamic torsional rigidity, $K_f G_f$	Dynamic bending rigidity, $E_f I_f$	ω
Acrilan	1.206×10^{-3} dyne-cm.^{2}	58.5×10^{-3} dyne-cm.^{2}	0.21
Dynel	0.525	37.9	0.14
Orlon† (cont. fil.)	0.523	83.5	0.06
Orlon	1.114	39.6	0.28
X-51	0.617	20.5	0.30
X-51	1.358	66.0	0.21
Fibro	0.894	49.5	0.18
Tenasco (cont. fil.)	0.383	35.6	0.11
Toramomen	0.303	21.4	0.14
Fibroceta	0.470	36.2	0.13
Nylon	0.970	33.5	0.29
Rilsan (cont. fil.)	0.750	26.1	0.29
Perlon L (cont. fil.)	0.680	21.5	0.32
Dacron† (cont. fil.)	0.500	30.4	0.16
Terylene (cont. fil.)	0.477	37.5	0.13
Terylene	1.457	86.2	0.17
Wool	3.30	46.6	0.71
Ardil	2.64	59.6	0.44
Fibrolane BX	2.55	39.0	0.65
Merinova	1.08	32.3	0.34

* From Guthrie, Morton, and Oliver [3].
† Du Pont trademark.

TABLE II. Values of $K_f G_f / E_f I_f$ for Nylon and Dacron* of Various Draws

Fiber	Draw	$\omega = K_f G_f / I_f E_f$
Nylon	1	0.62
Nylon	2	0.47
Nylon	3	0.33
Nylon	4	0.24
Nylon	5	0.23
Nylon	6	0.21
Dacron	1	0.80
Dacron	2	0.38
Dacron	3	0.15
Dacron	4	0.14
Dacron	5	0.11
Dacron	6	0.12

* From Wakelin et al. [11].

Dacron of various degrees of draw found by Wakelin et al. [11]. From both references one can observe that the possible range of ω is quite large. Wool, nonstretched Dacron, nonstretched Ardil, and Fibralane exhibit high values of ω. For all of the remaining fibers, ω ranges essentially between 0.1 and 0.3. For the former fibers, yarn torque due to fiber torsion greatly exceeds yarn torque from fiber bending.

The chief difficulty in applying the results of the analysis resides in the uncertainty of the extent to which extreme fiber torsional strain actually exists in spun yarns. Thus, fibers with a high ω, as indicated by Guthrie, Morton, and Oliver [3], may not be able to develop the end restraint by friction necessary to hold the fully twisted fiber state. If this is in fact the case, then fibers whose values of ω are large and from which one would otherwise expect high yarn torque due to fiber torque would be more or less "selfcompensating" with respect to their final torques, particularly at medium to high yarn twists; thus, even for such fibers, fiber bending may be the most significant contributor to yarn torque. Obviously, work beyond the scope of the present paper would be required to establish realistic limits to final fiber torsional strain in yarns. It is hoped that the discussions and geometric limits described herein aid in the formulations and assessing of such work.

Acknowledgment

The authors gratefully acknowledge the assistance of the following individuals for their helpful comments in many discussions relating to this work: Professors E. R. Schwarz and S. Backer of the Massachusetts Institute of Technology and Messrs. M. J. Coplan and H. M. Morgan of Fabric Research Laboratories, Inc. They are additionally particularly grateful to Professor S. Backer for pointing out via private communication the relationship given by Equation 37 in this work.

Literature Cited

1. Backer, S., TEXTILE RESEARCH JOURNAL **22**, 668 (1952).
2. Chow, T., unpublished Master's thesis, Massachusetts Institute of Technology, Textile Division, June 1948.
3. Guthrie, Morton, and Oliver, *J. Textile Inst.* **45**, No. 12 (1954).
4. Morton, W. E., *Congrès International de la Recherche Scientifique Appliquée à L'Industrie Textile*, 13 Numéro, published by Centre Scientifique et Technique de L'Industrie Textile, Belge, March 1956.
5. Platt, M. M., TEXTILE RESEARCH JOURNAL **20**, 1–15 (1950).
6. Platt, M. M., TEXTILE RESEARCH JOURNAL **20**, 519–538 (1950).
7. Platt, M. M., TEXTILE RESEARCH JOURNAL **20**, 665–667 (1950).
8. Platt, M. M., Klein, W. G., and Hamburger, W. J., TEXTILE RESEARCH JOURNAL **22**, 641–667 (1952).
9. Platt, M. M., Klein, W. G., and Hamburger, W. J., TEXTILE RESEARCH JOURNAL **24**, 907–939 (1954).
10. Schwarz, E. R., TEXTILE RESEARCH JOURNAL **20**, 175–179 (1950).
11. Wakelin, J. M., Voong, E. T. L., Montgomery, D. J., and Dusenbury, J. M., *J. Appl. Phys.* **26**, 786 (1955).
12. Woods, F. S., *Advanced Calculus*, New Ed., New York, Ginn & Company, 121–124 (1934).
13. Woods, H. J., *J. Textile Inst.* **24**, T317 (1933).

Manuscript received May 6, 1957.

Novel Mercerizing Technique to Establish "True" Length of Cotton Yarn

Charles F. Goldthwait[1] and Alton L. Murphy

Southern Regional Research Laboratory,[2] New Orleans, Louisiana

Abstract

A procedure is suggested for the determination of the length at which the yarn in a skein can be regarded as straightened but not stretched. This procedure requires the determination of the tensions developed in a series of mercerizings of skeins of yarn which are alike but are set in the mercerizing apparatus at lengths which differ by small percentages. When the maximum tensions attained are suitably plotted, a change in slope in the curve indicates a point which corresponds with the desired length. A unit measuring-tension for the precise measurement of skeins of yarn which are, for example, to be used subsequently for chemical treatment, can then be derived. More specifically, a suitable tension for measuring has been found to be 1.2 lb. per lea of 120 yds. of 40/2 yarn of mercerizing twist. Equivalent tensions can be calculated readily for other sizes of skein and many other yarns. The change in slope appears, further, to pinpoint a fundamental change in the response of cotton yarn under increasing tension just as it begins to stretch. It is suggested also that a measuring-tension for single threads derived from results with skeins may be suitable for determining the initial lengths of yarns for some of the common physical tests such as those for elongation and twist.

Introduction

Closely controlled mercerizations have aided in a solution of the old problem of determining the normal or "true" lengths of (certain) cotton yarns, that is, lengths at which the yarns can be considered straightened but not stretched. The method employed is based on that described for the measurement of the tension developed during the mercerization of yarn in the form of skeins [6]. An acceptable load or tension per unit of yarn (measuring-tension) has resulted for use in the measurement of skeins for processing as needed, for example, in the application of mercerizing techniques to aid in the characterization of cottons [3, 6]. Here, comparable results from the mercerization of yarns made from different cottons, even though of similar constructions, are obtainable only if carefully reeled skeins can be set in the mercerizing apparatus at equivalent initial or normal lengths.

The mercerizing procedure for establishing length of cotton yarn is also of possibly more fundamental interest because it appears to point out a rather sudden and pronounced change in response during the stressing of cotton yarns at low loads.

The "unit" tension which has been derived is applicable in general in the processing of yarn in skeins, and is especially useful when measurements are needed for the comparison of elastic properties of yarn before and after treatment. It will be of interest also for consideration for the routine testing of yarn, as for twist and elongation, if the unit tension can be established for the type of yarn that is to be tested.

The terms "length" and "straighten" are to be used and will be defined for their somewhat special usage for skeins of yarn. By length of a skein is meant its circumference as measured around the reel on which it is formed, or the distance around rollers on which it is mounted, as in a mercerizing apparatus. A skein of yarn obviously can not be fully straightened and still remain a skein, but when the skein is put under suitable tension the yarn in it can be straightened, as far as its measurement is concerned.

[1] Present address: School of Textiles, North Carolina State College, Raleigh, North Carolina.

[2] One of the laboratories of the Southern Utilization Research and Development Division, Agricultural Research Service, U. S. Department of Agriculture.

Background and Literature

The tension which is developed during mercerization is to be utilized, and one of the most important conditions for its determination is the reproducible setting of skeins of yarn in the mercerizing apparatus. This is a question of length and the tension at which it is measured; the latter would seem preferably to have some relationship to the tensions used for other yarn measurements.

In the absence at the time of anything very definite of this sort, a measuring-tension was determined by one of the authors [4] for 40/2 yarn of mercerizing twist, and has been used also with equivalent amounts of various other yarns. Although this (unit) tension has been in regular use, measuring-tension was studied again more recently in search of any more suitable value. The problem is much the same as that of measuring crimp or, more generally, of determining the tension and length at which a yarn would be straightened but not stretched —a logical basing point for measuring skeins for processing.

The subject of straightening cotton yarn without stretching it has been studied by others, and a review of the literature is summarized in Table I. Values are given for such purposes as measuring yarn for determinations of number, strength, elongation, twist, etc., particularly for measuring yarns which had been taken from bobbins or other packages, or from woven and knited fabrics, and contained waviness or crimp.

All of the values are given for 20/1 yarn, or for equivalent amounts of 40/2 or 60/3. The yarns on which observations were made were not necessarily strictly equivalent, but will serve to indicate the great differences between values suggested in different sources, even after reduction to a common denominator.

Values from Ball's method [2], Goldthwait's measuring-tension [4], and the single lea weight are the lowest of those found in the literature, and agree at about the weight of a lea. There were about twice as many values two or three times as high, and others ranging up to the highest at 13 times the weight of a lea. No attempt will be made to account for these great differences. In view of the

TABLE I. Tensions to Straighten But Not Stretch 20/1 or Equivalent Cotton Yarn *

Basis for tension	Reference**	Tensions as observed, calculated, or specified		
		For single thread, g.	For 120-yd. skein, g.	(1 lea), lb.
156 g. for 1's cord	1	7.8	1248	2.75
Wt. of 1 lea (120 yd.)		3.24	518	1.14
Wt. of 1 hank (7 leas, or 840 yd.)	10b	22.68	3629	8.00
Wt. of 1/3 hank (151/yarn number)	13	7.55	1210	2.67
Wt. of 440 yd. (400 m.)	12	11.9	1904	4.19
Yarn from warp-wound bobbins	2	2.86	458	1.01
Yarn from filling-wound bobbins	2	3.36	538	1.19
120 g./yarn number (twist)	11	6.0	960	2.11
Grex/20 g. (twist)	8	14.76	2362	5.20
Grex/40 g. (twist)	8	7.38	1181	2.60
Measure for mercerization, 40/2	4	3.4	545	1.20
131/Typp (Typp = 16.8 for 20/1)	1	7.8	1248	2.75
0.03 g./den. for cotton fiber	10a	8.0	1280	2.82
(1/30 g./den., consider same as 0.03)	13	8.0	1280	2.82
I.T.T. for crimp, 60/3	9	30.0	4800	10.6
I.T.T. for crimp, warp 20/1	9	32.0	5120	11.3
I.T.T. for crimp, filling 20/1	9	42.0	6720	14.8

* Most of these values have been given for measuring yarn straightened but not stretched, usually to remove crimp or waviness; a few more specific uses are indicated. The table is based on 20/1 yarn to utilize available data, but has some values for the approximately equivalent 40/2 and 60/3 yarns. Grams per 120 yd. is equal to grams per single thread times 160, the number of ends which support the weight used in measuring the skein.

** Literature Cited.

little supporting evidence for so many different tensions which were all supposed to do the same thing, none of them could be accepted for measuring without further study. Since the tension derived earlier [4] for measuring yarn for mercerization had been used so satisfactorily, it was singled out for more attention.

Derivation of Original Measuring-Tension

The tension mentioned in the previous article [6] was 2.4 lb./240-yd. skein of 40/2 yarn of 54-in. circumference, or 1 lb./100 yd., it having been arbitrarily changed to this convenient basis from the original observation of 25 lb./2400-yd. skein [4]. This tension finally has been accepted as essentially correct, although the basis for its original selection was found not entirely acceptable for such a "standard." The method of its derivation still may be of some interest if its limitations are understood; further experiments also brought out a few points, possibly unfamiliar, on elastic properties at very low tensions, i.e., below 1% of the breaking loads of the yarns.

The original work was done with yarn which is satisfactory for experimental mercerizing, a 40/2 combed peeler of mercerizing twist—with twist multipliers of about 3 in the singles, and 3 to 3.25 in the ply, twisted in the opposite direction.

The measuring-tension was derived from very low load stress–strain curves [4], and represented the maximum tension from which yarn would return immediately to its original length upon unloading. At that tension the yarn was regarded as just straightened and at its true or normal length, while above that tension the yarn would remain slightly elongated, and was then regarded as slightly stretched as well as straightened.

When the attempt was made to redetermine this tension at 65% relative humidity, the yarn did not return to its original length, and the measuring-tension could not be checked. Tests were then made in rooms at relative humidities of 15% to 50%, and results were substantially the same as obtained originally in an ordinary unconditioned room. Skeins of 480 yd. each, of several 40/2 yarns stressed to 4.8 lb., came back to the original length upon unloading. This was a good check on the previous experience. Since, however, the yarn would not return from the elongation at the higher humidity of normal test conditions, the method was decided to be unacceptable for general use.

Ball's Method Applied to Skein Yarn

Of the other tensions suggested, Ball's, which came down from Walen [14] and Haven ([7], p. 323), seemed possibly of most practical interest for skeins for chemical treatments because the tension obtained for any yarn by this method was intended particularly to free it from bends and waviness due to winding on bobbins in order to measure its true length.

The method was checked on various 40/2 and similar yarns; instead of tests on single threads, it was considered most practical for the immediate purpose to make the determinations on skeins of yarn similar to those which are usually mercerized.

The skeins were carefully made as usual for experimental mercerizing on a motorized laboratory reel running at uniform tension and a speed of 200 yd./min.

Data for stress–strain curves were obtained by manual loading of the skeins by weights while mounted on a balance-type mercerizing apparatus [6], where measurements were easily repeatable. Intermittent loading was preferable because no method of continuous loading, whether of single threads or skeins, has any close relationship to the usual static conditions under which skeins are measured or set at predetermined lengths or tensions during skein processing.

Increments of load were added, up to about ¼ of the estimated breaking strengths of the skeins when, upon plotting, there was a well-defined straight segment in the stress–strain curve. Each load was allowed 30 sec. to approach rest before the elongation was read, although this allowance of time was not entirely necessary; similar results were obtained with much shorter intervals between additions of load. When the straight portions of the curves were extended, etc., according to Ball's procedure, the tension values obtained ran from three to nearly five times as high as the original measuring-tension (4), which was similar to his values shown in Table I.

It was clear from experience that some of these new values would be too high for the purpose. No reason can be given now except that they were determined from skeins instead of single threads. Difference in method of loading seems not to have been significant because Ball's loading was chainomatic and, therefore, also intermittent. The tensions differed so much between rather similar yarns and were so high that some other approach seemed necessary.

Mercerization to Determine Tension for Measuring Yarn

This method is based on the mercerization of yarn in skeins, all reeled alike but mounted so that they will shrink or remain stretched at a series of different lengths from below to above the normal length determined by the earlier method [4], outlined above.

Skeins of 240 yd. or its equivalent were measured with tensions of 2.4 lb. to determine their normal lengths, that is, circumferences while in place around the rollers of a mercerizing apparatus of the balance type [6].

They were then mounted for the mercerizing, loosely or tightly, in separate experiments at roller settings corresponding with calculated lengths, usually within the range of 97% to 102% of the normal yarn length. Mercerizing proceeded with strain gauges and recorder so that typical curves were drawn which showed the course of the development of tension in each skein. The data from three or more skeins at each setting were averaged and a family of curves drawn for each group of tests, as illustrated by Figure 1. Then the maximum tensions reached during the actual mercerizings were plotted against the relative lengths of the yarns during their mercerization, as illustrated by Figure 2.

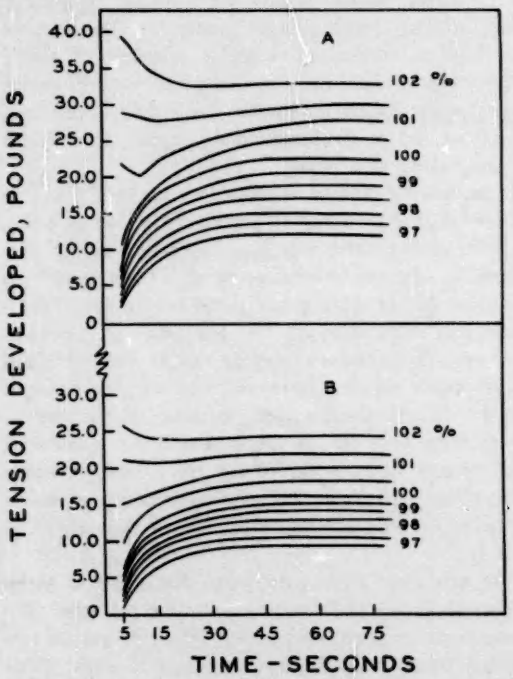

Fig. 1. Families of curves showing tensions developed during mercerization while maintaining different skein lengths, expressed as percentages of a reference length as described in text. (A) 31/2 cotton yarn, AHA variety, (B) 31/2 cotton yarn, Deltapine variety.

All mercerizings were alike except for length of skein and were performed in the ordinary laboratory atmosphere on air-dry yarn at room temperature with 23% concentration by weight of sodium hydroxide (containing 1% of a rapidly-acting penetrating agent), with manipulation as described in the previous paper [6].

Discussion of Mercerization Method

The mercerizings have been confined to a relatively narrow range from below to above normal length. Sometimes more tension was required to stretch the yarn to 2% above normal length than was developed later in the mercerizing process (Figure 1). Such high initial tension has not appeared to introduce error, since points observed for ½% intervals up to 2% stretch have fallen on the straight lines described below.

The range of lengths employed was sufficient for the purpose. If the range was extended too far downward, the skeins would be too slack to develop appreciable tension; in the other direction, the tensions required for further increases in length would soon be beyond the capacity of the apparatus. Also, with yarn stretched too much, there would not be the drop in tension upon entering the caustic soda solution and the subsequent rise to a maximum with the onset of swelling and mercerization, as shown in Figure 1. If this feature did not appear in the plotting of the data as in this figure, there would be uncertainty as to the significance of the tension developed in the mercerizing. Incidentally, after the maximum is reached, usually in about a minute, the tension tends to decline somewhat (not fully shown in Figure 1) with continued turning of the yarn on the rollers [6], probably due to slight deswelling from mechanical pressure.

The typical curve for maximum tensions developed in such a series of mercerizings was found to consist of two straight line segments which intersect at or near the point which corresponds with the normal length of the untreated skeins. This was typical in 13 out of 17 curves plotted, although it might be expected that two processes of elongation taking place on a yarn consecutively would tend to overlap,

and the line representing one of them run into that of the other through an actual curve. The lines appeared to join through a curve in only three cases, and if extended to intersect would still indicate the point being sought. If the intersection should occur at other than the 100% point, the desired value for the measuring-tension would be that required to set a skein of the same size of the same yarn to the indicated percentage of the base (100%) measured length. This can be determined very readily with the balance-type mercerizing apparatus used for this work.

Since the intersection was found usually to correspond with the normal length of the skein under the tension derived by the earlier method [4], that tension was confirmed as suitable for measurement of yarn in skein form for processing.

Since 1.2 lb./lea of 120 yd. of 40/2 yarn or its equivalent for other yarns was used to determine normal length before all mercerizations, it was considered possible that this weight may have imparted a semi-permanent stretch to the yarn, so that the intersect would have to occur at this point. In order to determine the effect of pretensioning on tension developed, skeins of yarn were stressed under 9 and 25 lb. and then mercerized at normal length as determined above. The skeins all developed the same maximum tension as skeins not pretensioned, indicating that within reasonable limits, tension applied prior to normal length mercerizations does not affect the tension developed during mercerization.

There seem to be no important sources of error which cannot be avoided readily. In each complete set of mercerizations for one given yarn there would be no yarn variables except that set up for length. The various conditions of mercerizing should be maintained constant, especially manner and extent of rotation of skeins on the rollers of the apparatus [6]. Although the exact levels of temperature and concentration of the mercerizing bath are not highly critical, the values should be the same from skein to skein. Effects of variations in caustic concentration can be judged from similar work [5].

There may be an error in the tension developed, seldom up to 1%, if the number of yards of yarn required does not correspond with a whole number of complete turns on the reel. This would make no significant difference in the relative values when the skeins were all alike. This point is illustrated by the unit tension by weight, 1 lb./100 yd. It has been more convenient with 40/2 yarn and the ordinary 54-in. reel to make skeins of the unit length of yarn (the lea of 120 yd. or desired multiples) and to measure them with tensions at the rate of 1.2 lb./lea.

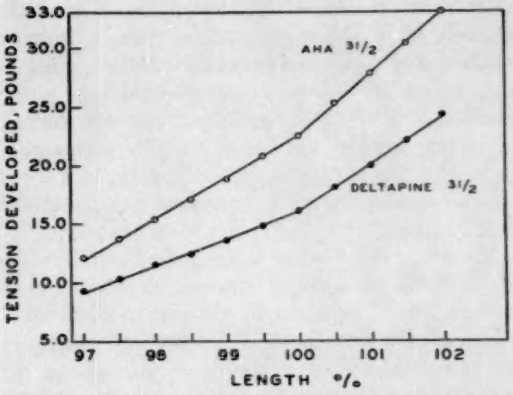

Fig. 2. Points at which yarns are at normal length, straightened but not stretched, are indicated by changes in slope of the curves of maximum tensions which were developed in the mercerizings of Figure 1.

Most of the determinations of normal lengths of skeins were made on 2-ply yarns of mercerizing or somewhat higher twist. The same lengths, expressed as percentages, were obtained with several 40/2 yarns. The results were substantially the same with 42/2, 36/2, 31/2, and even 8/1, for skeins reeled to yardages corresponding to equal weights, as calculated from yarn numbers, and mercerized as described, beginning with the same measuring-tension and yarn length as for the 40/2 yarn. In addition, these yarns represented cottons with very different properties, including Acala 4–42, AHA, Deltapine, Stoneville, Iquitos (Peruvian), and several combed peelers and other cottons of unknown variety. Hence, the conclusion has been drawn that yarns in general of low to medium twist, such as commonly would be selected for chemical processing, can be considered to be at normal length, straightened but not stretched, if measured at the unit tension determined from the mercerization of skeins of 40/2 yarn as described or at equivalent tensions calculated from it. Similar studies on the measurement of normal length have not been made on yarns of higher twist.

Explanation of Changes in Tension Developed

The curve consisting of the two straight lines meeting at an angle perhaps can be understood most

easily with the aid of an oversimplification of the structure of a cotton yarn. The fibers in a yarn which is under no tension at all can be regarded as lying somewhat loosely at appreciable angles to the yarn axis. When the yarn is put under slight and increasing tension, the fibers tend to decrease in angle with the yarn axis and ultimately, in a 2-ply yarn of mercerizing twist, to become nearly parallel to it.

No doubt there is the same general result when the stress is, in a sense, internal, as when due to mercerizing. The fibers in the yarn tend to swell in diameter at the expense of length, and, when they are restrained by the mounting of the yarn in the mercerizing apparatus, tension results. If the yarn is held loosely between supports, as at the 97% length employed above, it will tighten in the caustic, and fibers will be drawn nearer to the direction of the yarn axis. Since fibers were loose initially, take-up in length upon swelling prevents the building up of as great a tension as might otherwise be developed in the yarn. When the yarn is held slightly tighter so that it is partly straightened, the fibers are at initially smaller angles, so that there is less take-up and more tension is developed. This process was continued stepwise in the experiments described until, apparently, movement of the fibers into alignment with the yarn axis had practically ceased; the yarn was just straightened and had thus reached its normal or true length.

As skeins were mounted at increasingly greater lengths than normal, higher and higher tensions were developed, because the fibers in the yarns were more and more restrained and swelling was taking place against increasing resistance. The change in slope in Figure 2 indicated that there had also been some change in mechanism. Apparently, the fibers had begun to stretch or to bed together more closely in the yarn, so that tension was developed according to some other law than that in effect during the earlier straightening. The line below the intersection can be regarded as representing the resultant of straightening plus swelling of fibers, and that above as the resultant of stretching plus swelling.

Relaxation of tension with time might be thought to influence the drop from the tension in the yarn when stretched dry to that when wet with the caustic soda, but the time involved seems to have little, if any, determinative effect on the final tensions within the limits of the experiments described.

The drop from the relatively high tensions required to stretch yarns to 102% of the base length (Figure 1) is largely due to relaxation due to the wetting, this relaxation being sufficient to allow the yarn to come to a lower tension in the caustic soda than that finally reached in the mercerizing. As a check, when a skein mounted dry at 102% was held at that length for a time equal to that required for mercerizing, there was but slight relaxation of tension, but when it was run in water containing a wetting agent at room temperature the tension dropped from 30 lb. to about 5 lb.

In the caustic soda the tension drops similarly from the relaxation due to the wetting by the solution, but quickly builds up again with the onset of the swelling of mercerization. Apparently, as long as the relaxation would lower the tension during impregnation below that finally developed in the caustic soda, the straight line for maximum tensions would be followed.

A determination of normal yarn length or of measuring-tension by the procedure described is a rather long process, but a unit tension once established can be used for many yarns of similar constructions. That the method has still other possibilities is indicated by experience with strips of cloth.

Tensions Developed in Cloth

Tensions developed by fabrics mercerized in strips were determined in connection with possible studies on the mercerization of cotton piece goods [6]. When the strips were mercerized through a series of lengths such as employed with yarns, one of the most notable observations was the great difference between warp and filling in level of tension developed. This was due, of course, to previous stretch and setting of the warp (which led to the development of high tension) and to shrinkage in the filling with increase of crimp (resulting in a much lower tension). There were similar changes of slope in the curves of maximum tension to those for yarn in Figure 2.

Summary

A procedure is suggested for the determination of the normal or true lengths of skeins of yarn, i.e., lengths at which the yarn can be regarded as straightened but not stretched, and for the derivation of a suitable measuring-tension for establishing this length. This procedure requires the determina-

tion of the tensions developed in skeins of the yarn during a series of mercerizings at lengths in the range of about 97%–102% of an initial or base length previously determined. When the tensions thus developed are suitably plotted, a change in slope in a curve of maximum tensions attained indicates the percentage which corresponds with the desired length of skein. In the work described, the change usually came at 100%, or the base length, due to the fortunate use of the correct measuring tension as determined in a different way in earlier experiments. If the change is at other than 100%, the measuring tension being sought will be the load required to set a skein of the same yarn and of the same size at the indicated percentage of the base length. The value thus determined can be expressed as a unit tension, 1 lb./100 yd. of 40/2 yarn of mercerizing twist in a 54-in. skein or, more convenient in use, 1.2 lb./120-yd. lea. Skeins of different sizes and of yarns of different numbers, of low to medium twist, can be considered to be at normal length if measured under proportional or equivalent loads.

The break in the curve of maximum tensions developed during the mercerization of yarns stressed as described appears to point to a fundamental change in the behavior of cotton yarn as it begins to stretch under load.

It is suggested also that a measuring tension for single threads proportional to that determined as described for skeins may be suitable for determining the initial lengths of yarn specimens for some of the common physical tests, such as those for elongation and twist.

Literature Cited

1. ASTM (*a*) D 180–54T, paragraph 9; (*c*) D 39–49, paragraph 8, American Society for Testing Materials, Philadelphia.
2. Ball, H. J., *Bull. Lowell Textile Inst.*, Ser. 45, No. 2, 3 pp. (1941).
3. Brown, J. J., Howell, N. A., Fiori, L. A., and Sands, J. E., TEXTILE RESEARCH JOURNAL **25**, 404–414 (1955).
4. Goldthwait, C. F., *Am. Dyestuff Reptr.* **15**, 7–14 (1927).
5. Goldthwait, C. F., *Am. Dyestuff Reptr.* **27**, 70–76 (1938).
6. Goldthwait, C. F., Murphy, A. L., Lohman, I. W., and Smith, H. O., TEXTILE RESEARCH JOURNAL **22**, 540–8 (1952).
7. Haven, G. B., *Mechanical Fabrics*, John Wiley & Sons, New York, pp. 322–24 (1932).
8. International Organization for Standardization, ISO/TC 38 SC5 (USA Secretariat 11) 15, 3rd Draft Proposal (Jan. 30, 1954); ISO/TC 38 SC5 (USA Secretariat 18) 34, 4th Draft Proposal (Dec. 15, 1955), American Standards Association, New York.
9. Mereness, H. A., "Determination of Crimp in Cotton Yarns," *Inst. of Textile Technology, Report No. 7*, pp. 11–18.
10. (a) Meredith, R., *J. Textile Inst.* **36**, T116 (1945); (b) **47**, T503 (1956).
11. Sondhelm, W. S., *Textile Recorder* **64** (**761**), 43–45 (1946).
12. Tentative Textile Specification No. 11, *J. Textile Inst.* **38**, S15–S20 (1947).
13. Tentative Textile Specification No. 21, *J. Textile Inst.* **41**, S16–S19 (1950).
14. Walen, E. D. (quoted in Reference 2).

Manuscript received August 12, 1957.

Charge Transfer Upon Contact Between Metals and Insulators[1]

D. O. Van Ostenburg[2] and D. J. Montgomery

Department of Physics, Michigan State University, East Lansing, Michigan

Abstract

The equilibrium charge distribution between substances in contact is calculated in the one-dimensional approximation for metal–insulator and insulator–insulator contacts. The direction of charge transfer is such as to equalize the Fermi levels, and the magnitude of charge transferred depends on the positions of the energy bands in the substances in contact. For example, in an insulator it is possible to have a large charge density ($\sim 10^{11}$ esu) within a thin layer ($\sim 10^{-8}$ cm.) or a small charge density ($\sim 10^{-1}$ esu) in a thick layer ($\sim 10^{-1}$ cm.), to give the same potential shift (~ 1 ev), depending on the relative position of the bands. The energy levels in most insulators of high resistivities are too poorly known to allow strict quantitative comparison with experiment, but the results permit a semiquantitative explanation of some observations on static electrification.

Introduction

Sufficient reproducibility has been attained in recent experiments [2, 3] on static electrification to justify attempts at formulating theoretical explanations of the phenomena observed. In such attempts [2, 4] the process of electrification is broken down into two steps—the attainment of equilibrium charge distribution between the bodies during contact and the counterflow of part of the charge during separation. The present paper is concerned with the calculation of the equilibrium charge transferred upon contact. Calculations of this kind have been made by other authors for metal–insulator [6] and metal–semiconductor [1, 6] contacts with special relations between energy bands and for metal–metal [1] contacts. We have extended the calculations to other metal–insulator contacts and to insulator–insulator contacts, restricting ourselves to the one-dimensional approximation. No consideration has been given to surface states or to impurity levels.

In equilibrium the laws of classical electrodynamics apply, specifically in the one-dimensional form of Poisson's equation, $d^2V/dx^2 = -(4\pi/\epsilon)\rho$. Here V is the electrostatic potential, x the spatial coordinate normal to the interface, ϵ the dielectric constant, and ρ the volume charge density. According to the theory of the solid state, the charge density is a function of the potential, the form of the function being determined by the details of the band structure. The function can be written as the product of a density of states times the Fermi-Dirac statistical factor giving the probability of occupation. In practice, it is frequently possible to simplify the computations by taking the statistics as degenerate (i.e., the statistical factor equals unity) everywhere within a metal and sometimes within an insulator near the interface, or by taking the statistics as classical (i.e., the statistical factor becomes a simple exponential) within an insulator, at least far from the interface.

The resulting differential equation, of the form $d^2V/dx^2 \sim \rho(V)$, can always be solved by an elementary transformation, although the exact solution can seldom be given in closed form. The constants of integration are fixed by the requirements that the field strength vanishes at infinity, since the system remains neutral, and that the field strength is continuous across the interface, since the charge density is finite there. One other condition must be fulfilled in accordance with the requirements of thermodynamics: in equilibrium the Fermi level is uniform throughout the system.

[1] This paper is based on a dissertation submitted by D. O. Van Ostenburg in partial fulfillment of the requirements for the degree of Doctor of Philosophy at Michigan State University.

[2] Present address: Armour Research Foundation, Chicago 16, Ill.

The exact height of the Fermi level, depending as it does on the geometry of the objects in contact, is unimportant for the problem at hand. It is, however, convenient to choose a geometry such that the depth of the Fermi level after contact represents the energy released when an electron at rest at infinity is taken into the interior of either object.

In the body of the paper these points will be illustrated by carrying out the solutions for most of the cases of interest. Numerical examples will be cited to show the orders of magnitudes of the potential shifts and effective surface charges.

Model

It is assumed that sufficient periodicity in the lattice structure exists to allow the use of a band model. To illustrate the notation, Figure 1 shows a schematic energy-band diagram for the case of metal–metal contacts, Figures 2*a*, *b*, *c*, and *d* show diagrams for metal–insulator contacts, and figures 3*a* and *b* for insulator–insulator contacts. Before contact the levels are constant up to the edge of the crystal. After contact, as a result of the transferred charge, $-eV(x)$, the potential energy of an electron within the crystal will change, the levels shifting accordingly. The total shift from one substance to the next is $e(\Delta V_1 - \Delta V_2)$, where ΔV_1 is the shift in the electrostatic potential of an electron in the substance on the left and ΔV_2 the corresponding quantity for the substance on the right. In the metal we are concerned with the work function ϕ_0, the energy released when an electron at rest outside the crystal is taken to the Fermi level ζ or absorbed when an electron is taken from the Fermi level to a point outside the crystal. In a sense ϕ_0 may be considered the analog of either the electron affinity or the ionization potential for a free molecule. We are concerned also with the energy of an electron at the bottom of the half-filled band in the metal, and designate this by ω_0. In the insulator we are concerned with the energy χ_0 released when an electron at rest outside the crystal is taken into the lowest level in the uppermost nearly empty band. This quantity is the analog of the electron affinity A for a free molecule. We are concerned also with the energy v_0 necessary to remove an electron from the highest level of the uppermost nearly filled band. This quantity is the analog of the ionization potential I for a free molecule.[3]

In the figures, the energy parameters of the substance on the left contain the subscript 1, those of the substance on the right the subscript 2. The subscript 0 indicates a value for a parameter before contact. For example, Figure 1 represents a metal–metal contact in which electrons flow from metal 2 to metal 1. As a result the levels in metal 1 are shifted upward by an amount $e\Delta V_1$, those in metal 2 downward by $e\Delta V_2$. Near the contact the potential energy of an electron is not constant, and the variation is designated by $\omega_1 \equiv -eV_1$ and $\omega_2 \equiv -eV_2$ in the two metals, respectively. With contacts involving insulators, the variable energy parameters χ and v are also needed, as will be seen in detail later.

The charge density due to electrons having either direction of spin is given by

$$-2e\int n(E)f(E)dE \qquad (1)$$

where $n(E)$ is the number of energy levels per unit volume for electrons of one direction of spin with energy lying in dE at E and $f(E)$ is the probability of occupation of the levels at E. We assume the Fermi-Dirac energy distribution,

$$f(E) = 1/[e^{(E-\zeta)/kT} + 1] \qquad (2)$$

where ζ is the Fermi energy and kT is Boltzmann's constant times the absolute temperature T.

To allow analytic representation of the results, we assume energy bands of standard form [7],

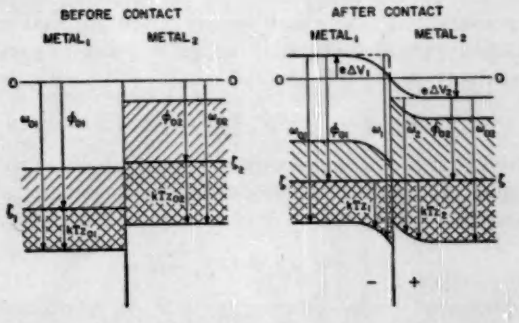

Fig. 1. Schematic diagram of energy levels for metal–metal contact.

[3] The quantity χ_0 is usually called "electron affinity" in solid-state literature, but we would prefer some designation differentiating it from the quantity A for a free molecule. The quantity v_0 does not seem to have been called "ionization potential," though the reasons are just as cogent as those for "electron affinity." At present we wish neither to introduce a new terminology nor to continue what to us is an undesirable usage; hence we shall use symbols only.

neglecting exchange and correlation energy. For the dependence of the energy E on k, the component of the propagation vector normal to the interface, we have

$$\begin{cases} E = \frac{1}{2}\hbar^2k^2/m^* \\ \qquad \text{(normal band of standard form)} \\ E = A_0 - \frac{1}{2}\hbar^2k^2/m^* \\ \qquad \text{(inverted band of standard form)} \end{cases} \tag{3}$$

where $\hbar$ is Planck's constant h divided by 2π, m^* is the effective mass of the electrons, and A_0 is the energy at the top of the inverted band.

In the usual way the number of energy levels per unit volume for one direction of electron spin lying in dE at E is

$$\begin{cases} n(E)dE = 2\pi(2m^*/h^2)^{\frac{1}{2}}E^{\frac{1}{2}}dE \quad \text{(normal band)} \\ n(E)dE = 2\pi(2m^*/h^2)^{\frac{1}{2}}(A_0 - E)^{\frac{1}{2}}dE \\ \qquad \text{(inverted band)} \end{cases} \tag{4}$$

For each case, to find the equilibrium distribution one must solve Poisson's equation. In the one-dimensional approximation, taking the origin of coordinate x at the interface,

$$d^2(-eV)/dx^2 = (4\pi e/\epsilon)\rho(x) \tag{5}$$

where ϵ is the dielectric constant and $\rho(x)$ is the net charge density obtained from Equation 1 with appropriate use of the relations in Equation 4. In order to get the net charge density, the positive charge density of the atomic cores must be added to the electron charge density.

The potential energy variation $-eV(x)$ is obtained by solution of Equation 5. The field strength E follows immediately from the definition $E \equiv -dV/dx$, as does the net charge density ρ from the relation $-4\pi\rho = \epsilon d^2V/dx^2$.

The constants appearing in the solution for the potential are determined by the conditions that at infinity the field strength vanishes (since the entire system remains neutral)

$$(dV_1/dx)_{x=-\infty} = 0 \quad (dV_2/dx)_{x=\infty} = 0 \tag{6}$$

and that the field strength is continuous across the interface (since the volume charge density there, as elsewhere, is finite)

$$(dV_1/dx)_{x=0} = (dV_2/dx)_{x=0} \tag{7}$$

Moreover, from thermodynamics or statistical mechanics it is known that at equilibrium the Fermi potential ζ is constant for the entire system. It is convenient to introduce an equivalent surface charge density,

$$\sigma_2 \equiv \int_0^\infty \rho_2(x)dx = -\sigma_1 \equiv -\int_{-\infty}^0 \rho_1(x)dx \tag{8}$$

which would give the same field as the total volume charge. The quantity σ_2 is most easily obtained as

$$\sigma_2 = (1/2\pi)(dV_2/dx)_{x=0} = -\sigma_1 = (1/2\pi)(dV_1/dk)_{x=0} \tag{9}$$

Metal–Metal Contacts

From Figure 1 it is clear that the net charge density in metal 1 is

$$\rho_1(x) = -4\pi(2m_1^*/h^2)^{\frac{1}{2}}e \cdot \left\{ \int_{\omega_1+e\Delta V_1}^{\zeta} [E - (\omega_1 + e\Delta V_1)]^{\frac{1}{2}}dE - \int_{\omega_{01}+e\Delta V_1}^{\zeta} [E - (\omega_{01} + e\Delta V_1)]^{\frac{1}{2}}dE \right\} \tag{1.1}$$

if the temperature is so low that the electron gas may be considered completely degenerate. Poisson's equation then takes the following form, after the elementary integrations in Equation 1.1 have been carried out:

$$d^2(eV_1/kT)/dx^2 = d^2(\omega_1/kT)/dx^2 = d^2z_1/dx^2 = (2/3l_1^2)(-z_{01})^{-\frac{1}{2}}[(-z_{01})^{\frac{1}{2}} - (-z_1)^{\frac{1}{2}}] \tag{1.2}$$

where we have introduced the following abbreviations:

$$z_1 \equiv (\omega_1 + e\Delta V_1 - \zeta)/kT \tag{1.3}$$

and

$$1/l_1^2 \equiv (16\pi^2e^2/\epsilon_1)(2m_1^*/h^2)^{\frac{1}{2}}(-kTz_{01})^{\frac{1}{2}} \quad \text{(for metals)} \tag{1.4}$$

The first integration of Equation 1.2 leads to the following result for the derivative of z_1:

$$dz_1/dx = (2z_{01}/\sqrt{3}l_1) \times [\tfrac{3}{5} + \tfrac{2}{5}(z_1/z_{01})^{\frac{5}{2}} - (z_1/z_{01})] \tag{1.5}$$

The second integration of Equation 1.2 leads to hyperelliptic functions; but, as Fan [1] has shown, it is often sufficient to expand the first term on the right hand side of Equation 1.5 in powers of $(z_{01} - z_1)/z_{01}$. The solution for ω_1 then is

$$\omega_1 - \omega_{01} = -e\Delta V_1 e^{x/l_1} \quad (x \leq 0) \tag{1.6}$$

In exactly the same fashion we find the variation of potential energy of an electron in metal 2 to be

$$\omega_2 - \omega_{02} = -e\Delta V_2 e^{-x/l_2} \quad (x > 0) \tag{1.7}$$

where the definition of l_2 is analogous to that of l_1.

To find ΔV_1 and ΔV_2, considered as unknowns to be determined from given parameters ω_{01}, ω_{02}, ϕ_{01}, and ϕ_{02}, assume the system at equilibrium so that

$$\phi_{01} + e\Delta V_1 = \zeta = \phi_{02} + e\Delta V_2 \qquad (1.8)$$

and apply Equation 7 to get

$$\Delta V_1/l_1 = -\Delta V_2/l_2 \qquad (1.9)$$

Then

$$e\Delta V_1 = (\phi_{02} - \phi_{01})/(1 + l_2/l_1) \qquad (1.10)$$

$$-e\Delta V_2 = (\phi_{02} - \phi_{01})/(1 + l_1/l_2) \qquad (1.11)$$

$$\zeta = \phi_{01}/(1 + l_1/l_2) + \phi_{02}/(1 + l_2/l_1) \qquad (1.12)$$

From equations similar to (9) and (1.5) it is seen that

$$\begin{aligned}\sigma_1 &= -(1/2\pi)(dV_1/dx)_{x=0} \\ &= (kT/2\pi e)(dz_1/dx)_{x=0} \\ &= [(\omega_{01} - \phi_{01})/\sqrt{3}\pi e l_1] \\ &\times \{\tfrac{2}{3} + \tfrac{2}{3}[(\omega_{01} - \zeta)/(\omega_{01} - \phi_{01})]^{\frac{3}{2}} \\ &\qquad - [(\omega_{01} - \zeta)/(\omega_{01} - \phi_{01})]\}^{\frac{1}{2}}\end{aligned}$$

From Equations 1.2 and 1.3 is obtained

$$\begin{aligned}\rho_1(0) &= (\epsilon_1/4\pi e)d^2(-eV_1)/dx^2 \\ &= [(\omega_{01} - \phi_{01})\epsilon_1/6\pi e l_1^2] \\ &\qquad \times \{[(\omega_{01} - \zeta)/(\omega_{01} - \phi_{01})]^{\frac{1}{2}} - 1\}\end{aligned}$$

Expressions for $\sigma_2 = -\sigma_1$ and for $\rho_2(0)$ are obtained in obvious fashion.

Numerical example: Let $m_1^* = m_2^* = m$, the normal electronic mass, and take $\epsilon_1 = \epsilon_2 = 1$. Suppose

$\phi_{01} = \zeta_1 = -6.23$ ev $\quad \phi_{02} = \zeta_2 = -4.00$ ev

$\omega_{01} \equiv \phi_{01} + z_{01} = -8.23$ ev $\quad \omega_{02} \equiv \phi_{02} + z_{02} = -7.00$ ev

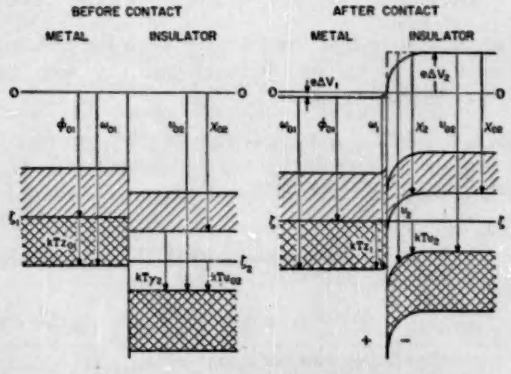

Fig. 2a. Schematic diagram of energy levels for metal–insulator contact, Case *a*.

Then we find by substitution in the equations given

$$l_1 = 0.68 \times 10^{-8} \text{ cm} \qquad l_2 = 0.62 \times 10^{-8} \text{ cm}.$$

and

$$e\Delta V_1 = 1.17 \text{ ev} \qquad e\Delta V_2 = -1.06 \text{ ev} \qquad \zeta = -5.04 \text{ ev}$$

The charge densities for metal 1 are

$$\sigma_1 = -9.6 \times 10^4 \text{ esu} \qquad \rho_1(x) = -7.65 \times 10^{12}\, e^{z_1/l_1} \text{ esu}$$

At the interface the volume charge density corresponds to an excess electron density of 1.6×10^{22} electrons/cm.^{3}, several times the normal density. Here the quantity $(z_{01} - z_1)/z_{01}$, in powers of which Equation 1.5 has been expanded, attains the value 0.58. We cannot then take the numercial results very seriously, since neither the model nor the calculation has strict validity.

Metal–Insulator Contacts

For metal–insulator contacts the method of calculation depends on the relative positions of the bands. Figures 2*a*, *b*, *c*, and *d* are schematic diagrams of the qualitatively different cases.

Case 2a

Figure 2*a* represents the contact between a metal and an insulator where before contact the Fermi level in the metal lies above the Fermi level in the insulator and where the Fermi level in the metal lies above the bottom of an empty band in the insulator. Then electrons can spill from the half-filled band of the metal into the empty band of the insulator. Large charge is lost by the metal from a small spatial region, and a large amount gained by the insulator within a small spatial region. Hence the potential shift within the insulator is no more than an order of magnitude larger than that within the metal.

For the metal we have the same type of solution as that just given for the metal–metal contact. The chief result needed is Equation 1.6, written here as Equation 1.6′:

$$x/l_1 = \ln[(\omega_1 - \omega_{01})/(-e\Delta V_1)] \qquad (1.6')$$

From Figure 2*a* it is clear that the charge density in the insulator is

$$\rho_2(x) = 4\pi(2m_2^*/h^2)^{\frac{1}{2}}e \qquad (2a.1)$$

$$\times\left\{\int_{-\infty}^{v_2+e\Delta V_2} \frac{[(v_2 + e\Delta V_2) - E]^{\frac{1}{2}}}{e^{(\zeta-E)/kT} + 1}\,dE - \int_{\chi_2+e\Delta V_2}^{\infty} \frac{[E - (\chi_2 + e\Delta V_2)]^{\frac{1}{2}}}{e^{(E-\zeta)/kT} + 1}\,dE\right\}$$

Upon defining the auxiliary quantities $u_2(x)$ and γ

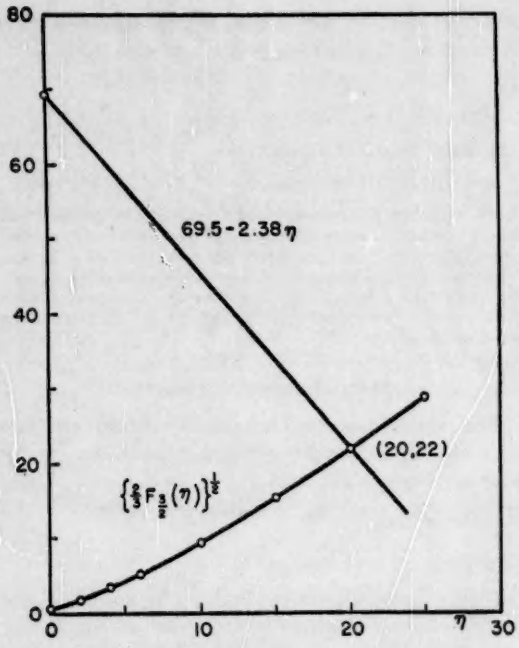

Fig. 2a'. Graph for solution of transcendental equation for potential shift in an insulator for metal–insulator contact, Case *a*.

(see Figure 2*a*, p. 25) by the following equation:

$$kTu_2(x) \equiv v_2(x) + e\Delta V_2 - \zeta$$

and

$$kT\gamma_2 \equiv v_2(x) - \chi_2(x) = v_{02} - \chi_{02}$$

and introducing the notation [5]

$$F_n(\zeta) \equiv \int_0^\infty [t^n/(e^{t-\zeta}+1)]\,dt$$

Poisson's equation becomes

$$d^2(-eV_2/kT)/dx^2 = d^2(v_2/kT)/dx^2 = d^2u_2/dx_2 = (1/2l_2^2)[F_{\frac{1}{2}}(u_2) - F_{\frac{1}{2}}(\gamma_2 - u_2)] \quad (2a.2)$$

where

$$1/l_2^2 \equiv 2(16\pi^2e^2/\epsilon_2)(2m_2^*/h^2)^{\frac{3}{2}}(kT)^{\frac{1}{2}} \quad \text{(for insulator)} \quad (2a.3)$$

The first integration of Equation 2*a*.2 leads to the following result for the derivative of u_2:

$$du_2/dx = (1/l_2)\{\tfrac{2}{3}[F_{\frac{3}{2}}(u_2) - F_{\frac{3}{2}}(u_{02})] - \tfrac{2}{3}[-F_{\frac{3}{2}}(\gamma_2 - u_2) + F_{\frac{3}{2}}(\gamma_2 - u_{02})]\}^{\frac{1}{2}} \quad (2a.4)$$

Here we have made use of the relation given [5]

$$\tfrac{2}{3}F_{\frac{3}{2}}(\zeta) = \int_a^\zeta F_{\frac{1}{2}}(\zeta')d\zeta' + \tfrac{2}{3}F_{\frac{3}{2}}(a)$$

Usually the only term of appreciable size within the braces is that of argument $\gamma_2 - u_2$.

The second integration of Equation 2*a*.2 gives an implicit expression for u_2 as a function of x:

$$x/l_2 = \int_{u_{02}-e\Delta V_2/kT}^{u_2(x)} \{\tfrac{2}{3}[F_{\frac{3}{2}}(u_2') - F_{\frac{3}{2}}(u_{02})] - \tfrac{2}{3}[F_{\frac{3}{2}}(\gamma_2 - u_{02}) - F_{\frac{3}{2}}(\gamma_2 - u_2')]\}^{-\frac{1}{2}}du_2' \quad (2a.5)$$

From figure 2*a* it is seen that

$$\gamma_2 < u_{02} < 0 < e\Delta V_2/kT$$

The function $F_{\frac{3}{2}}(\zeta)$ increases rapidly for positive values of its argument, but is small for negative values. If one stays at distances such that u_2' is sufficiently far from u_{02}, one needs retain only the last term in the braces of Equation 2*a*.5. This equation thus reduces to

$$x/l_2 = \int_{u_{02}-e\Delta V_2/kT}^{u_2(x)} [\tfrac{2}{3}F_{\frac{3}{2}}(\gamma_2 - u_2')]^{-\frac{1}{2}}\,du_2' \quad (2a.5')$$

Here we have made the restriction $u_2 \leq u_{02} - \delta$, δ being a positive quantity whose magnitude depends on the accuracy desired in the approximation.

Equations 1.6′ and 2*a*.5′ are implicit expressions for the variation of potential energy of an electron as a function of distance within the metal and insulator. They contain $e\Delta V_1$ and $e\Delta V_2$ as unknowns to be evaluated in terms of ϕ_{01}, ω_{01}, v_{02}, and χ_{02} through imposition of Equation 7 and a constant Fermi potential at equilibrium. Therefore,

$$\phi_{01} + e\Delta V_1 = \zeta = v_{02} + e\Delta V_2 - kTu_{02} \quad (2a.6)$$

Let us assume that the Fermi level in the isolated insulator lies halfway between the full and the empty bands. Then

$$kTu_{02} = \tfrac{1}{2}(v_{02} - \chi_{02}) = \tfrac{1}{2}kT\gamma_2 \quad (2a.7)$$

From Equation 7 we have

$$(dv_2/dx)_{x=0} = \{\tfrac{2}{3}F_{\frac{3}{2}}(\tfrac{1}{2}\gamma_2 + e\Delta V_2/kT)\}^{\frac{1}{2}}(kT/l_2) \quad (2a.8)$$

and

$$(d\omega_1/dx)_{x=0} = -e\Delta V_1/l_1 \quad (2a.9)$$

Upon introducing the notation

$$\eta \equiv \tfrac{1}{2}\gamma_2 + e\Delta V_2/kT \quad (2a.10)$$

we find by appropriate substitution that the term

$$[\tfrac{2}{3}F_{\frac{1}{2}}(\eta)]^{\frac{2}{3}} = \{[(\phi_{01} - \chi_{02})/kT] - \eta\}(l_2/l_1) \quad (2a.11)$$

This equation may be solved graphically for η and then for $e\Delta V_2$. The values of $e\Delta V_1$ and ζ follow from Equation 2a.6. The variation of the potential and of the volume charge density throughout the metal and the insulator follows from Equations 1.6′ and 2a.5. The equivalent surface charge is obtained from Equations 8 and 2a.8.

Numerical example: Let $m_1^* = m_2^* = m$, and $\epsilon_1 = \epsilon_2 = 1$. Take $T = 290°$ K. Suppose

$$\phi_{01} = -6.27 \text{ ev} \quad \chi_{02} = -7 \text{ ev}$$
$$\zeta_1 = -6.27 \text{ ev} \quad \zeta_2 = -8.5 \text{ ev}$$
$$\omega_{01} = -9.46 \text{ ev} \quad v_{02} = -10 \text{ ev}$$

Then we find

$$l_1 = 0.673 \times 10^{-8} \text{ cm} \quad l_2 = 1.59 \times 10^{-8} \text{ cm} \quad l_2/l_1 = 2.38$$

Equation 2a.11 becomes

$$[\tfrac{2}{3}F_{\frac{1}{2}}(\eta)]^{\frac{2}{3}} = 69.5 - 2.38\,\eta$$

Figure 2a′ is a plot of each side of this equation. The curves intersect at the point (20, 22), whence by Equations 2a.7 and 2a.10 we see $e\Delta V_2 = 2$ ev. From Equations 2a.6 and 2a.7 we find $\zeta = -6.50$ ev, and from Equation 2a.6, $e\Delta V_1 = -0.23$ ev. We may now determine $\omega_1(x)$ from Equation 1.6′, just as in the case of the metal–metal contact. We obtain $x(u_2)$ from Equation 2a.5, and upon inverting the expression get the potential energy as a function of x. Within the insulator we have then:

$$x = (1.59 \times 10^{-8}) \int_{u_2(0)=-140}^{u_2(x)} [\tfrac{2}{3}F_{\frac{1}{2}}(-120 - u_2')]^{-\frac{2}{3}}\, du_2'$$

The results are plotted as part of Figure 2a.

To obtain the volume charge density use Equation 2a.1 or 2a.2, inserting the result for $u_2(x)$ just found. For the numerical example under discussion see Table I.

The equivalent surface charge density is calculated from Equation 2a.8 to be $\sigma_2 = -18{,}300$ esu.

Case 2b

Figure 2b represents the contact between a metal and an insulator where before contact the Fermi level in the metal lies below the Fermi level in the insulator and where the top of a filled band in the insulator lies above the Fermi level in the metal. Electrons can spill from the filled band in the insulator to the half-filled band in the metal. Much charge is lost by the insulator from a small spatial region and much gained by the metal within a small spatial region. An analysis of Figure 2b shows that the charge density is given by an expression just like that in Equation 2a.1. However, $e\Delta V_1$ is now positive and $e\Delta V_2$ negative. The treatment is almost exactly the same as that in Case 2a.

TABLE I. Volume Charge Density within Insulator for Case 2a

$u_2(x)$	$\gamma_2 - u_2(x)$	x(A)	$\rho_2(x)$(esu)	$100\rho_2(x)/\rho_2(0)$
−140	20	0	770 $\times 10^0$	100%
−120	0	7	8.8 $\times 10^0$	1.1
−116	− 4	26	0.21 $\times 10^0$	0.027

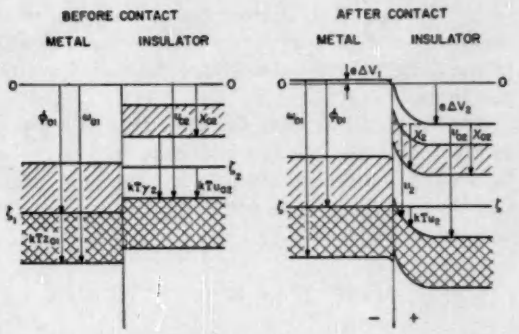

Fig. 2b. Schematic diagram of energy levels for metal–insulator contact, Case *b*.

Numerical example: Let $m_1^* = m_2^* = m$, and $\epsilon_1 = \epsilon_2 = 1$. Take $T = 290°$ K. Suppose

$$\phi_{01} = -6.27 \text{ ev} \quad \chi_{02} = -2.54 \text{ ev}$$
$$\zeta_1 = -6.27 \text{ ev} \quad \zeta_2 = -4.04 \text{ ev}$$
$$\omega_{01} = -9.46 \text{ ev} \quad v_{02} = -5.54 \text{ ev}$$

Then we find again

$$l_1 = 0.67 \times 10^{-8} \text{ cm} \quad l_2 = 1.59 \times 10^{-8} \text{ cm} \quad l_2/l_1 = 2.38$$

The solution of the equation for η leads to the same graphs as in Figure 2a′, the curves intersecting at the same point. Assuming that in the isolated insulator the Fermi level lies halfway between the occupied and empty bands, we find that

$$e\Delta V_2 = -2.00 \text{ ev} \quad e\Delta V_1 = 0.23 \text{ ev} \quad \zeta = -6.04 \text{ ev}$$

The values of the parameters have been chosen so that the results for the volume charge density and the equivalent surface charge density are the same as those for Case 2a, provided the sign is changed.

Case 2c

Figure 2c represents the contact between a metal and an insulator where in isolation the Fermi level in the metal lies above the Fermi level in the insulator and where the bottom of the empty band of the insulator lies above the Fermi level in the metal. Electrons escape by thermal agitation from the filled band in the metal to the empty band of the insulator. A little charge is lost from the metal in a small spatial region, and the same amount is gained by the insulator in a large spatial region. This case was treated originally by Mott and Gurney

[6]. We extend their treatment by using a more accurate solution in order to remove the difficulty of the infinite potential arising from their logarithmic form.

For the metal we have the same type of solution as given earlier. For the insulator, an analysis of figure 2*c* leads to Equation 2*a*.2. Since the arguments of $F_{\frac{1}{2}}$ are always negative, we may use the series representation [5]

$$F_{\frac{1}{2}}(\zeta) = \Gamma(\tfrac{3}{2}) \sum_{s=1}^{\infty} (-1)^{s-1} e^{s\zeta}/s^{\frac{1}{2}} \quad (\zeta < 0)$$

If ζ is sufficiently negative, only the first term need be retained. The error is only about 0.5% for $\zeta = -4$, and is completely negligible for $\zeta = -10$, the greatest value occurring in our example.

Poisson's equation becomes

$$d^2u_2/dx^2 = B_2^2 \sinh (u_2 - \tfrac{1}{2}\gamma_2) \qquad (2c.1)$$

where

$$B_2^2 \equiv \Gamma(\tfrac{3}{2}) e^{\frac{1}{2}\gamma_2}/l_2^2$$

The first integration of Equation 2*c*.1 leads to the following result for the derivative of u_2:

$$du_2/dx = -2B_2 \sinh [\tfrac{1}{2}u_2(x) - \tfrac{1}{4}\gamma_2] \qquad (2c.2)$$

The second integration of Equation 2*c*.1 yields

$$u_2(x) = \tfrac{1}{2}\gamma_2 - 4 \tanh^{-1} \times \{e^{-B_2 x} \tanh [\tfrac{1}{8}\gamma_2 - \tfrac{1}{4}u_2(0)]\} \quad (x \geq 0) \qquad (2c.3)$$

To evaluate $e\Delta V_1$ and $e\Delta V_2$, we impose the condition expressed in Equation 6

$$\phi_{01} + e\Delta V_1 = \zeta = v_{02} + e\Delta V_2 - kTu_{02} \qquad (2c.4)$$

and, by incorporating Equation 7,

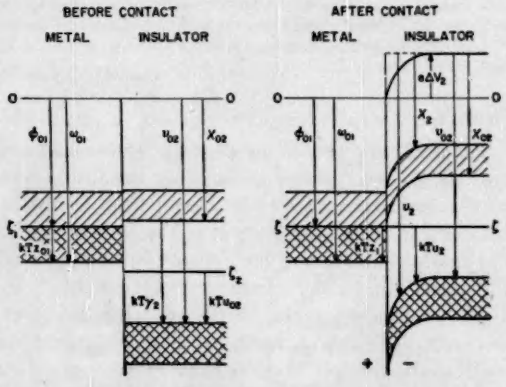

Fig. 2c. Schematic diagram of energy levels for metal–insulator contact, Case *c*.

$$(-e/kT)(\Delta V_1/l_1) = -2B_2 \sinh [\tfrac{1}{2}u_2(0) - \tfrac{1}{4}\gamma_2] = 2B_2 \sinh (\tfrac{1}{2}e\Delta V_2/kT) \qquad (2c.5)$$

Elimination of $e\Delta V_1$ from Equation 2*c*.5 by use of 2*c*.4 leads to a transcendental equation for $e\Delta V_2$ whose solution can be approximated, in those cases where the Fermi levels before contact differ by more than 0.1 ev or so, by

$$e\Delta V_2 \cong \phi_{01} - \tfrac{1}{2}(\chi_{02} + v_{02}) \qquad (2c.6)$$

The approximate solution for $e\Delta V_1$, which is also the correction of next order to be added to Equation 2*c*.6 for $e\Delta V_2$, is

$$-e\Delta V_1 \cong kT(l_1/l_2)\sqrt{\Gamma(\tfrac{3}{2})}\, e^{\frac{1}{2}(\phi_{01} - \chi_{02})/kT} \qquad (2c.7)$$

The approximate value of the Fermi potential is obtained immediately from Equation 2*c*.4.

The variation of the potential within the insulator is obtained from Equation 2*c*.3 with the result 2*c*.6 inserted. We write this variation as

$$u_2(x) = \tfrac{1}{2}\gamma_2 - 4 \tanh^{-1}[e^{-B_2 x} \tanh (e\Delta V_2/4kT)]$$

For small x, $u_2(x)$ takes the form

$$u_2(x) = \tfrac{1}{2}\gamma_2 - 2 \ln [2/(B_2 x + 2e^{-e\Delta V_2/2kT})] \qquad (0 < B_2 x \ll 1)$$

When the second term within the parentheses is negligible compared with the first term, this expression gives the logarithmic variation found by Mott and Gurney [6].

For large x, $u_2(x)$ is given approximately by

$$u_2(x) = \tfrac{1}{2}\gamma_2 - 4e^{-B_2 x} \tanh (e\Delta V_2/4kT) \qquad (B_2 x \gg 1)$$

usually

$$e\Delta V_2/kT \gg 1$$

and we have simply

$$u_2(x) = \tfrac{1}{2}\gamma_2 - 4e^{-B_2 x}$$

The equivalent surface charge density is calculated by use of Equation 2*c*.5 to be

$$\sigma_2 = (1/2\pi)(dV_2/dx)_{x=0} = -(kT/2\pi e)(du_2/dx)_{x=0} = -[kT\sqrt{\Gamma(\tfrac{3}{2})}/\pi e l_2] e^{\frac{1}{2}\gamma_2} \sinh (e\Delta V_2/2kT)$$

Upon making the approximation $\sinh y \cong \frac{1}{2}e^y$ for large y, and upon taking the value of $e\Delta V_2$ from Equation 2*c*.6, we get

$$\sigma_2 \cong -[kT\sqrt{\Gamma(\tfrac{3}{2})}/2\pi e l_2] e^{(\phi_{01} - \chi_{02})/2kT}$$

The volume charge density is obtained from Equation 2*c*.1 with the value for u_2 given in Equation

2c.3. The result is complicated except for small x; then we find

$$\rho_2(x) = (\epsilon_2 kT/4\pi e)d^2u_2/dx_2 = -\epsilon_2 kT/[2\pi e(x + x_0)^2]$$

where

$$x_0 \equiv [2l_2/\sqrt{\Gamma(\tfrac{3}{2})}]e^{-(e\Delta V_2/2kT)-\frac{1}{2}\gamma_2} = 2.19 l_2 e^{(\phi_{01}-\chi_{02})/2kT}$$

The characteristic distance x_0 is that at which the volume charge density falls to one-quarter its value at the interface,

$$\rho_2(0) = -[\epsilon_2 kT\Gamma(\tfrac{3}{2})/8\pi e l_2^2]e^{(\phi_{01}-\chi_{02})/kT}$$

Numerical example: Let $m_1^* = m_2^* = m$, and $\epsilon_1 = \epsilon_2 = 1$. Take $T = 290°$ K. Suppose

$$\phi_{01} = -6.27 \text{ ev} \quad \chi_{02} = -6.00 \text{ ev}$$
$$\zeta_1 = -6.27 \text{ ev} \quad \zeta_2 = -8.50 \text{ ev}$$
$$\omega_{01} = -8.27 \text{ ev} \quad v_{02} = -11.00 \text{ ev}$$

Then we find

$$l_1 = 0.67 \times 10^{-8} \text{ cm.} \quad l_2 = 1.59 \times 10^{-8} \text{ cm.}$$
$$e\Delta V_1 = -45 \times 10^{-6} \text{ ev} \quad e\Delta V_2 = 2.23 \text{ ev}$$

Furthermore, $\zeta = -6.27$ ev $\quad x_0 = 750 \times 10^{-8}$ cm. The charge densities are

$$\sigma_2 = -\sigma_1 = -3.51 \text{ esu}$$
$$\rho_1(0) = 2.62 \times 10^{6} \text{ esu} \quad \rho_2(0) = -2.35 \times 10^{5} \text{ esu}$$

The effective surface charge density, ~3 esu, is less than that producing dielectric breakdown from a plane surface in atmospheric air. The excess electron densities are small compared with the normal densities. The depth of penetration in the insulator as measured by x_0 is about 10^2 times the depth in the metal as measured by l_1. The potential shift is accordingly much smaller in the metal.

Case 2d

Figure 2*d* represents the contact when in isolation the Fermi level in the metal lies below the Fermi level in the insulator and when the top of the filled band of the insulator lies below the Fermi level in the metal. Electrons escape from the insulator only by thermal agitation from the filled band in the insulator to the half-filled band in the metal. Small charge is lost by the insulator from a large spatial region and an equal charge gained by the metal within a small spatial region. The solution for this case proceeds in almost the same fashion as that for Case 2*c*, except that the sign of charge is reversed.

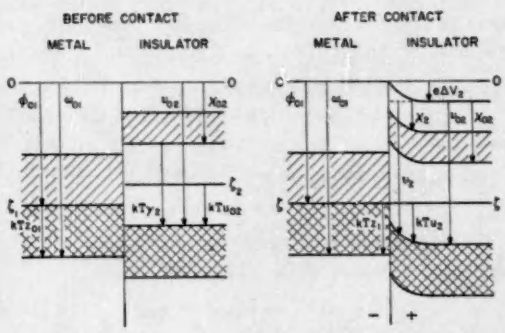

Fig. 2d. Schematic diagram of energy levels for metal–insulator contact., Case *d*.

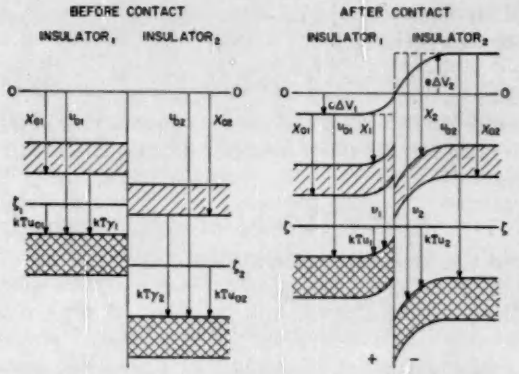

Fig. 3a. Schematic diagram of energy levels for insulator–insulator contact, Case *a*.

Insulator–Insulator Contacts

For insulator–insulator contacts the method of calculation depends on the relative positions of the bands, much as in the case of metal–insulator contacts. Figures 3*a* and 3*b* are schematic diagrams of the qualitatively different cases.

Case 3a

Figure 3*a* respresents the contact between two insulators where electrons can escape from the left-hand insulator to the right-hand one only by thermal agitation from a filled band into an empty band lying above it. Hence, small charge is lost by the left-hand insulator from a large spatial region, and an equal charge gained by the right-hand insulator within a large spatial region. From figure 3*a* it is seen that the charge density for the insulator on the right is the same as that for the insulator in Case 2*c*. The solution for the potential energy variation in the right-hand medium is therefore the same as in Equation 2*c*.2. For the insulator on the left, we find for the charge density an expression

of the form occurring in Equation 2*c*.1, except that the sign is changed:

$$d^2u_1/dx^2 = -B_1^2 \sinh [u_1(x) - \tfrac{1}{2}\gamma_1] \quad (3a.1)$$

where the definition of B_1 is analogous to that of B_2 in Case 2*c*. The first integration of Equation 3*a*.1 gives

$$du_1/dx = 2B_1 \sinh [\tfrac{1}{2}u_1(x) - \tfrac{1}{4}\gamma_1] \quad (3a.2)$$

and the second integration gives

$$u_1(x) = \tfrac{1}{2}\gamma_1 - 4 \tanh^{-1} \times \{e^{B_1 x} \tanh [\tfrac{1}{8}\gamma_1 - \tfrac{1}{4}u_1(0)]\} \quad (x \leq 0) \quad (3a.3)$$

To evaluate $e\Delta V_1$ and $e\Delta V_2$ we assume uniformity of the Fermi level, whence

$$v_{01} + e\Delta V_1 - kTu_{01} = \zeta = v_{02} + e\Delta V_2 - kTu_{02} \quad (3a.4)$$

Upon use of Equation 7,

$$e^{\frac{1}{2}\gamma_1} l_1^{-1} e^{-e\Delta V_1/2kT} = e^{\frac{1}{2}\gamma_2} l_2^{-1} e^{e\Delta V_2/2kT} \quad (3a.5)$$

The solution of these equations is

$$-e\Delta V_1 = \tfrac{1}{2}(\chi_{01} - \chi_{02}) - kT \ln (l_2/l_1) \quad (3a.6)$$

and

$$e\Delta V_2 = \tfrac{1}{2}(v_{01} - v_{02}) + kT \ln (l_2/l_1) \quad (3a.7)$$

The position of the Fermi level is obtained from Equation 3*a*.4:

$$\zeta = \tfrac{1}{2}(v_{01} + \chi_{02}) + kT \ln (l_2/l_1) \quad (3a.8)$$

The variation of the potential energy of an electron within the left-hand insulator may now be found from Equation 3*a*.3; the volume charge density may be obtained from Equation 3*a*.1. The surface charge density follows from Equation 3*a*.2, and may be approximated by

$$\sigma_2 = -\sigma_1 \cong -[kT\sqrt{\Gamma(\tfrac{3}{2})/2\pi e l_2}]\, e^{(v_{01}-\chi_{02})/2kT}$$

For the right-hand insulator a similar procedure is followed. The results are analogous to those for Case 2*c*.

We may expect that unless the energy gaps are no greater than several times kT, the charge transferred will be much smaller than that necessary to produce breakdown.

Numerical example: Let $m_1^* = m_2^* = m$, and $\epsilon_1 = \epsilon_2$. Take $T = 290°$ K. Suppose

$\chi_{01} = -4.00$ ev $\quad \chi_{02} = -6.00$ ev
$\zeta_1 = -5.50$ ev $\quad \zeta_2 = -8.50$ ev
$v_{01} = -7.00$ ev $\quad v_{02} = -11.00$ ev

Then we find

$l_1 = l_2 = 1.59 \times 10^{-8}$ cm. $\quad \zeta = -6.50$ ev
$e\Delta V_1 = -1$ ev $\quad e\Delta V_2 = 2$ ev

The equivalent surface charge density is

$$\sigma_2 = -\sigma_1 = -7.70 \times 10^{-6} \text{ esu}$$

It is so small primarily because one-half the energy gap $v_{01} - \chi_{02}$ amount to 1 ev, or 40 times kT. In general, energy gaps more than a few tenths of an electron volt result in very small charge formation.

Case 3b

Figure 3*b* represents the contact between two insulators where electrons can spill from the filled band of the left-hand material into the empty band of the right-hand material. Large charge is lost by the left-hand insulator from a small spatial region, and an equal charge is gained by the right-hand material in a small spatial region. It is seen from the figures that the insulator on the right has a band structure identical with that of the insulator in Case 2*a*; therefore the solution is of the same form as that developed for Case 2*a*. Assumption of equilibrium and utilization of Equation 7 leads to

$$\{\tfrac{2}{3}F_{\frac{1}{2}}(\tfrac{1}{2}\gamma_1 + e\Delta V_1/kT)\}^{\frac{1}{3}}(kT/l_1) = \{\tfrac{2}{3}F_{\frac{1}{2}}(\tfrac{1}{2}\gamma_2 + e\Delta V_2/kT)\}^{\frac{1}{3}}(kT/l_2) \quad (3b.1)$$

and

$$v_{01} + e\Delta V_1 - kTu_{01} = \zeta = v_{02} + e\Delta V_2 - kTu_{02} \quad (3b.2)$$

Solving these equations for $e\Delta V_1$ and $e\Delta V_2$ is awkward unless $l_1 = l_2$. Then we have

$$-e\Delta V_1 = \tfrac{1}{2}(\chi_{01} - \chi_{02}) \quad (3b.3)$$

$$e\Delta V_2 = \tfrac{1}{2}(v_{01} - v_{02}) \quad (3b.4)$$

$$\zeta = \tfrac{1}{2}(\chi_{02} + v_{01}). \quad (3b.5)$$

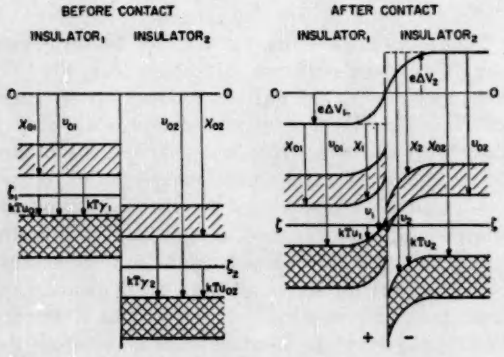

Fig. 3b. Schematic diagram of energy levels for insulator–insulator contact, Case *b*.

For the surface charge density, in this case

$$\sigma_2 = -\sigma_1 = -(kT/2\pi e l_1) \times [\tfrac{2}{3}F_{\frac{1}{2}}(\tfrac{1}{2}v_{01}/kT - \tfrac{1}{2}\chi_{01}/kT)]^{\frac{1}{2}} \quad (3b.6)$$

The expressions for volume charge density are obtained readily.

Numerical example: Let $m_1^* = m_2^* = m$, and $\epsilon_1 = \epsilon_2$. Take $T = 290°$ K. Suppose

$$\chi_{01} = -4.00 \text{ ev} \quad \chi_{02} = -7.00 \text{ ev}$$
$$\zeta_1 = -5.00 \text{ ev} \quad \zeta_2 = -8.50 \text{ ev}$$
$$v_{01} = -6.00 \text{ ev} \quad v_{02} = -10.00$$

Then we find

$$l_1 = l_2 = 1.59 \times 10^{-8} \text{ cm.} \qquad \zeta = -6.50 \text{ ev}$$
$$e\Delta V_1 = -1.50 \text{ ev} \qquad e\Delta V_2 = 2.00 \text{ ev}$$

The equivalent surface charge density is

$$\sigma_2 = -\sigma_1 = -18{,}400 \text{ esu}$$

For charge transfer of this amount, the volume charge densities are so great that the numerical values are not very meaningful. The chief point to be noted is that large amounts of charge may be transferred even between good insulators.

Applications

Hersh and Montgomery [3] described the techniques and gave the results of an experimental study on the static electrification of filaments of various materials rubbed against one another, and in a subsequent paper [4] outlined the basis for a theory of the subject. Harper [2] described his work on the charge transferred when spheres of various materials are touched against one another, and gave a theoretical treatment to correlate the results for metal–metal contacts. The present paper constitutes an attempt to provide a specific quantitative basis for explanation of some of the results obtained in the studies mentioned.

One may consider static electrification to consist of two processes—the direct flow of charge from one substance to another upon making contact and the reverse flow upon separation. The latter flow will take place between the materials during the breaking of the contact, but will be directed towards other objects in the neighborhood as well when dielectric breakdown of the atmosphere occurs. In the present paper we consider only the equilibrium charge while the materials are in contact. The charge observed in the experiments mentioned may be reduced from the equilibrium value by quantum-mechanical tunneling through the gap during the separation and by discharge through the surrounding atmosphere.

In the experimental work mentioned [2, 3], the point relevant to the present paper is that in certain cases of insulator–insulator and metal–insulator contacts the transfer of charge is observed to be small; in others, it is observed to be appreciable and even large. The mechanism discussed provides for these phenomena, and in fact permits the assignment to some extent of energy parameters for different materials [4]. Unfortunately, for most insulators of high enough resistivity to make static electrification practicable, so little is known independently about energy levels that quantitative comparisons cannot be made.

It is concluded that for phenomena involving contact between metals and insulators, a mechanism for charge transfer based on the band picture of conventional solid-state theory affords at least semi-quantitative agreement with experiment. Additional data will be necessary to see whether strictly quantitative predictions can be made successfully.

Literature Cited

1. Fan, H. Y., *Phys. Rev.* **61**, 365 (1941); **62**, 388 (1942).
2. Harper, W. R., *Proc. Roy. Soc.* **A205**, 83 (1951); **A218**, 111 (1953).
3. Hersh, S. P. and Montgomery, D. J., TEXTILE RESEARCH JOURNAL **25**, 279 (1955).
4. Hersh, S. P. and Montgomery, D. J. TEXTILE RESEARCH JOURNAL **26**, 903 (1956).
5. McDougall, J. M. and Stoner, E. C., *Trans. Roy. Soc.* **237**, 67 (1938).
6. Mott, N. F. and Gurney, R. W., *Electronic Processes in Ionic Crystals*, Oxford, Chap. 5 (1948).
7. Wilson, A. H., *The Theory of Metals*, 2nd ed., Cambridge, Chap. 1–2 (1953).

Manuscript received July 16, 1957.

Penetration and Supercontraction of Keratin Fibers by Lithium Bromide Solutions

A. R. Haly and June Griffith

Physics and Engineering Unit, Wool Textile Research Laboratories, Commonwealth Scientific and Industrial Research Organization, The Hermitage, Ryde, N.S.W., Australia

Abstract

With the aid of a microscope, measurements were made of the diametral swelling and degree of supercontraction of wool fibers in lithium bromide solutions at room temperature. Considerable differences were found between supercontractions measured around the orthocortical and around the paracortical sides the fibers. The mode of pentration of the solutions into the fibers was studied, and it was concluded that the epicuticle is an important barrier to the entry of the reagent. In addition, rates of supercontraction of wool, kid mohair, and human hair fibers in lithium bromide solutions at 89° and 100° C. were determined. Supercontraction-time curves exhibit three well-defined zones; an attempt is made to explain these characteristics. Some histological observations are reported.

Introduction

Supercontraction of keratin fibers has been the subject of many investigations, and a number of attempts have been made to account satisfactorily for the phenomenon. Alexander [1] invoked a model in which keratin polypeptide chains are set in a three-dimensionally cross-linked cement, and this model was discussed recently by Jeffrey et al. [12]. On the other hand, Carter et al. [4] and Elöd and Zahn [6] have based their discussions on the assumption that the keratin structure which is significant in supercontraction is a system of cross-linked polypeptide chains.

In a previous communication from this laboratory [11], the latter viewpoint was adopted and, subject to certain assumptions, the average number of residues between positions of cross-linking was calculated.

Studies of the interaction of keratin fibers and reagents which will cause supercontraction have not been confined to this phenomenon alone. In the case of the uptake of lithium bromide solutions by human hair, Barnard and White [3] investigated the resulting swelling; Barnard et al. [2] reported on the rate of uptake of solutions of different concentrations, the molarity of the reagent within the fibers, and a number of other factors.

In this paper observations relating to diffusion of lithium bromide solutions into wool are reported, together with swelling data and histological observations. In addition, supercontraction–time curves for various fibers in solutions at 89° and 100° C. are presented and discussed. It is shown that an equation can be derived which is consistent with the cross-linked polypeptide chain model of keratin and which fits these curves.

Experimental

All the work was done microscopically. Fiber snippets (0.5–2 mm. in length) or cross-sections (5–10μ in length) were immersed in the solution in a cell about 0.02 mm. deep and 2 cm. in diameter. To make this cell, a microscope coverglass was recessed into a stainless steel ring, and the ring sealed with silicone grease to a microscope slide. A small opening allowed for expansion of LiBr solution during experiments at elevated temperatures.

The stage heater which was constructed for the work at elevated temperatures is shown diagrammatically in Figure 1. This device was made of copper and, in use, was clipped to the existing microscope stage. Glass slides, with immersed fiber samples, could be slipped into channel A. The copper below this channel was about 1.5 mm. thick, so that a good approach to optimum illuminating conditions could be obtained with the standard microscope condenser. The mercury-in-glass thermom-

eter was calibrated according to temperature measurements made with a fine thermocouple mounted on a glass slide and placed in channel A.

For experiments on rates of contraction[1] at elevated temperatures, the heater was brought to the required temperature and a slide with immersed fiber snippets was placed in channel A at zero time. The full length of the snippets was measured. Fibers which remained straight during contraction were measured using an eye-piece scale. Fibers which curled were photographed at a number of times, and measurements were made on enlarged positives of these photographs. In all experiments, three snippets from the same fiber were mounted in the reagent. When wool was being studied it was usual for one or more of these to curl in such a way that its full length was not in focus. This was rare when kid mohair and human hair were used, and often all three snippets were measured during the course of an experiment.

Diameter measurements were made on fiber cross-sections.

Three concentrations of aqueous LiBr were used: 10.4 *M*, 8.3 *M*, and 6.3 *M*, corresponding respectively to the 125%, 100%, and 75% solutions used by Alexander [1]. The solutions were made up as described by Griffith and Alexander [8], any traces of bromine being removed by the addition of a small amount of sodium thiosulfate.

Modification of the fiber surface was produced by treatment in a solution of KOH (2 g.) in n-butanol (100 ml.) followed by neutralization in a solution of H_2SO_4 (1 ml.) in ethanol (100 ml.). The fibers were then washed in distilled water.

Fibers used were strong Merino wool, fine Corriedale wool, human hair, and kid mohair. The wool samples were from one fleece of each type. Samples of human hair and kid mohair were kindly provided by Dr. Menkart of the Textile Research Institute.

Results

Diffusion of LiBr into Wool at Room Temperature (14°–18° C)

Corriedale fiber cross-sections were immersed in each of the three solutions. In all cases, even with sections 5μ in length, penetrating fronts could be seen moving radially in a manner similar to that described by Haly [10] for the absorption of ethanolic KOH. This behavior suggests that axial diffusion of LiBr solution is relatively slow.

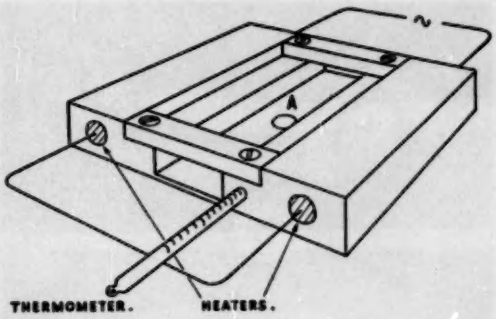

Fig. 1. Drawing of stage heater designed to receive 3 × 1 in. microscope slides.

When penetration was complete, orthocortical and paracortical segments could be distinguished. It was found that penetration radially through the orthocortex was faster than through the paracortex. The ratio of the rates was less than 2:1.

Penetrating fronts could be seen in fibers viewed in profile under ordinary conditions of transmitted light microscopy. However, with 10.4 *M* and 8.3 *M* solutions, fiber birefringence was almost completely destroyed as the reagent advanced, and the position and shape of the penetrating front could be seen with great clarity under the polarizing microscope. Figures 2 and 3 are photographs of fibers between polaroids just sufficiently rotated from the crossed position that the fiber outline was visible. The fiber in Figure 2b had been deliberately damaged at the position indicated.[2] Near the ends of the fibers of Figure 2 and on both sides of the damaged position, conical fronts developed. At other places penetration was not uniform, but began in localized areas; one such area is shown in Figure 2a.

The conical fronts are usually fully developed before penetration begins in other regions. This indicates that somewhere in the cuticle there is an important barrier to transfer of LiBr, and that penetration axially is considerably more rapid near the periphery of the fiber cortex, or between two cuticular components, than near the axis of the fiber.

Other workers (see, for instance, Lindberg [14, 15, 16] have concluded that the wool fiber epicuticle is a barrier to certain acids and dyes.

---

[1] For the sake of brevity "contraction" will be used henceforth instead of "supercontraction."

[2] The fiber was arranged on a flat surface at such a distance from a wire that when a razor blade made contact with the surface and wire a cut was made to a suitable depth in the fiber.

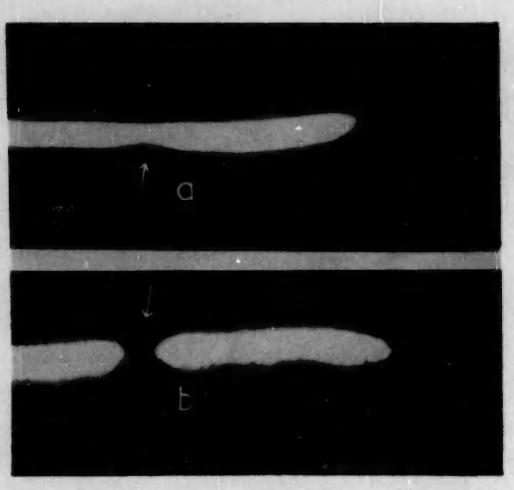

Fig. 2. Merino fibers in 8.3 *M* LiBr under the polarizing microscope. (a) shows conical front of penetrant at end of fiber, and a zone of "local" penetration indicated by the arrow. Immersion time: 300 min. (b) shows conical fronts at end and on both sides of a position of fiber damage. The damaged position is indicated by the arrow. Immersion time: 220 min.

In an attempt to determine whether or not this membrane was responsible in the present instance, fibers were cut in halves and half of each fiber treated with butanolic KOH as already described. The other half of each fiber was treated with ethanolic H_2SO_4 and water only. After 5 sec. in butanolic KOH, radial penetration of the LiBr solution was fairly uniform, whereas the fiber halves not pretreated in this way showed characteristic local penetration. Figure 3 is a photograph of a treated fiber after immersion in 8.3 *M* LiBr for the same time (220 min.) as the fiber of Figure 2b. Since butanolic KOH does not cause wool to swell to an appreciable extent in a number of days, its action in 5 sec. is probably confined very closely to the fiber surface. Hence it would appear that LiBr does not readily penetrate an undamaged wool fiber epicuticle. Increasing the time of pretreatment from a few seconds to 16 hr. appeared to increase the rate of absorption of LiBr only slightly.

The times required for complete penetration into Corriedale fibers (initial diameter about 35μ) pretreated with butanolic KOH for 16 hr. were: 10.4 *M*, 7–8 da.; 8.3 *M*, 5–7 hr.; and 6.3 *M*, 30–45 min. Corresponding times for penetration into sections about 20μ in length were shorter, presumably due to reaction at the cut ends of the sections and to the greater surface:volume ratio. However, the proportionality between the times was about the same.

Before appreciable LiBr penetration, the wool must lose or gain water to approach a regain corresponding to the water vapor pressure of the salt solutions. The approximate relative humidities over the solutions were: 10.4 *M*, 11%; 8.3 *M*, 29%; and 6.3 *M*, 46%. The corresponding wool regains are 5, 9, and 13%. Thus the process of LiBr penetration can be considered in terms of diffusion into wool at these regains. It is known [13] that the rate of diffusion of water through keratin increases very rapidly with increase of regain. The very slow diffusion of LiBr from highly concentrated solutions emphasizes the important effect of water content on accessibility.

Phenomena Resulting from LiBr Absorption at Room Temperature (14°–18° C.)

In a crimped wool fiber the orthocortex is on the outside of the crimp curve. When such a fiber is allowed to stand in 8.3 *M* or 10.4 *M* LiBr solution at 14–18° C., there is a contraction in length accompanied by curvature reversal; i.e., the fiber moves so that the orthocortex is on the inside of the curve. Curling begins before penetration is quite complete. Lengths were measured around both the outside and the inside of the curve. The average contraction of Merino wool fibers in each of the abovementioned solutions was $10 \pm 0.5\%$ of the initial length, but there was a considerable difference between the values obtained for the orthocortical and paracortical sides. For instance, in one case of a fiber in 8.3 *M* solution, the contraction measured around the orthocortical side was 16%, while that measured around the paracortical side was 4.5%. The length of fine Corriedale fibers, which curl during contraction, was reduced by approximately the same amount. Coarser Corriedale fibers did not curl appreciably, probably

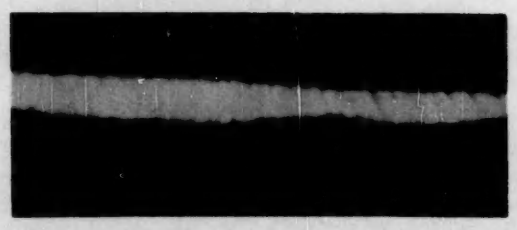

Fig. 3. Merino fiber pretreated with butanolic KOH and immersed in 8.3 *M* LiBr. Immersion time at this stage: 220 min. Magnification is twice that in Figure 2.

because of their radial cortical asymmetry, and their contraction was slightly less. There was no contraction, little or no loss of birefringence, and no curvature reversal in 6.3 *M* solution at room temperature. Human hair did not contract to an appreciable extent in any of the solutions. Its contraction, if any, was less than 1%.

Equilibrium diametral swellings of Corriedale fiber cross-sections were: 10.4 *M*, 35%; 8.3 *M*, 30%; and 6.3 *M*, 16%. These values are based on diameters after sufficient time had elapsed for the fiber regain to approximate standard regain at the relative humidity over the solutions.

Contracted fibers, whether the contraction has taken place at room temperature or at a higher temperature, exhibit cuticular corrugations. The number and depth of these corrugations increase as the amount of contraction increases. As is shown in Figure 4, the corrugations are approximately perpendicular to the fiber axis, do not cross scale edges, and do not form in the vicinity of the upper scale edge. They may have a depth of up to about 1μ, and are unchanged in appearance when viewed through either a chlorine or bromine Allworden bubble. This suggests that the corrugations are not confined to the epicuticle and exocuticle, but exist also in the endocuticle. The reason why they are not present near the upper scale edge may be that the plates of endocuticle overlap [7] in this region. The conclusion may be drawn that the wool fiber cuticle does not contract, but is forced into folds by the contracting cortex. If the cuticle is compelled to fold in this way, it is likely that the endocuticular plates remain firmly fused together and firmly attached to the cortex during the reaction.

All the visible changes in a fiber contracted at room temperature are reversed when it is washed in water. Birefringence, length, and curvature are restored, and the cuticular corrugations vanish. Birefringence is restored very rapidly, but no measure of the time taken was obtained.

Fig. 4. Micrograph of surface of Corriedale fiber contracted 35%, showing features of corrugations in cuticle. Gold-shadowed fiber.

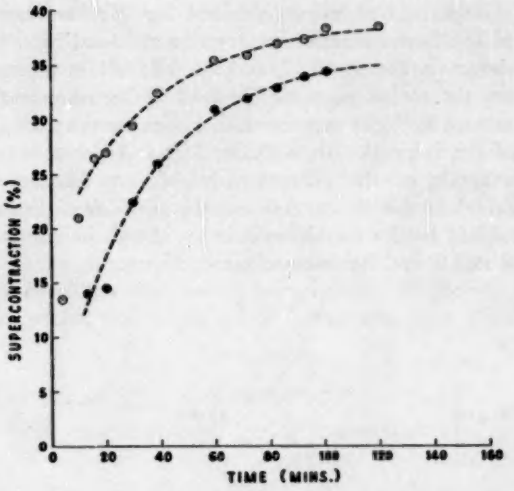

Fig. 5. Experimental results and curves calculated, using Equation 2, for contraction of two snippets from same Merino fiber, in 6.3 *M* LiBr at 89 ± 1° C.

Absorption of LiBr at 89° and 100° C.—Supercontraction

At temperatures up to 100° C. nonuniform (localized) penetration takes place in fibers whose surface has not been damaged, and radially moving fronts are seen in cross-sections. That there is a surface barrier to the penetration of the reagent at 89° C. is shown by Figure 6, which gives the supercontraction vs. time curves for a normal and a treated fiber in 8.3 *M* LiBr. Contraction of the normal fiber was at first delayed, but later the contraction rates of the two fibers were almost identical.

The error in the measurement of contraction in a single experiment is unlikely to exceed 1% contraction in the case of wool, and about 0.5% for kid mohair and human hair. However, temperature could be controlled only to ±1° C. at 89° C. and ±1.5° C. at 100° C.; the situation was complicated by differences in degree of contraction between snippets from the same fiber as well as between different fibers from the same sample. The magnitude of these differences will be indicated later. When two fibers were to be compared directly, snippets from the two fibers were immersed on the same slide. It was then certain that the snippets were being treated under identical conditions.

Experimental points obtained for Merino fibers of 25–30μ dry diameter contracting at 89 ± 1° C. are shown in Figures 5, 6, and 7. The values plotted are the means of those obtained by measurements around both the orthocortical and paracortical sides of the snippets. In addition, Figure 7 presents an example of the differences which are frequently found in the contractions on the two sides. Some typical results for kid mohair are shown in Figures 8 and 9, and for human hair in Figure 10.

Wool, kid mohair, and human hair exhibited an early rapid contraction which began just before the fibers were completely penetrated by the reagent. This stage, once begun, was completed so rapidly that often no experimental points were obtained (see Figure 9). The time at which it began varied with fiber diameter and the state of the epicuticle, and was considerably reduced in fibers pretreated with butanolic KOH. There followed an intermediate period (best seen in C and D of Figure 9 and C of Figure 10) during which little or no contraction took place. A second contraction stage ensued, the rate of contraction at first increasing and finally decreasing as equilibrium was approached.

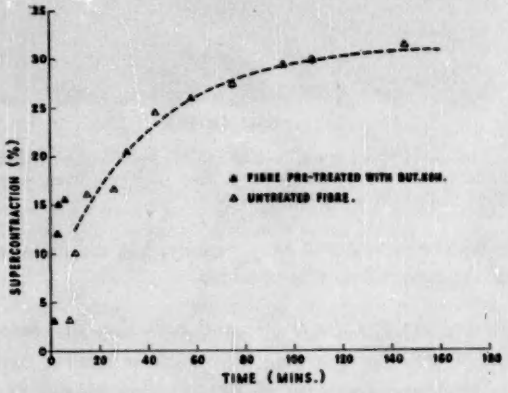

Fig. 6. Experimental results and curve calculated, using Equation 2, for a Merino fiber contracting at 89 ± 1° C. in 8.3 *M* LiBr.

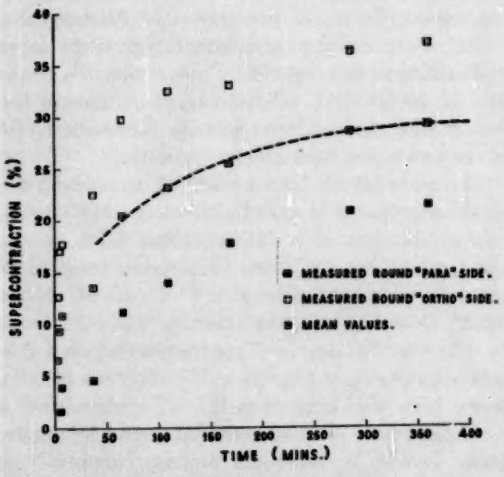

Fig. 7. Experimental results and curve calculated, using Equation 2, for a Merino fiber contracting at 89 ± 1° C. in 10.4 *M* LiBr, showing differences between measurements around orthocortical and paracortical sides.

Equilibrium contractions at 89° C. of different snippets from the same wool fiber may differ as much as 3–4%. The experimental points for two snippets from the same fiber mounted side by side on the same slide are shown in Figure 5; differences in degree of contraction are apparent at a relatively small value of time, after which the curves remain approximately parallel. A very noticeable difference in the behavior of these two snippets was that the one yielding the lower final contraction curled to a much greater extent than the other. In the case of wool, such phenomena often seemed to be associated with the amount of curling that took place, but similar differences have been found in kid mohair fibers (C and D of Figure 9), which do not curl to an appreciable extent during contraction. Furthermore, in the case of kid mohair considerable interfiber differences were found. Experiments were done with ten different fibers, and the results fell into two groups. In one group (fibers referred to as type F) the range of intermediate stage contraction was 15–19% and that of equilibrium contraction was 40–44%. In the other group (referred to as

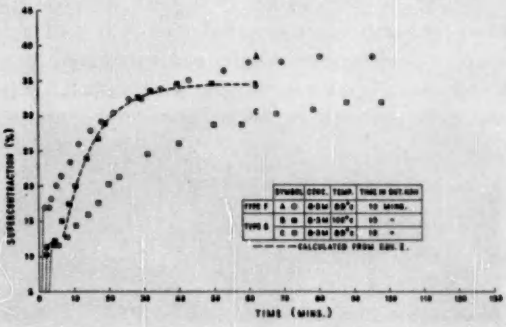

Fig. 8. Experimental results for two types of kid mohair fibers contracting under the conditions shown on the figure. Curve B was calculated using Equation 2.

type S) the intermediate stage contraction was 10–12% and the equilibrium contraction was approximately 35%. These results suggest the presence of two fairly distinct kinds of fibers in the kid mohair sample, but it is possible that further work would reveal a continuous variation between the values quoted. Typical curves are shown in Figure 8, A and C being obtained in one experiment. Curve B of Figure 8 is included to show that the degree of contraction at the intermediate stage was unaffected by a temperature increase from 89° to 100° C. Snippets from the same fiber yielded the results B and C.

Interfiber and intrafiber variations among fibers from the same sample may be caused by differences in the arrangement of the two cortical segments and by differences in the ortho- to paracortex ratio. It is noteworthy that agreement between results for different human hairs from the same head was very good; this may be construed as evidence in support of the deduction of Dusenbury and Jeffries [5] that human hair has only one type of cortical cell.

The degree of contraction achieved by human hair both at the intermediate stage and at equilibrium was much less than for either wool or kid mohair. It was similar to that measured on the paracortical side of a wool snippet which curled strongly during contraction. Since the cortex of human hair is considered to be analogous to wool paracortex [5], this result might have been anticipated.

The necessity to guard against anomalous contraction behavior should be stressed. The effect of traces of bromine in the lithium bromide solutions has been reported [8]. In addition, we have observed that fibers which were allowed to stand in lithium bromide solutions at room temperature for a number of days, when subsequently contracted in the same solution at 89° C., appeared to reach a low equilibrium degree of contraction. The rate of contraction in the latter part of these experiments was extremely slow. Similar behavior was occasionally found in an ordinary contraction experiment, but it was impossible to determine whether or not in this case the cause was some unusual variation in the keratin material.

Discussion

Swelling at Room Temperature

The diametral swellings of Corriedale fibers in LiBr solutions at room temperature are shown in Table I. Values based on the water-saturated diameter of the fibers were calculated from these using the relation

$$S = \frac{(1 + s_c)(1 + s_r)}{1 + s_w} - 1$$

where S = diameter swelling based on water-saturated diameter, s_c = measured diameter swelling quoted in Table I, s_r = diameter swelling, based on the dry diameter, of fibers at the standard regain corresponding to the relative humidity over the solutions, and s_w = diameter swelling, based on the dry diameter, of fibers when saturated with water.

Barnard and White [3] have published figures for the volume swelling based on the water-saturated volume of human hair in various LiBr solutions. For comparison with these, the approximate volume

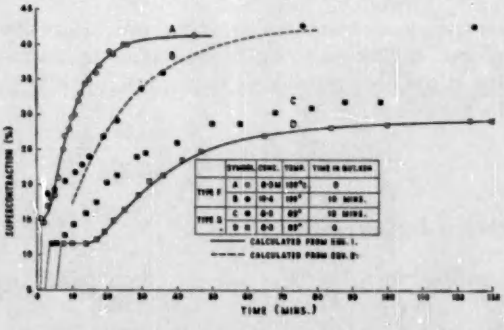

Fig. 9. Experimental results for two types of kid mohair fibers contracting under the conditions shown on the figure. Curves A and D were calculated using Equation 1; the dashed curve B was calculated using Equation 2.

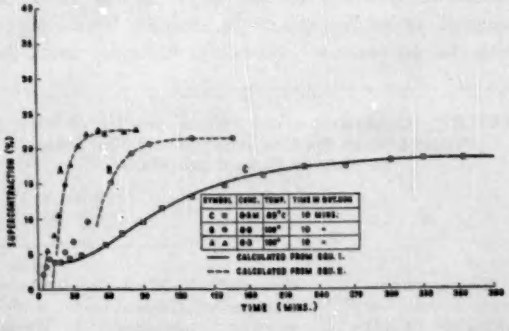

Fig. 10. Experimental results and calculated curve for human hair contracting under the conditions shown on the figure. Curve C was calculated using Equation 1; the dashed curves A and B were calculated using Equation 2.

swelling of wool can be computed from the diametral swelling and the longitudinal contraction, assuming that the fibers are cylindrical. This volume swelling is given by

$$\frac{V - V_w}{V_w} = 2S + S^2 - C(1 + S)^2$$

where C = contraction based on initial length and V_w = water-saturated volume.

A comparison between the present results and those of Barnard and White, for the hair which gave greater swelling, is shown in Table I.

Agreement is excellent. This was not expected in the case of the more concentrated solutions since, under the present temperature conditions, 7–8 days were required for wool of 35μ diameter to be completely penetrated by 10.4 M LiBr, and the time required by the coarser hair was greater. It had seemed unlikely that Barnard and White allowed a sufficiently long time of immersion.

Supercontraction

Assuming keratin to be made up of polypeptide chains stabilized by disulfide cross-linkages and by a large number of weaker linkages, a complete contraction curve can be explained in a manner somewhat similar to that previously reported [9].

Since in the case of wool a temperature of no more than 18° C. is sufficient to cause two-thirds of the total contraction achievable in the first stage, this part of the contraction probably results from the action of the reagent on weak secondary bonds. This stage of contraction can be completely reversed by washing the fibers in water, whereas if contraction proceeds beyond the first stage complete recovery cannot be obtained in this way. Before the final stage of contraction can begin, stronger bonds, which may be cooperative secondary linkages, must be broken. The intermediate stage of little or no shortening continues until a sufficient number of these are destroyed for the mechanical resistance of the remainder to be overcome. When this condition is satisfied, the final stage begins and the rate of contraction increases as more and more of these linkages are broken. The rate reaches a maximum for the stage, and then necessarily becomes less as equilibrium is approached.

TABLE I. Comparison of the Volume Swelling of Wool in Various Lithium Bromide Solutions with That Found for Hair by Barnard and White

Concentration		Measured diameter swelling	$\frac{(V - V_w)}{V_w} \times 100$	
Molarity	Molality		Wool (present results)	Hair (Barnard and White)
6.3	7.6	16	12	13
8.3	10.7	30	23	25
10.4	14.5	35	28	28

In terms of this model, an attempt can be made to develop a mathematical description of the final contraction stage. It will be assumed that the intermediate stage has been completed, and that at this time the fiber is made up of n_0 constrained, contractile elements in series. Suppose these elements are freed at a rate given by

$$\frac{dn}{dt} = k_1 n$$

where n is the number of constrained elements at time t and k_1 is a constant for a particular material, solution concentration, and temperature. By integration we find that the number of free elements at time t is $n_0(1 - e^{-k_1 t})$. The maximum percentage contraction the fibers can achieve with this number of free elements is $(1 - e^{-k_1 t})C_e$, where C_e is the maximum percentage contraction of an element. (C_e is also the maximum percentage contraction of the fiber.)

Now suppose that the rate of contraction of the fiber is proportional to the amount of contraction which would remain to take place if no more contractile elements were freed after time t; i.e.,

$$\frac{dC}{dt} = k_2(C_m - C)$$

where k_2 = a constant, C = actual percentage contraction at time t, and C_m = the maximum contraction of the fiber possible at time t, = $(1 - e^{-k_1 t})C_e$. We then have

$$\frac{dC}{dt} = k_2 C_e(1 - e^{-k_1 t}) - k_2 C$$

whence, by integration,

$$\frac{C_e - C}{C_e} = \frac{k_2}{k_2 - k_1} e^{-k_1 t} - \frac{k_1}{k_2 - k_1} e^{-k_2 t} \quad (1)$$

To evaluate k_1 and k_2 by reference to experimental supercontraction–time curves, it was assumed that at relatively large values of time a

negligible number of contractile elements were constrained, so that $e^{-k_1 t}$ was small and the above equation became

$$\frac{C_e - C}{C_e} = -\frac{k_1}{k_2 - k_1} e^{-k_2 t} \qquad (2)$$

The slope of the plot of $\ln\left(\frac{C_e - C}{C_e}\right)$ against large values of t then gave k_2, and k_1 was found by trial, using in the complete equation an experimental value of C at a smaller value of t. Supercontraction–time curves over the range from the intermediate stage to final equilibrium were then calculated. Graphs A and D of Figure 9 show the comparison between experimental points for kid mohair and curves calculated from Equation 1. In the case of A, $k_1 = 0.6$ and $k_2 = 0.13$, while in D, $k_1 = 0.3$ and $k_2 = 0.04$. A similar comparison for human hair is given in curve C of Figure 10. In this case $k_1 = 0.03$ and $k_2 = 0.014$. The curves fit the data within the degree of accuracy of measurement. In general the fit seemed to be better when contraction was done at 100° C. than at 89° C. This is perhaps not surprising, since equilibrium contraction is lower at 89° than at 100°.

Analyses of this kind showed that the first term on the right hand side of Equation 1 became negligible at approximately the region of maximum slope in the final contraction stage. Furthermore, with fibers of one type the value of k_1 varied considerably from fiber to fiber, while that of k_2 showed little interfiber variation. In other words, the shape of a curve from the region of maximum slope to equilibrium was approximately constant for a particular fiber type, solution concentration, and temperature. Furthermore, it should be noted that, in the case of crimped wool, the value of k_2 was the same when measurements were made on the orthocortical side, the paracortical side, or when the mean of these two measurements was used. It therefore seemed most useful to evaluate k_2 by fitting Equation 2 to the latter part of the various contraction–time curves. The dashed curves of Figures 5–10 were calculated from Equation 2; values of k_2 which were used in both equations are shown in Table II.

For the LiBr concentrations used, k_2 increased as the concentration decreased; it was of interest to determine what function of concentration was important. It was found that in all cases the proportionality between the values of k_2 was not very different from the proportionality between the relative humidities at room temperature of the solutions. (Both relative humidities and values of k_2 may be in error by about ±5%.) The comparison between proportionalities is shown in Table II. That there should be a correlation between the rate of contraction and the relative humidity of the reagent might have been expected, since it is probable that the greater the free energy of water in the wool–lithium bromide system, the less will be the viscosity of the system; i.e., the less will be the cohesion between molecular chains.

Activation energies were estimated from the values

TABLE II. Values of k_2 Under Various Experimental Conditions, and a Comparison of the Proportionality Between k_2 Values and Between Corresponding Values of the R.H. of the LiBr Solutions

Fiber	LiBr concentration, M	R.H. over solution at 20° C.	Temp., ° C.	k_2	Proportionalities	
					R.H.	k_2
Merino wool	6.3	46	89	0.030	4.2 : 2.6 : 1	3.8 : 3.0 : 1
	8.3	29	89	0.024		
	10.4	11	89	0.008		
Hair	6.3	46	100	0.104	4.2 : 2.6	4.7 : 2.6
	8.3	29	100	0.057		
	8.3	29	89	0.014		
Kid mohair (Type F)	8.3	29	100	0.13	2.6 : 1	2.5 : 1
	10.4	11	100	0.053		
	8.3	29	89	0.047		
Kid mohair (Type S)	8.3	29	100	0.11		
	8.3	29	89	0.038		
	8.3	29	89	0.040		

of k_2 at 89° C. and 100° C., the values being 34 kcal./mol. for human hair and 25 kcal./mol. for kid mohair. These values are only approximate because of the small temperature range studied and because of lack of precision in temperature measurement. However, activation energy did not appear to be a function of the concentration of the LiBr solution. In the only case in which experiments were done using wool, kid mohair, and human hair under the same conditions of concentration and temperature (8.3 *M* LiBr at 89°), k_2 for wool was intermediate between k_2 for kid mohair and k_2 for human hair.

Conclusions

1. The wool fiber epicuticle is an important barrier to the penetration of LiBr solution into the fiber.

2. Axial diffusion of LiBr solution is slower than radial diffusion. Axial diffusion is considerably more rapid near the fiber periphery than near its axis.

3. Supercontraction of the fiber cuticle is negligible.

4. Snippets of fibers with a bilaterally asymmetric cortex curl during contraction because of greater and faster contraction in the orthocortex than in the paracortex. Snippets of fibers with a radially asymmetric cortex do not curl to an appreciable extent, but their degree of contraction is probably between the degrees of contraction which would be reached under the same conditions by the orthocortical segment and by the paracortical segment. Intra- and interfiber variation in degree of contraction of fibers from the same sample may well result from variations in the arrangement of the two segments and from differences in the ortho- to paracortex ratio.

5. Supercontraction at 89° C. and at 100° C. takes place in two distinct stages, separated by an intermediate period during which little or no contraction takes place. The first contraction stage probably results from the breakdown of weak secondary bonds.

6. The second contraction stage is well represented by an equation derived from a simple model. Rate constants, obtained by fitting this equation to experimental curves, show that there is a strong correlation between rates of contraction in the second stage and the relative humidity over the LiBr solution.

Acknowledgments

The authors wish to thank Professor A. E. Alexander for his interest in this work.

Literature Cited

1. Alexander, P., *Ann. N.Y. Acad. Sci.* **53**, 653 (1951).
2. Barnard, W. S., Palm, A., Stam, P. B., Underwood, D. L., and White, H. J., TEXTILE RESEARCH JOURNAL **24**, 863 (1954).
3. Barnard, W. S. and White, H. J., TEXTILE RESEARCH JOURNAL **24**, 695 (1954).
4. Carter, E. G. H., Middlebrook, W. R., and Phillips, H., *J. Soc. Dyers Colourists* **62**, 203 (1946).
5. Dusenbury, J. H. and Jeffries, E. B., *J. Soc. Cosmetic Chemists* **6**, 355 (1955).
6. Elöd, E. and Zahn, H., *Melliand Textilber.* **30**, 17 (1949).
7. Fraser, R. D. B. and Rogers, G. E., *Biochim. et Biophys. Acta* **16**, 307 (1955).
8. Griffith, June and Alexander, A. E., *Chem. and Ind.* **47**, 1424 (1956).
9. Griffith, June and Alexander, A. E., TEXTILE RESEARCH JOURNAL **27**, 755 (1957).
10. Haly, A. R., TEXTILE RESEARCH JOURNAL **27**, 82 (1957).
11. Haly, A. R. and Feughelman, M., TEXTILE RESEARCH JOURNAL **27**, 919 (1957).
12. Jeffrey, G. M., Sikorski, J., and Woods, H. J., TEXTILE RESEARCH JOURNAL **25**, 714 (1955).
13. King, G., *Trans. Faraday Soc.* **41**, 479 (1945).
14. Lindberg, J., TEXTILE RESEARCH JOURNAL **23**, 67 (1953).
15. Lindberg, J., TEXTILE RESEARCH JOURNAL **23**, 225 (1953).
16. Lindberg, J., TEXTILE RESEARCH JOURNAL **23**, 573 (1953).

Manuscript received July 22, 1957.

of k_2 at 89° C. and 100° C., the values being 34 kcal./mol. for human hair and 25 kcal./mol. for kid mohair. These values are only approximate because of the small temperature range studied and because of lack of precision in temperature measurement. However, activation energy did not appear to be a function of the concentration of the LiBr solution. In the only case in which experiments were done using wool, kid mohair, and human hair under the same conditions of concentration and temperature (8.3 *M* LiBr at 89°), k_2 for wool was intermediate between k_2 for kid mohair and k_2 for human hair.

Conclusions

1. The wool fiber epicuticle is an important barrier to the penetration of LiBr solution into the fiber.

2. Axial diffusion of LiBr solution is slower than radial diffusion. Axial diffusion is considerably more rapid near the fiber periphery than near its axis.

3. Supercontraction of the fiber cuticle is negligible.

4. Snippets of fibers with a bilaterally asymmetric cortex curl during contraction because of greater and faster contraction in the orthocortex than in the paracortex. Snippets of fibers with a radially asymmetric cortex do not curl to an appreciable extent, but their degree of contraction is probably between the degrees of contraction which would be reached under the same conditions by the orthocortical segment and by the paracortical segment. Intra- and interfiber variation in degree of contraction of fibers from the same sample may well result from variations in the arrangement of the two segments and from differences in the ortho- to paracortex ratio.

5. Supercontraction at 89° C. and at 100° C. takes place in two distinct stages, separated by an intermediate period during which little or no contraction takes place. The first contraction stage probably results from the breakdown of weak secondary bonds.

6. The second contraction stage is well represented by an equation derived from a simple model. Rate constants, obtained by fitting this equation to experimental curves, show that there is a strong correlation between rates of contraction in the second stage and the relative humidity over the LiBr solution.

Acknowledgments

The authors wish to thank Professor A. E. Alexander for his interest in this work.

Literature Cited

1. Alexander, P., *Ann. N.Y. Acad. Sci.* **53**, 653 (1951).
2. Barnard, W. S., Palm, A., Stam, P. B., Underwood, D. L., and White, H. J., TEXTILE RESEARCH JOURNAL **24**, 863 (1954).
3. Barnard, W. S. and White, H. J., TEXTILE RESEARCH JOURNAL **24**, 695 (1954).
4. Carter, E. G. H., Middlebrook, W. R., and Phillips, H., *J. Soc. Dyers Colourists* **62**, 203 (1946).
5. Dusenbury, J. H. and Jeffries, E. B., *J. Soc. Cosmetic Chemists* **6**, 355 (1955).
6. Elöd, E. and Zahn, H., *Melliand Textilber.* **30**, 17 (1949).
7. Fraser, R. D. B. and Rogers, G. E., *Biochim. et Biophys. Acta* **16**, 307 (1955).
8. Griffith, June and Alexander, A. E., *Chem. and Ind.* **47**, 1424 (1956).
9. Griffith, June and Alexander, A. E., TEXTILE RESEARCH JOURNAL **27**, 755 (1957).
10. Haly, A. R., TEXTILE RESEARCH JOURNAL **27**, 82 (1957).
11. Haly, A. R. and Feughelman, M., TEXTILE RESEARCH JOURNAL **27**, 919 (1957).
12. Jeffrey, G. M., Sikorski, J., and Woods, H. J., TEXTILE RESEARCH JOURNAL **25**, 714 (1955).
13. King, G., *Trans. Faraday Soc.* **41**, 479 (1945).
14. Lindberg, J., TEXTILE RESEARCH JOURNAL **23**, 67 (1953).
15. Lindberg, J., TEXTILE RESEARCH JOURNAL **23**, 225 (1953).
16. Lindberg, J., TEXTILE RESEARCH JOURNAL **23**, 573 (1953).

Manuscript received July 22, 1957.

Compressional and Absorptive Behavior of Bulk Fiber Systems[1]

Irvin M. Gottlieb, Helmut Wakeham[2], and Hester M. Virgin[3]

Textile Research Institute, Princeton, N. J.

Abstract

Methods are presented for the determination of (a) the interfiber volume of fibers in bulk form when immersed under pressure in water, and (b) the volume of water which can be absorbed by systems of initially dry fibers at various pressures. Data are given for acetate, Acrilan, cotton, Dacron[4], glass, Fortisan, nylon, Orlon[4], ramie, silk, Vicara, vicuna, and viscose rayon.

Introduction

The objective of this study was to develop methods for the evaluation of two characteristics of bulk fiber systems. One method would permit the determination of the interfiber volume of fiber systems immersed under pressure in water, and the other, the determination of the volume of water which could be taken up by a system of initially dry fibers at various pressures. No attempt was made to distinguish between the water taken up by swelling of the fibers and that taken up by filling the interstices between the fibers.

The natural, synthetic, derivative, and regenerated fiber types included in this research represented commercially available materials and were indicative of industrial production (Table I). The materials were available in bulk form. The staple length of the various fiber types was approximately 1.5 in. The denier of most of the manmade fibers was 1.5, with the following exceptions: Orlon—3 den., Acrilan and Vicara—2 den., and Fortisan—0.58 den. The samples of the natural fibers were selected so as to approach as closely as feasible the requirements of 1.5 in. staple length and 1.5 den. Therefore, vicuna was chosen to represent the wool-like fibers. The characteristics of the glass fiber differed somewhat. A commercially available material with a diameter of 6μ was the nearest approach to the denier requirement obtainable. The calculated value for its denier was 0.9.

Apparatus

The apparatus used to measure the compressional behavior of bulk fiber systems when immersed under pressure in water (Figure 1) consisted of a clear plastic cylindrical chamber 1.65 in. in internal diameter and 8 in. in height, which could be mounted on the crosshead of an Instron tensile tester. This chamber held the fibers and the water. For the application of pressure a piston-plunger arrangement which fitted into the chamber was attached to the load sensing cell of the Instron tensile tester through a 14-lb. brass dead weight. The head of the piston consisted of a disc of plastic 1.56 in. in diameter which yielded a surface area of 1.92 sq. in. The disc was perforated with holes $\frac{1}{16}$ in. in diameter, randomly spaced to allow for the unrestricted passage of the water through the fiber systems. Clearance was provided between the edge of the piston head and the walls of the chamber in order to permit frictionless operation and to eliminate edge effects.

A second plastic cylindrical chamber of similar dimensions was constructed to measure the uptake of water by fiber systems under pressure (Figure 2). The chamber was divided into two segments by a perforated plastic disc. The smaller, bottom compartment, approximately $1\frac{3}{8}$ in. in height, functioned to provide the liquid surface and to serve as a liquid reservoir, and was connected to the source of supply of water in an auxiliary tube. The larger, upper segment of the chamber contained the fiber systems under pressure, which was applied by means of the piston-plunger attachment previously described.

---

[1] This paper was presented at a meeting of The Fiber Society, Clemson, South Carolina, May 1, 1957.

[2] Present address: Ahmedabad Textile Industry's Research Association, Ahmedabad 9, India.

[3] Present address: Princeton, New Jersey.

[4] Du Pont trademark.

A mechanical cotton blender similar to that developed by the U. S. Department of Agriculture [1] was used to prepare the systems of fibers.

Although the equipment can be used with any liquid, in the experiments to be reported an 0.055% (by weight) solution of Ultrawet 30 DS surfactant prepared in distilled water was used exclusively. Ultrawet 30 DS is essentially a medium molecular weight alkyl aryl sulfonate and is manufactured by the Atlantic Refining Company, Philadelphia, Pennsylvania. The surface tension of the solution was approximately 35 dynes/cm.

TABLE I. Description of Fiber Types

Fiber	Description	Classification	Density (g./cc.)*
Acetate	1.5 den. 1½ in. bright staple	derivative-cellulosic	1.33
Acrilan	2 den., 1 9/16 in. semidull staple	synthetic-acrylic	1.14
Cotton	cotton roving kier boiled carded, twisted	natural-cellulosic	1.55
Dacron	1½ in. type 5400 semidull staple 1.5, 3.0, 4.5, 6.0 den.	synthetic-polyester	1.38
Fortisan	0.58 den., 1½ in. carded sliver form	regenerated-cellulosic	1.52
Glass	Pyrex brand wool filtering fiber	synthetic-inorganic	2.56
Nylon	1.5 den., 1½ in. type 200 semidull staple	synthetic-polyamide	1.14
Orlon	3 den., 1½ in. type 42 semidull staple	synthetic-acrylic	1.17
Ramie	sliver	natural-cellulosic	1.51
Silk	silk noils from combing silk Peigree	natural-protein	1.35
Vicara	2 den., 1½–2 in. bright, natural staple	synthetic-protein	1.25
Vicuna	Peruvian vicuna roving-130's yarn	natural-protein	1.32
Viscose rayon	1.5 den., 1 9/16 in. bright staple, high tenacity, viscose 32	regenerated-cellulosic	1.53

* Harris, M., "Handbook of Textile Fibers," 1st Ed., Harris Research Laboratories, Inc., Washington, D. C. (1954).

Procedures

To provide a common basis for the analysis of the data, it was necessary to select either a constant weight or a constant volume of solid fiber substance. Since the effects to be studied were more closely related to volume, a constant volume of 1 cc. (0.06 cu. in.) of solid fiber substance was used. If the weight in grams of solid fiber substance was equal to the numerical value for its density (Table I), the volume of the material would be equal to 1 cc., or 0.06 cu. in. Fiber samples were made into loose battings in the blender, cut into the shape of cylindrical biscuits, and weighed to the requisite amounts.

Two experimental procedures were designed: one to measure the compressional behavior of fiber systems when wet, and the other to measure the amount

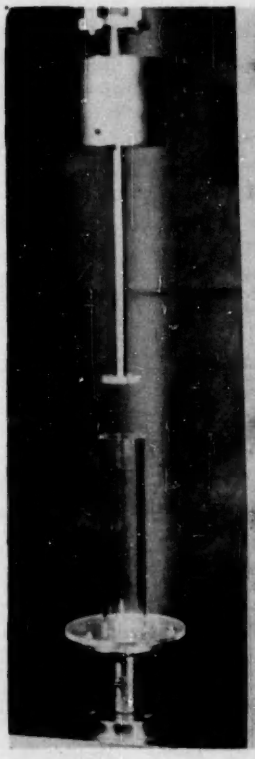

Fig. 1. Apparatus for the determination of interfiber volume.

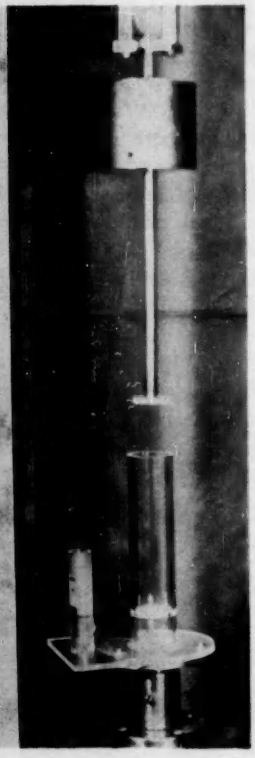

Fig. 2. Apparatus for the determination of fiber system absorptivity.

of water systems of initially dry fibers could absorb from a liquid surface. Dry refers to the equilibrium state at 65% RH, 70° F., approached from the dry side.

Procedure for the Determination of Interfiber Volume

a. The weighed fiber sample was placed in the cylinder of the first apparatus (Figure 1).

b. A volume of water sufficient to saturate completely and to cover the fibers was carefully poured down the walls of the cylinder while allowing for the gradual release of entrapped air bubbles and without disturbing the material.

c. Pressure was applied to the fiber system by moving the crosshead of the Instron tensile tester upward against the piston head atached to the load sensing cell through a dead weight.

d. The height of the specimen under the piston at various pressures was read from the dials of the Instron tensile tester. The bulk volume (cu. in.) of the material is the product of the piston area (1.92 sq. in.) and the piston height h (in.) above the bottom of the cylinder. The interfiber volume was obtained by subtracting the volume occupied by the solid dry fibers (0.06 cu. in.) from the observed bulk volume: $(1.92h)-(0.06)$. The data represent averages of three independent determinations.

Procedure for the Determination of Fiber System Absorptivity

a. The weighed dry sample was placed on the perforated inner disc in the cylinder of the second apparatus (Figure 2).

b. The crosshead of the Instron tensile tester was then allowed to ascend; the piston head entered the chamber and compressed the fibers. The pressure exerted by the fiber systems decreased with time due to relaxation phenomena; therefore, it was necessary to allow an equilibrium to be reached.

c. Water was introduced into the bottom compartment of the main cylinder through the auxiliary tube from a buret. The height of the water in the auxiliary tube was maintained equal to the top surface of the supporting perforated disc in the main cylinder. As the system of fibers absorbed water, the height of this column of water dropped. An additional quantity of water was added by titration from a buret in order to restore the system until no water was absorbed further and the height of the water remained constant in the auxiliary tube. The volume of water added was equal to the volume of water absorbed by the system of fibers.

d. The bulk volume of the dry fiber system was determined as previously described. The bulk density of the dry fiber system was calculated from this value and from the weight of dry fibers.

e. All curves shown (Figures 4, 5, and 6) represent the data obtained at at least six points.

The load cell "C" of the Instron tensile tester was used at a 20-lb. full-scale range to measure pressure changes. The crosshead speed was 0.2 in./min.

Observations and Results

Figure 3 illustrates the effect of pressure on the interfiber volume of systems of various fibers in water. Interfiber volume is defined as the air space between the individual fibers of 1 cc. solid dry fiber substance. If the pressure becomes infinitely high,

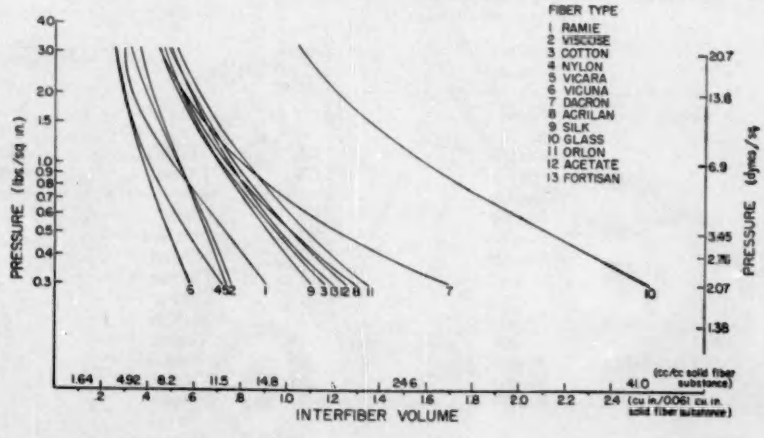

Fig. 3. Effect of pressure on interfiber volume.

thereby eliminating the space between the individual fibers and causing a compression of the fiber substance into a solid mass, the fiber material would occupy a volume of 1 cc., or 0.06 cu. in. The curves of Figure 3, therefore, at very high (extrapolated) pressures tend to approach zero for the interfiber volume of all the fiber types.

The fibers studied can be divided into three groups. For example, at a pressure of 3.0 p.s.i. the glass fiber displays the largest interfiber volume—17 cc./cc. solid fiber substance—and should be considered in a group by itself. The second group—Dacron, Orlon, Fortisan, Acrilan, acetate, cotton, and silk—has an interfiber volume of approximately 8 cc./cc. solid fiber type. The third group—ramie, viscose, Vicara, nylon, and vicuna—has an interfiber volume of approximately 5 cc./cc. solid fiber type.

At lower pressures these groupings are still maintained, but individual differences within a group become more pronounced. Table II shows the interfiber volume for each of the fibers studied at a pressure of 0.30 p.s.i.

To obtain an interfiber volume of 10 cc., various pressures are required for the different fibers. These values are listed in Table III. The fibers may again be divided into three groups. The glass fiber, in a group by itself, requires a pressure in excess of 13 p.s.i. The remaining fiber types range in value from 2.1 p.s.i. for Orlon to 0.27 p.s.i. for vicuna. The second group—cotton, silk, Acrilan, Dacron, Fortisan, acetate, and Orlon—has a value of approximately 1.7 p.s.i. The third group—vicuna, nylon, Vicara, viscose, and ramie—has a value of approximately 0.55 p.s.i.

The fiber systems of ramie, Acrilan, and silk did not absorb water. The volume of water absorbed by the nylon system was small compared to that of the other systems of fibers. It should be noted that the data are applicable only to the particular samples herein tested.

As shown in Figure 4, the systems of the other fiber types appear to exhibit a common pattern of water uptake. As the dry bulk volume increases, the volume of water absorbed into the system also increases, but only to a maximum value characteristic of the fiber type. The corresponding bulk volume is the "optimum dry bulk volume" for that fiber type. The volume of water taken up at this point for the various fiber types studied is given in Table IV. Beyond this point the volume of water ab-

TABLE II. Interfiber Volume
(Pressure = 0.30 p.s.i.)

	Fiber type	Volume (cc./cc. of solid fiber substance)
Group I	Glass	41.8
	Silk	18.1
	Cotton	18.9
	Fortisan	19.0
Group II	Acetate	20.2
	Acrilan	21.0
	Orlon	24.8
	Dacron	27.9
	Vicuna	9.4
	Nylon	11.6
Group III	Vicara	12.0
	Viscose	12.3
	Ramie	14.7

TABLE III. Pressure Required to Obtain Interfiber Volume of 10 cc.

	Fiber type	Pressure (p.s.i.)
Group I	Glass	>13
	Cotton	1.4
	Silk	1.5
	Acrilan	1.5
Group II	Dacron	1.6
	Fortisan	1.7
	Acetate	1.9
	Orlon	2.1
	Vicuna	.27
	Nylon	.43
Group III	Vicara	.63
	Viscose	.68
	Ramie	.73

TABLE IV. Maximum Water Uptake

Fiber type	Maximum water absorbed (cc./cc. of fiber)	Optimum dry bulk volume value for maximum water uptake (cc./cc. of solid fiber substance)
Glass	29	31.5
Fortisan	25	32.0
Viscose	24	>35.0
Dacron	23	24.2
Cotton	23	22.0
Acetate	22	23.6
Vicara	17	20.8
Orlon	17	14.8
Vicuna	14	14.8
Nylon	4	28.3

sorbed decreases. A tendency exists for systems of the fibers which absorb water to group together at low dry bulk volumes. Apparently, equal volumes of water are taken up. It is only after the optimum dry bulk volume is reached that differences are manifested, depending upon the physical, chemical, and surface characteristics of the fibers. At dry bulk volumes greater than the optimum, the distance between adjacent fibers may be too large for the maximum rise of water to occur. At the optimum point, the maximum rise takes place. As the pressure is increased, the dry bulk volume of the system decreases because of the collapse of the capillary tube system. This phenomenon can be observed when a fiber at a dry bulk volume greater than the optimum value, which has absorbed water, is subjected to increasing pressure. As the pressure is increased, the water level in the auxiliary tube of the apparatus (Figure 2) will fall, indicating that additional liquid is being taken up by the system. As an example illustrating this phenomenon, the data for vicuna are shown in Table V.

When water is absorbed by a system of initially dry fibers, there is a loss in pressure at constant bulk volume. The loss in pressure has been related by Preston and Nimkar [2] to a swelling of fibers in water and a change in the mechanical properties of the fibers in going from the dry to the wet state.

TABLE V. Relation Between Bulk Volume and Volume of Water Absorbed by the Vicuna System

Bulk volume (cc. total volume for 1 cc. solid fiber substance)	Volume water absorbed (cc. water/cc. of solid fiber substance)
4.7	5.2
9.4	7.6
12.2	13
15.8	8.0
17.3	4.7
18.9	2.5

TABLE VI. Loss in Pressure at Constant Volume Due to Wetting

Fiber type	Loss in pressure (%)
Vicara	81
Acetate	70
Cotton	66
Fortisan	63
Viscose	56
Vicuna	31
Orlon	6
Acrilan	5
Glass	5
Nylon	2
Dacron	2

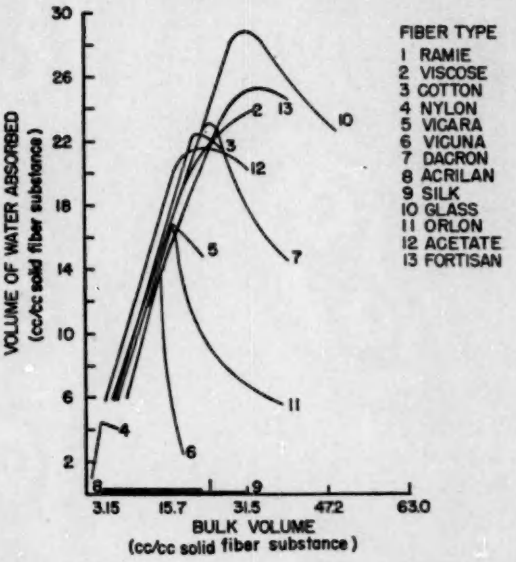

Fig. 4. Effect of bulk volume on fiber system absorptivity.

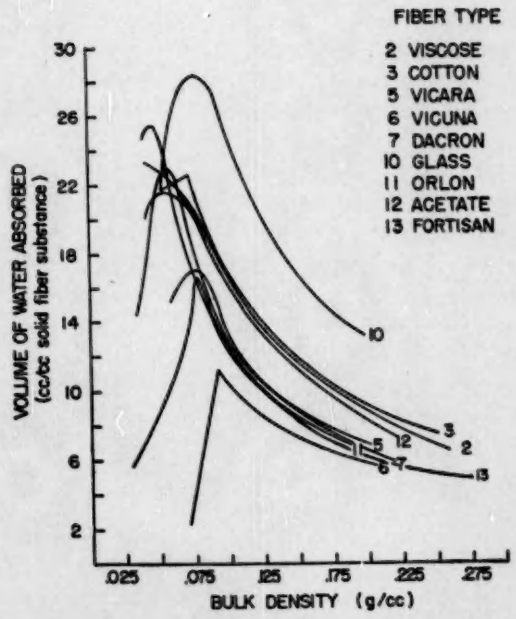

Fig. 5. Effect of bulk density on fiber system absorptivity.

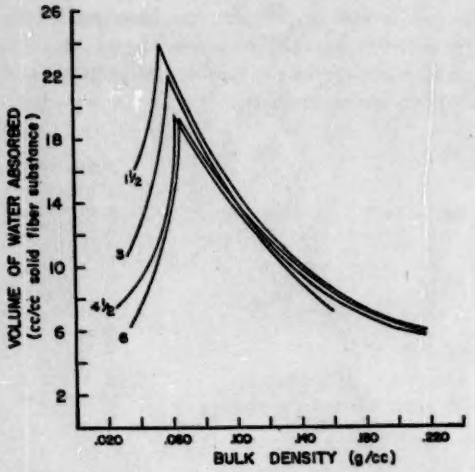

Fig. 6. Effect of denier on fiber system absorptivity.

The data of Table VI distinguish between two classes of fibers. The first class includes those fibers which absorb considerable quantities of water and whose mechanical properties are changed thereby. The second class includes those fibers which do not absorb much water and which maintain their properties to the effect that the bulk system can take up large quantities of water interfiberwise.

Figure 5 illustrates the effect of changes in system bulk density on the volume of water absorbed. The density at which maximum absorption occurs can be considered to be the "optimum bulk density" (dry) for that particular system of fibers.

The effect of fiber fineness on interfiber volume and on the volume of water absorbed was investigated. Similar values of interfiber volume were obtained for various finenesses. However, significant differences were noted in the volume of water absorbed and the bulk density, shown in Figure 6 for Dacron.

Based on the theoretical concepts of Preston and co-workers [2], the amount of water absorbed should increase linearly with the reciprocal of the square root of the product of the true density and denier

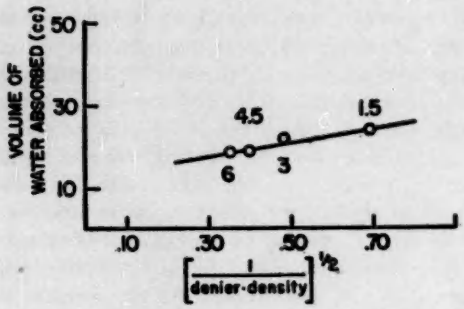

Fig. 7. Relationship between denier-density and water absorbed.

of the fiber. The data for Dacron, shown in Figure 7, are consistent with this concept.

Summary

It was shown that there is an optimum dry bulk volume and correspondingly an optimum bulk density at which maximum absorption of water by a system of fibers will take place. The pressure necessary to achieve the optimum bulk volume for the system is characteristic of the fiber type. This value is dependent upon the physical properties of the fibers when wet and on the chemical and physical natures of the surfaces of the fibers.

Systems of fibers of glass, Fortisan, and Dacron show high values for interfiber volumes and for the amount of water absorbed. Since these materials possess high elastic moduli, it is reasonable to assume that this property may be an important factor in attaining a high bulk volume at a given pressure. This observation suggests that a successful way of improving the capacity of a system of fibers to take up water would be achieved by increasing their stiffness by chemical or physical means.

Literature Cited

1. Gaus, G. E. and Larrison, J. E., "A Mechanical Cotton Fiber Blender for Use in Fiber Testing Laboratories," mimeographed by Cotton Branch, P.M.A., U. S. Department of Agriculture (August 1951).
2. Preston, J. M. and Nimkar, M. V., *J. Textile Inst.* **40**, P674 (1949).

Manuscript received July 26, 1957.

INDUSTRIAL SECTION

Some Dynamometric Applications of an Electronic Integrator-Differentiator[1]

J. Grignet and F. Monfort

Peltzer & Fils, Verviers, Belgium

Abstract

One of the authors (J. G.) has devised an electronic integrator-differentiator which can be connected to two recorders which will then record in one operation the classical load–extension curve, the work of stretching, and the slope of the load–extension curve. The recorders give a continuous trace from which at any moment can be read off as ordinates the corresponding work of stretching and the rate of loading or rate of extension. The technique can be applied equally well to measurements made by dynamometers on fibers, yarns, rovings, or slivers. Moreover, the integrator-differentiator circuit which is used is also appropriate for many additional uses, since it can be fed by the variable voltage which is produced in many types of apparatus now being widely used in the laboratory. In this way, without any additional work, both the integrated and the differentiated curve can be obtained for whatever function is being measured.

The authors have employed this circuit for (1) a critical study of the extent to which the constancy of rate of loading or extension is realized in two yarn dynamometers which have been put on the market recently, and (2) for the continuous measurement of the work of stretching and the rate of loading of wool, nylon, Terylene, and other fibers when they are being tested on a dynamometer supposed to give a constant rate of extension.

Quite apart from the advantage of having the integration and the differentiation proceeding instantaneously, this electronic device also allows a careful investigation of the effect of time in various dynamometric studies of fibers, rovings, and yarns.

Introduction

There is a tendency nowadays to prefer dynamometers working under constant rate of loading (CRL) or constant rate of extension (CRE) to the older pendulum type of machines. While it is certain that we understand the way in which the load is applied in testing machines of the CRL and CRE types more completely, several questions still remain to be answered on this subject. They are: (1) Do the CRL and CRE machines, which are already commercially on the market, actually attain constant rate of loading or constant rate of extension during the entire duration of the test? If the answer is no, how can they be improved in this respect? and (2) If the constant rate of loading or constant rate of extension conditions are effectively realized, does the behavior of the fiber or the yarn during extension depend on the application of one or the other of these conditions? Is, for example, the variation of load or of extension as a function of time affected in some way by the molecular structure of the fibers, or by the characteristics of the yarns? In general, recording dynamometers provide a trace of the load–extension curve. If we are not certain whether

[1] This paper was presented to the Technical Committee of the International Wool Textile Organization at its meeting in Cannes, May 1957; it also has been published in the *Bulletin de l'Institut Textile de France* **69**, 32 (1957).

either constant rate of loading or constant rate of extension is being realized, then the effect of time on such extension phenomena will remain obscured. The difficulties disappear, however, if we can study the first derivative of the load F as a function of time dF/dt, or the derivative of the extension e, also with respect to time de/dt.

Such studies are greatly facilitated if there is available an electronic differentiator circuit to which can be applied the variable voltage corresponding to the variations in the physical property being studied and if such a circuit permits this calculation of the first derivative to be made instantaneously.

In fact, electronic circuits which integrate or differentiate have existed for many years and are now used in analog-type calculators. The accuracy of the elements (D.C. amplifiers and components, condensers and resistors in the feedback network) which are used in such calculators varies in general from 0.01 to 0.1%, and the stabilized supply systems used give voltages which are regulated to an accuracy of about 0.01%. In consequence, the price of these elements and of the supply systems is high. On the other hand, for the greater part of the usual applications which could be made in the textile field, an accuracy of ±1% would be more than sufficient. By taking suitable precautions, it is possible to use satisfactorily individual commercial components; provided they are of the very best quality in this field and certain tricks of circuit design are utilized, it is possible to obtain an accuracy of 1% with a relatively simple apparatus which can be made at quite a low price. J. Grignet has devised a circuit of this kind which can be used in connection with many forms of apparatus commonly found in research institutes and could be reproduced easily in any laboratory.

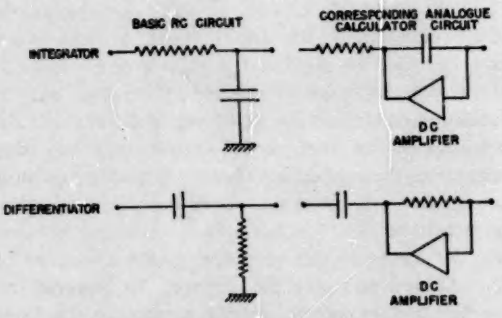

Fig. 1a. The principle of the electronic integrator-differentiator.

In using such a circuit with various dynamometers two cases must be considered: (1) the dynamometer may itself be an electronic one which provides at its outlet variations in voltage which correspond either to load or extension, or (2) the dynamometer may be a purely mechanical one. In this event some device which will transform the mechanical variations into electrical ones must be introduced.

In the following section will be described applications to the Statigraph sliver and yarn dynamometer made by Stein; the automatic dynamometer for yarns made by Zellweger-Uster, Switzerland; and the Fafegraph dynamometer for single fibers also made by the Stein Company of München-Gladbach, Germany.

In addition to the differentiating circuit, it is convenient to add another integrating circuit capable of carrying out the inverse operation; that is, integrating the function $F(t)$. If F varies as a function of time, the integrating circuit will calculate instantaneously the work of stretching. Such a parameter is particularly interesting during fiber stretching and will certainly prove very useful in dynamometry in general and in particular during the examination of the behavior of high polymers.

Description of the Electronic Integrator-Differentiator and the Special Arrangement for Use with the Statigraph, Fafegraph, and the Zellweger-Uster Dynamometers

The working principles of analogic integrators and differentiators are well known, so we will describe only the actual apparatus which was built and the details of its application to the different dynamometers; more specific information is available [1]. The electronic integrator-differentiator is an improvement on the resistance-capacity integrator-differentiator circuits which are commonly applied in radio and television techniques (Figure 1*a*); the accuracy of the integration or differentiation of the function derives from the gain and stability of the special direct-current amplifiers.

A dynamometer working on an electronic basis which already provides an output voltage of sufficient amplitude (a minimum of 6 volts full-scale reading, corresponding either to the load or to the extension) necessitates the employment of the following apparatus (see Figure 1*b*): (1) an automatic A.C. voltage stabilizer (working on the saturation principle), giving at its outlet an A.C. voltage which

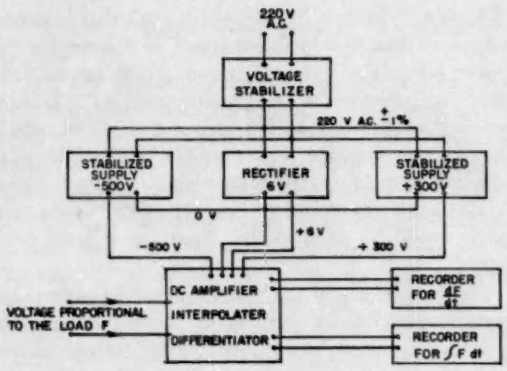

Fig. 1b. Integrator and differentiator schemes.

is controlled to ±1%, whatever may be the fluctuations of the main supply or of the load, (2) an electronically stabilized supply delivering a D.C. voltage of +300 volts under a minimum loading of 30mA and regulating to ±0.1%. (A degree of regulation of up to ±0.2%, or even ±0.5% to 1% might in the limit also be acceptable, but this would affect the stability and would require readjustment of the zero at much more frequent intervals.), (3) a stabilized supply of the same kind as that just described, delivering −500 volts under a minimum loading of 30mA, (4) a rectification system (bridge-connected selenium rectifiers) which is fed from the stabilized A.C. supply and which gives a D.C. voltage of 6 volts under a load of 2 amps. and which is used as supply to the valve filaments, (5) two special D.C. amplifiers having a voltage gain of 2,000 to 10,000, (6) a chassis carrying the integration and differentiation circuits, the automatic relay control device, and the range-changing equipment, and (7) two recorders giving a trace on paper strips and having sufficient sensitivity and linearity. The recording of the work of stretching can be made on any kind of pen recorder, providing it is sufficiently sensitive (the output of the integrator gives at full-scale 100 volts and 10 milliamps.) and has a paper speed of the order of 20–40 cm./min. We prefer an apparatus with rectangular coordinates which uses a paper chart width of about 10 cm. In our own work, which is described below, we have used the normal recorder made by Evershed and Vignoles on the Murday system. (This recorder is used with the Fielden regularimeter.) We have found its characteristics to be in every way suitable for this purpose.

On the other hand, the recording of the differentiated diagrams imposes certain other requirements, particularly as regards the response to different frequencies of the recording system used. It is indeed essential to use a pen system which has a very slight inertia and which will respond at 10–30 cycles. We have again used the recorder described above, but with an appropriate readjustment to the damping control obtained by trial and error. In this way we have obtained a truthful response for sudden variations going as high as 50% of the total amplitude of the diagrams. Above this level we have observed a slight excessive reaction which at the most reaches 2–5% of the reading. However, it would be better to use a special high-speed recorder; many types exist on the market already, i.e., the special model Evershed-Vignoles, Ediswan, Hartman and Braun.

The German firm, Stein, is making both a dynamometer called the Statigraph, appropriate for yarns, slivers and rovings, and a Fafegraph, which is suitable for single fibers. Both are stated to give constant rate of extension, and we have used the device just described to examine these dynamometers. The output voltage corresponding to the load can be tapped directly from two terminals situated to the left of the main frame of the apparatus. The output voltage corresponding to elongation is drawn from two plugs placed at the back of the electronic amplifier.

When working with a dynamometer which is not electronic in character, the arrangement must become a little more complicated, since the load and extension must now be converted into corresponding electrical changes. For this purpose the fixed jaw of the dynamometer must be replaced by a strain gauge of the variable resistance type, or by a measurement head made of a cantilever and a variable inductance (magnetic strain gauge).

A resistance strain gauge has certain advantages over a magnetic strain gauge, since it is very much smaller and has practically no inertia. Moreover, it is essentially linear and is very stable over a period of time. On the other hand, it is somewhat fragile and calls for certain precautions during manipulation; in addition, its output voltage is extremely small and requires a much higher amplification than that which is necessary for a magnetic strain gauge. Experiments using a nonelectronic dynamometer therefore involve the following additional equipment: (1) a resistance strain gauge, (2) an A.C. amplifier

with a very precisely linear response and a gain regulatable from 1,000 to 10,000, followed by a bridge-connected rectifier, and (3) a D.C.-to-A.C. converter device, if the strain gauge is fed with D.C., or a 50- to 100-cycle oscillator, if the feed is with A.C. (see Figure 2).

We have used this arrangement on the automatic Zellweger-Uster dynamometer, which is claimed to give constant rate of loading. On this dynamometer the lower (fixed) jaw is fastened by three screws to the frame of the apparatus. We have used these three screws as a support for a piece of rigid steel 4 mm. thick and resting against the machined surface of the frame (see Figure 3). The resistance strain gauge was attached to the front surface of this piece of steel by four screws. The latter is therefore fastened rigidly to the frame of the apparatus in the same way as is the lower jaw under normal conditions of use.

The strain gauge which was used is a model intended to deal with a load of ±10 oz. (280 g.). The output voltage is led by a shielded cable to the A.C. amplifier. The D.C. voltage after rectification at the output of the amplifier is of the order of 12 volts for 200 g. This voltage is then applied as the input to the integrator-differentiator; the rest of the circuit is identical with that which has been described above. A detailed description of the electronic part of the apparatus is published elsewhere [3].

Experimental Verification of the Performance of Various Dynamometers

Verification of the Constancy of the Rate of Extension of the Statigraph Dynamometer

Constant rate of extension conditions are very much more easily arranged for than constant rate of loading. In fact, in the first case all that is necessary is to ensure a constant speed of descent for the lower jaw. For example, there would be no difficulty in employing a D.C. motor with an electronic speed-stabilizer followed by a rigid drive in which no play or slippage was possible and which was coupled directly to the lower jaw. With a drive of this kind, the speed of descent of the lower jaw easily could be fixed within limits of ±1 or even ±0.1%.

This rather costly solution to the problem has not been adopted in the commercial dynamometers. If certain precautions are taken during the use of the apparatus, it is possible to obtain a sufficiently constant speed of descent without introducing supplementary complications into the construction of the device. Thus the Statigraph dynamometer uses for the drive to the lower jaw a common type of 3-phase motor. The movement is transmitted through a friction clutch to a steel blade on which the lower jaw is mounted. This steel blade controls a potentiometer, from the moving contact of which a voltage which is proportional to the displacement of the lower jaw can be tapped.

After amplification, this voltage can be differentiated directly, thus giving an experimental value for the rate of extension de/dt; i.e. the slope of the extension–time curve. In fact, it is the instantaneous speed with which the lower jaw is descending.

In this way we have determined 18 different diagrams by varying the various operating conditions, making some tests as soon as the motor was switched on (i.e., during the period when the motor was still cold), repeating these after the apparatus has been running for half an hour, making the tests with a single 32's yarn between the clamps, making tests without any yarn, etc. From these diagrams we have picked out three for publication; these may be seen in Figures 4.1, 4.2, and 4.3.

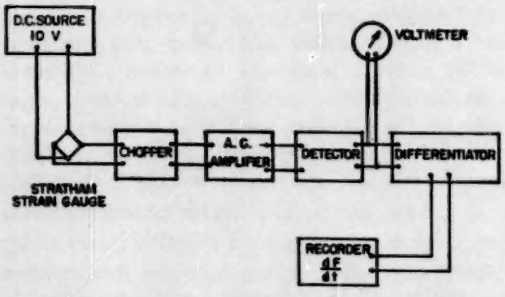

Fig. 2. Additional equipment for a nonelectronic dynamometer.

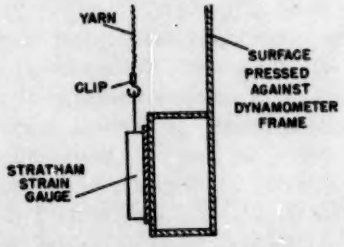

Fig. 3. Attachment device for use with the Uster apparatus.

From these diagrams the following conclusions can be drawn:

(1) No difference can be detected between diagrams recorded with or without a yarn between the jaws. Thus the average velocity, the amplitude, and the shape of the instantaneous variations of speed around this average remain constant. Evidently this result could have been foreseen, since the lower jaw is being driven through a quasi-rigid linkage by a powerful motor so that the reactions from the yarn being extended can be neglected.

(2) In order to obtain a sufficiently constant speed, it is necessary to allow for a certain time of warming up which is adequate both for the motor and for the remainder of the transmission mechanism. Thus the curve 4.1 in Figure 4 shows that after one minute preliminary warming up for the motor, there is a rapid increase in the rate of extension during the course of a subsequent normal test lasting 20 sec., and at the end of the recording the speed is 75% higher than the speed at the beginning of the movement of the jaw.

When we made recordings every 3 min. with the motor kept running continuously between these times, we obtained sufficiently horizontal speed diagrams only after the third period. Therefore, in order to make reliable tests it is necessary to run the drive mechanism to the lower jaw for a period of about 10 min., during this time making the lower jaw execute a series of descents and returns at a speed of about 1 cm./sec. Even when the motor has been warmed up, if there is any interruption of more than 5 min. between two series of tests it is necessary to repeat four or five extension–return movements of the jaw before restarting with the tests in order to ensure that the same average rate of extension will be reobtained.

(3) Once the regular speed has been obtained, the average rate of extension calculated for a period of 2–3 sec. remains constant during the duration of a normal test (about 20 sec.).

Among the twelve recordings which were made with the apparatus in a warmed-up condition, using different speeds for the jaw, ten were found to have a satisfactory constant mean speed from the beginning to the end of the test. On the other hand, two tests corresponding to one particular speed showed a small fall of the order of 10% in the velocity during the test.

(4) The instantaneous value of the rate of extension shows variations of the order of ±5 to ±10% around its mean value, the maximum range being from +12% to −12% in the least favorable case. These variations in the instantaneous velocity of descent of the jaw correspond to variations in the speed of the motor brought about by fluctuations in the main supply and also by fluctuations in the load brought about by such variations in the transmission mechanism as frictional changes, shocks in the chain and the gear-wheels, etc.

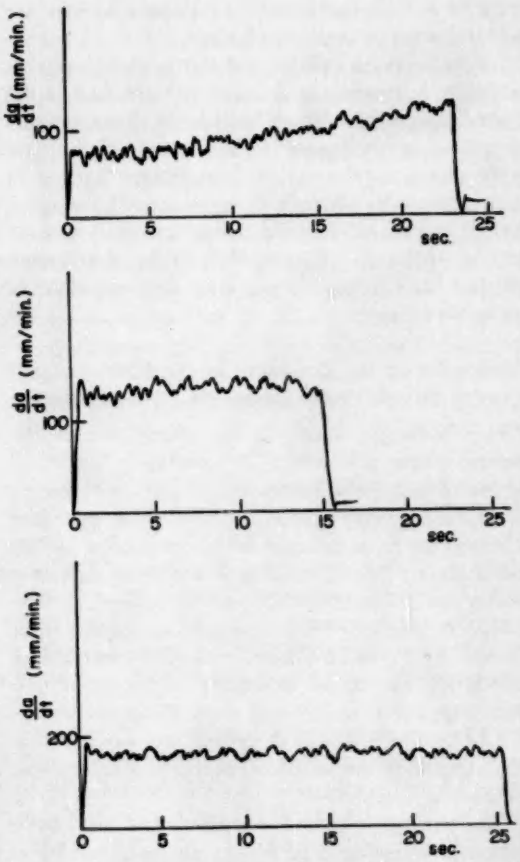

Fig. 4.1. Stein Statigraph after 1 min. **Fig. 4.2.** After 10 min. **Fig. 4.3.** At high speed.

It should be noted, in fact, that the speed of the motor is affected when the voltage of the mains varies. For this reason there are noticeable differences between the speeds indicated by the maker, which are calculated for the nominal mains voltage, and the actual speeds observed. However, in general, the variations are fairly small, being of the

order of 5–10% maximum. Diagram 4.2 of Figure 4 well illustrates these conclusions.

In summary, it can be said that constant rate of extension is reasonably satisfactorily obtained in the Stein Statigraph. Nevertheless, the instantaneous variations in the speed of movement of the jaw bring about corresponding momentary changes in load in the yarn which is being examined, and such variations can be detected in the recorded rate of loading diagram. It has still to be determined whether their effect on the final breaking load is negligible or not.

Verification of the Constancy of the Rate of Loading of the Automatic Zellweger Dynamometer

The Zellweger dynamometer makes use of the inclined plane principle and stretches a length of 50 cm. of yarn held in the vertical position between two jaws, the lower jaw being fixed. The upper jaw is connected to a carriage which moves on an inclined plane; this connection is made through two flexible steel blades which roll up around a first pulley; a chain attached to the carriage unrolls from a second pulley which is connected solidly to the first one during the actual stretching of the yarn. A more complete description is available in the literature [4]. For the tests described, we substituted a strain gauge of the variable resistance type, as was described above.

The working procedure is as follows: a small auxiliary clip weighing 8 g. which can be closed by a screw is suspended from the lower end of the yarn. This clip can be attached by means of two hooks to the strain gauge which replaces the lower jaw.

The yarn is passed under tension between the jaws of the upper clamp. The apparatus is then put into motion for a normal cycle of stretching and unloading. The measurements are thus made under conditions which are identical with those existing during the normal use of the apparatus.

It might be objected that the measurement head would be affected not only by the load imposed by the inclined plane but also by the possible reactions of the yarn; e.g., slippages or breakages of the individual fibers composing it.

In order to eliminate the result of these yarn reactions and to isolate the effect of the inclined plane, we have carried out similar tests on a homogeneous test material giving only a negligible extension under the loads which are used in the experiment. For this purpose we have used a copper wire of diameter 0.45 mm.

Among textile yarns we have tested worsted yarns of counts 32–60 metric (31–16.5 tex). In this manner a total of 20 diagrams have been recorded. A carriage was selected which would give a maximum load of 200 g.; this was used in all the tests, employing the speeds marked as 1, 2, or 3 on the speed-controller button. This was done in order to assure the breaking of the yarn being tested in an average time of 20 sec., as is required by the I.S.O. standards.

In order to follow the progress of the tests, the output voltage from the strain gauge representing the instantaneous load F being borne by the yarn is read on a voltmeter after amplification. The same voltage is transmitted to the electronic differentiator, from the output of which is recorded dF/dt, the rate of loading as a function of time.

If the rate of loading was perfectly constant, the diagram $(dF/dt, t)$ should be a line parallel to the time axis. We will consider the records obtained in practice for the copper wire and for the textile yarns of count 32 and 60.

We must, however, first point out one supplementary check which was carried out. The strain gauge being attached directly to the apparatus as described above should, of course, give a zero voltage when no pull is being exerted on the fixing system. Nevertheless, we have noted the appearance of a very small pulsating output voltage as soon as the motor is switched on to cause the inclined plane to descend. The average value of this voltage is almost nil, but it corresponds to a series of brief impulsions derived from the vibration both of the motor and the whole of the driving mechanism to the inclined plane, and this vibration is transmitted to the main frame of the apparatus. When fed into the differentiator, this slight pulsating voltage gives a recording on the ordinate which, though small, cannot be neglected. We have therefore made a series of supplementary tests in which the strain gauge was screwed to a support attached directly to the table supporting the apparatus but insulated from it by two layers of rubber. In these circumstances, the impulses caused by the motor vibration had a negligible effect on the record of the rate of loading, being of the order of only 1% of the maximum when calculated as a proportion of the rate of loading being tested.

When this second series of diagrams was compared with the first, it was found to be identical from a general point of view, both as regards the shape and the amplitude of the variations, etc. The new diagrams thus obtained are only a little "cleaner"; i.e., certain of the rapid variations of small amplitude have now disappeared. We have therefore concluded that the special precaution of insulating the measurement head from the main body of the apparatus with a view to suppressing the propagation of these vibrations is unnecessary, the form of the diagrams not being substantially changed by these precautions. Such a precaution may be regarded as indeed undesirable, because similar shocks will certainly be transmitted by the body of the machine to yarns via the lower jaw during the normal test procedure. The recordings which were obtained with the strain gauge fixed to the apparatus therefore correspond more exactly with the normal conditions of use.

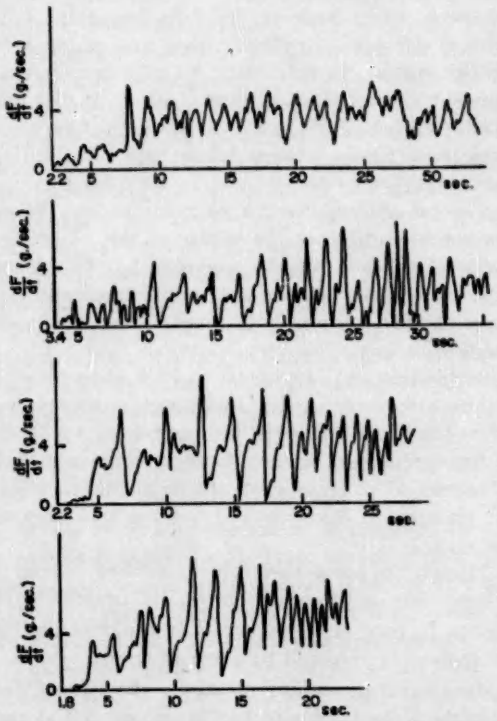

Fig. 5.1. Copper wire, 0.45 mm. diameter, Uster dynamometer. **Fig. 5.2.** Worsted yarn, 1/60. **Fig. 5.3.** Worsted yarn, 1/32. **Fig. 5.4.** Worsted yarn, 1/32.

Diagrams obtained with a copper wire. An examination of the five recorded diagrams at first sight reveals certain common features. Thus, there is an initial section where there is no indication of rate of loading taking place, or where this indication is very slight. This is followed by a sudden rise in the rate of loading, after which the rate of loading becomes roughly stable for the greater part of the period of the test and oscillates in a quasi-periodic manner around a constant average value (see Figure 5.1).

When the diagrams are examined more closely, the following features can also be detected:

(1) The variations of the rate of loading around its mean value are of two kinds: (a) a long period of oscillation (1.6 sec.) of very great amplitude, which may reach 55% of the mean ordinate, and (b) an oscillation of higher frequency (with a period of the order of 0.1 sec.), which has a very much smaller amplitude, the highest reaching 5% of the mean value.

(2) The amplitude and frequency of these oscillations are not constant throughout the whole period of extension. Thus (a) the period of the oscillation of the first type (i.e., with high amplitude) remains practically constant, but its amplitude decreases progressively as the load increases. Thus it changes from ±55% to ±18% during the course of one test. (b) The high-frequency oscillation period decreases progressively as the load is increased, but the amplitude increases from ±2% to ±5% of the mean value.

(3) In order to understand these results more completely, it is necessary to examine the working of the apparatus closely, and in particular to observe the wire which is being put under tension. Moreover, it is also necessary to take account of the working procedure used.

The first section of the recording showing a zero rate of loading can easily be explained in terms of the operating procedure. The yarn is fixed between the two clamps with an initial tension of 8 g. corresponding to the weight of the auxiliary clip; this tension is then increased by a supplementary tension derived from the connecting of the hooks to the attachment bar of the strain gauge. It is the sum of these two tensions which constitutes the initial total tension.

At the beginning of the test, when the upper clamp is set free, it remains pressed against the lower stop under the action of this initial tension. It is only

when the inclined plane has reached a position where it balances this initial pretension that the clamp actually starts to move. During the whole of this period the pull on the strain gauge remains constant (as can be verified by reading the output voltmeter, which shows the value of the load F) and the rate of loading, dF/dt, remains zero.

Observations of the copper wire which is being extended also provides an explanation of the second kind of oscillations (i.e., those of short period of the order of 0.1 sec. and of rather small amplitude). It can be observed that the wire is undergoing transverse vibrations and behaving like a vibrating string actuated by shocks transmitted from the drive mechanism and oscillating at its own natural frequency.

If on one of these diagrams we count the number of vibrations per second around the point corresponding, for example, to a load of about 150 g., we find a periodicity of 0.1 sec. For a wire of diameter 0.45 mm. such as was being used, if the normal formula for transverse vibrations of a vibrating string is applied one obtains

$$f = \frac{1}{2L}\sqrt{\frac{T}{m}} = \frac{1}{100}\sqrt{\frac{1.5 \times 10^4}{1.415 \times 10^{-2}}} \doteqdot 10$$

Turning to the first system of oscillation (i.e., the more important one with the long period of 1.5 sec. and a rather large amplitude), we have found an explanation, though we have not yet been able to verify it entirely.

It is that when the wire submitted to the test does not extend, as is almost exactly the case here, then the carriage mounts regularly up the length of the inclined plane and the chain to which it is attached rolls onto the corresponding pulley. The number of links in the chain which pass onto the pulley during the period of extension corresponds almost exactly to the number of oscillations which are recorded on the diagram. It therefore appears that the shocks which are produced in the wire by the rolling-up of the chain may well be responsible for the very substantial changes in the rate of loading.

Apart from this particular explanation, it is almost certain that the first system of oscillation is due to some irregularity in the movement of the carriage on the inclined plane or to a discontinuous transmission of this movement through the linkages between the carriage and the upper jaw. Indeed, the number of oscillations is always proportional to the distance covered by the carriage on the inclined plane.

Tests on undyed wool yarns of count 1/60's (16.1 tex). Here, after an initial period of zero rate of load followed by a sudden rise (Figure 5.2) which may be explained by the pretension which exists in the yarn, we observe once again a rate of loading which remains on the average constant but which undergoes rather large variations around this average. Once again these oscillations are of two kinds:

(1) An oscillation of very large amplitude which here rises to as much as 100% of the mean value and which has a rather long period. During the determination of the extension this amplitude decreases progressively from 100% to 50%, and its period also decreases from 2 to 1 sec.

(2) An oscillation of small amplitude (10%) and of shorter period (0.2–0.3 sec.) which is superimposed on the first one.

Tests on undyed 1/32 wool yarn (Figures 5.3 and 5.4). In general the observations are similar to the preceding case; however, the behavior of the 1/32 yarn is distinguished clearly from that of the 1/60 by two special characteristics: (a) the amplitude of the first system of oscillations is much smaller and rarely reaches 100%, and (b) its period is much greater and varies between 3.3 sec. and 1 sec. during the test.

General observations on all wool yarns. When we consider together the whole of the recordings for wool yarns it is quite apparent that the second type variations (i.e., those of small amplitude and short period), are clearly less well-defined than with the copper wire.

In addition and in contrast to what happens with copper wire, these oscillations are very much reduced when the strain gauge is insulated from the body of the apparatus. We are therefore concerned with vibrations of more or less random character which are transmitted from the body of the apparatus to the yarn.

Though the wool yarn which is being extended behaves like a vibrating string, its resonant frequency is very much higher than the wire and is too high to be recorded by a recording pen.

Once again the rolling up of the chain could explain the large amplitude oscillations as well as the variation in the observed period. In the final region during extension, the extension becomes very much

larger than at the beginning; the carriage therefore descends much more quickly and the number of links of the chain wound onto the pulley is greater. In consequence the period between any two successive shocks is decreased.

Present conclusions. The Zellweger-Uster dynamometer succeeds in giving a rate of loading which is *on the average* constant. On all the recorded diagrams the mean rate of loading (taken from the intervals of 3 to 1 sec.) appears to be reasonably constant and corresponds to the mean theoretical value, which can be calculated from the weight of the carriage and its speed of descent along the inclined plane.

But there are momentary variations in the rate of loading which are very large, and this rate can reach twice its mean value or can at certain moments fall to zero. In consequence, the momentary rate of loading dF/dt at the point of rupture seems to be extremely variable. Certain authors in fact attach a great importance to the rate of loading at break. (Consider for example the "equivalent time of break" used by Peirce.)

The existence of large oscillations in the rate of loading may be explained as due to shocks transmitted to the yarn during its extension and probably arising from the particular mechanism used in this apparatus. These shocks correspond to a relatively small amount of energy, but at the final stages, when considerable extensions are being realized, it can reach a level such as will have the effect of causing the actual moment of break to occur earlier than would otherwise be the case.

Analysis of this kind, which leads to the determination of the periodicity of the shocks, is particularly suitable for indicating the origin of the shocks, with a view to their possible elimination.

Measurement of the Work of Stretching and of the Rate of Loading [2, 3]

When using a dynamometer at constant rate of extension it is possible to obtain simultaneously with the load–extension curve a curve showing the rate of loading and a curve for the work of stretching as a function of time. On such diagrams one can read off as ordinates much interesting data which can be considered in relation to the parameters of the fibers themselves and will probably provide explanations of the mode of action of the dynamometers.

For example, we can easily read from the rate of loading diagram (Figure 6.2) the value for the maximum rate of loading corresponding to the short straight-line Hooke's law period. Sometimes this peak is a very sharp one and almost corresponds to

[2] Figures 6.1, 6.2, and 6.3 correspond to simultaneous recordings. No reduction of the scale on the abscissas of the load–extension diagram (6.1) could be made to render it identical with that used for both 6.2 and 6.3; this is apparent when the figures are placed side by side. This same situation exists with the three figures in each of the sets 7.1, 7.2, 7.3, 8, and 9.

[3] Term a on graphs $= e$ in text; allongement = extension.

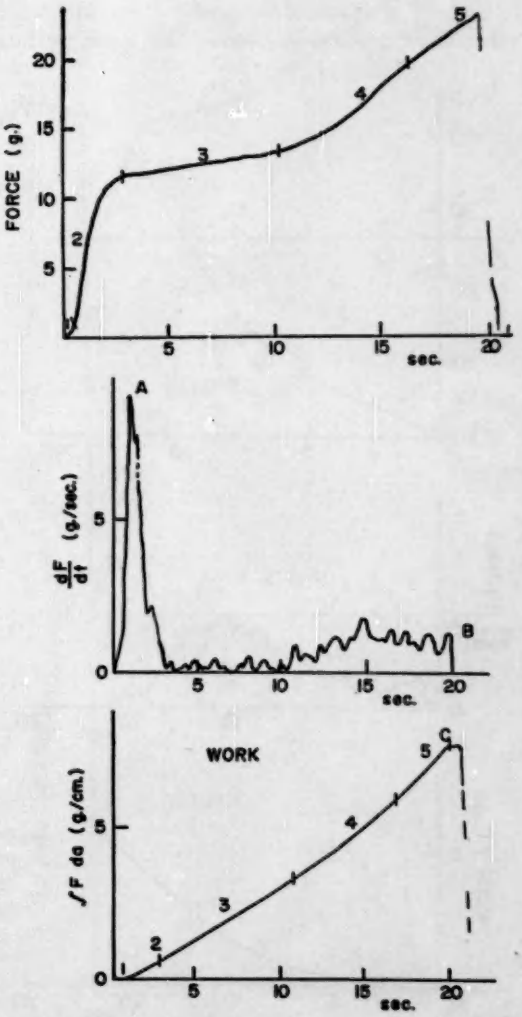

Fig. 6.1. Fafegraph dynamometer—single wool fiber. **Fig. 6.2.** dF/dt vs. sec. **Fig. 6.3.** Work vs. sec.

a point of inflexion on the load–elongation curve (see point A, Figure 6.2). The value of the rate of loading at break may also be seen. This value is considered by some authors to have the controlling influence on the value of the breaking load (point B, Figure 6.2).

As regards the diagram for the work of stretching (Figure 6.3), one can determine from this curve, for example, the total work of the stretching (point C), the work of stretching corresponding to any predetermined extension (for example to a 25% extension), and, the work of stretching corresponding to the end of Hooke's law period. For this latter value, one can choose as abscissa that corresponding to the minimum value (equal or near to zero), which is reached by the rate of loading after its maximum value corresponding to the point of inflexion.

Curves for some 250 wool fibers have been recorded for later publication. Meanwhile we will give only a brief summary of them and examine the general shape and overall properties of the diagrams which show the rate of loading and work of stretching for wool fibers, nylon, Dralon, and Tergal. In addition data is given on wool yarns and rovings.

Wool Fibers

Considering the whole 250 recorded diagrams together, a fairly general and typical shape to the curves can be discerned if we divide the load–extension curve into five regions separated by transition zones. These regions are chosen to correspond to sections where the rate of loading and the work of stretching curves have characteristic properties.

In doing so all the cases which have been met dur-

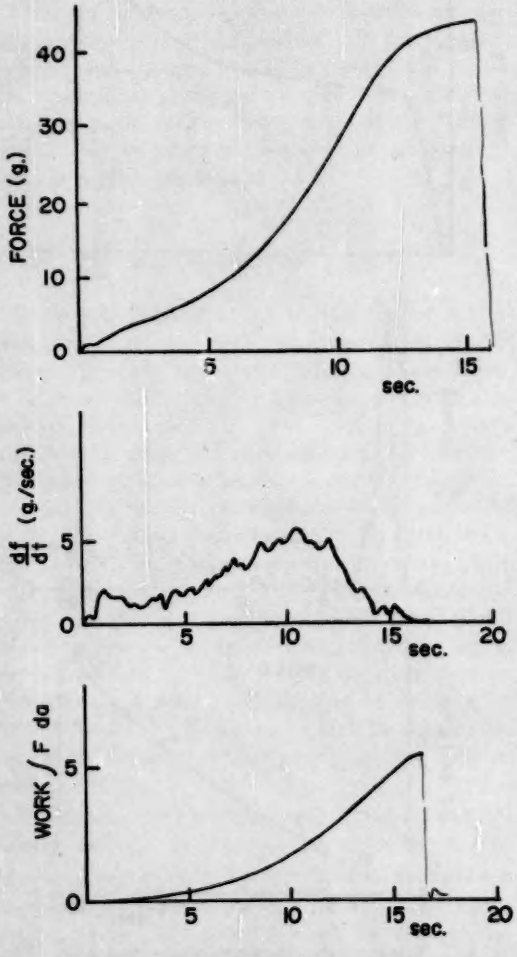

Fig. 7.1. Fafegraph dynamometer—nylon fiber.

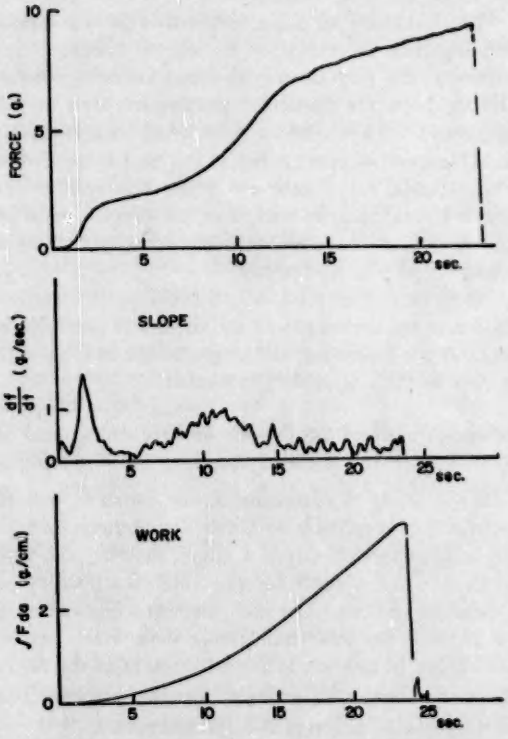

Fig. 7.2. Fafegraph dynamometer—Tergal fiber.

ing the course of this analysis were taken into account. Nevertheless, there were numerous fibers for which certain of the five zones were smaller, less well defined, or even completely nonexistent.

Load–extension diagram. The diagram can be divided into five sections (Figure 6.1): (1) the uncrimping region, (2) the Hooke's law region, characterized by a steep slope, (3) the rather long region with a slight slope approximating to zero, (4) a region with a greater slope (though this is sometimes absent or not very well characterized), and (5) a final short region, where the slope is again less. For a considerable number of fibers this last zone is either nonexistent or can be detected only with difficulty.

Work of stretching curve (Figure 6.3). The area under the first region of the load–extension curve being almost negligible as compared to the total area, the corresponding work of stretching is practically undetectable on the diagrams. The ordinate therefore remains practically zero right to the end of this region. (Evidently if we wish to do so it is possible even at this stage to obtain by amplification an ordinate corresponding to the total breadth of the paper record, if, for example, we wish to make a special study of say the work of decrimping.)

In the second region the increase in work per unit time increases progressively, but the work of stretching corresponding to the Hooke's law region is relatively quite small. We thus have a region with increasing curvature, but where the ordinate remains quite small throughout.

In the third region the ordinate of the load–extension curve remains almost constant, and the integrated diagram takes approximately the form of a straight line inclined to the axis. This region is in fact nearly always the longest and the most important; it is for this reason that at first glance the work curve appears to take the form of a triangle.

In the fourth region the load once again begins to increase very rapidly with time; on the work of stretching diagram a line is obtained which is curved with its concavity upwards.

Corresponding to the fifth region of the load–extension curve, where the slope is appreciably reduced, a final zone of very slight curvature is found on the integrated diagram.

The rate of load curve. Throughout the uncrimping region, the rate of loading is quite small, but increases progressively (see Figure 6.2). In the Hooke's law region the rate of loading increases abruptly to a high value and thereafter remains stable for a short period at this maximum value; finally it again falls rapidly to a value near to zero. Occasionally the peak zone is very short and corre-

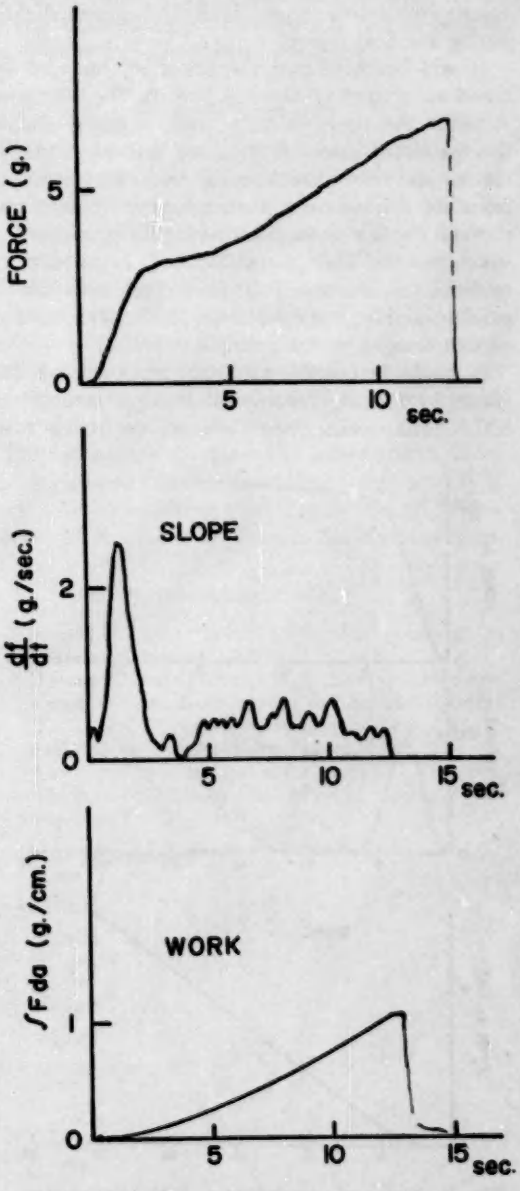

Fig. 7.3. Fafegraph dynamometer—Dralon fiber.

sponds to a point of inflexion on the load–extension curve.

The rate of loading retains a value near to zero throughout the third region and then increases steadily throughout the zone of transition between this and the fourth region.

The rate of loading again attains quite a high value in the fourth region; finally it decreases slightly during the final region.

It will be noted that the preceding remarks are based on a kind of average line for the diagrams. Actually the curve is of a quite irregular shape; this probably arises from three factors: (1) the shocks and vibrations coming from the motor or from the driving mechanism which are transmitted through the jaw to the fiber during its extension and which set the fiber in oscillation, (2) momentary variations in the speed at which the lower jaw is moving, and (3) the reactions of the fiber itself—sudden elongation, for example.

It would be possible to obtain more regular diagrams by filtering the applied voltages through an R.C. circuit, which would average the values over a short chosen time interval. Nevertheless, we have thought it preferable for our first trials to record the diagrams without any modification of this kind. It is, moreover, essential to do this in order to obtain the true instantaneous value of the slope at break.

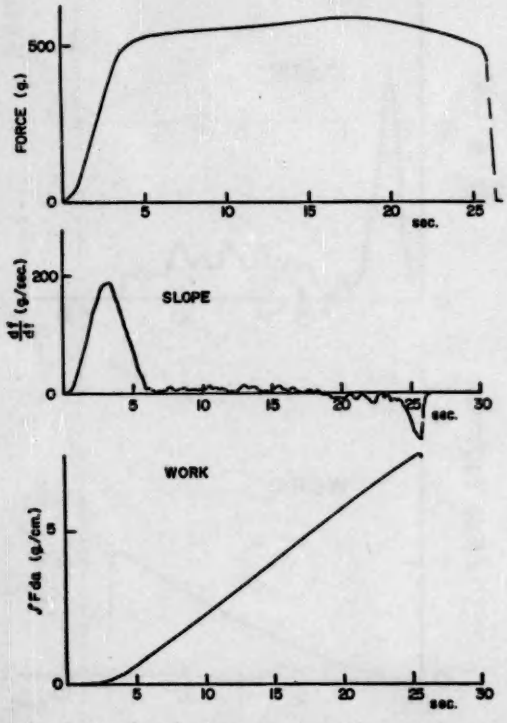

Fig. 8. Statigraph dynamometer—1/10 worsted yarn.

Nylon, Dralon, and Tergal Fibers

Since our tests have been made only on about ten of each of these fibers, it is a little difficult to draw general conclusions concerning the shape of the diagrams. It can nevertheless be stated that the general shape of the diagram and its slope is very characteristic for each of the fibers. The diagram for the work of stretching is also very clearly distinguished from that which is obtained from wool fibers. In Figure 7 we have included one diagram for each type of fiber.

Yarns and Rovings of Wool

The diagram for yarns can be divided into four regions (see Figure 8). The first of these regions are analogous to those given by the wool fiber. Region 4 consists of a decrease in load just before break; this is represented by a negative value on the differential diagram. This zone, however, sometimes does not exist. The shape of the diagrams, both for the rate of increase of load and for the work of stretching, is very comparable to that obtained for wool fibers. Nevertheless, three essential distinctions must be drawn. The maximum value for the rate of loading is much less well marked and the transitions are very much more gradual. Region 3 is much longer, and there is no longer a Region 4 with a rising slope for the load–extension curve. The break actually takes place in Region 3, or in a fourth region which corresponds to a *decrease* in load.

We have also produced several diagrams for wool rovings (Figure 9). These diagrams are characterized by a long region with a negative gradient, corresponding to the slipping of the fibers before breakage.

Conclusions

As we have been able to show, the integrator–differentiator circuit which we propose allows a more accurate analysis of (1) the principle and the functioning of commercial dynamometers, and (2) the phenomena exhibited when fibers, rovings, and yarns are stretched.

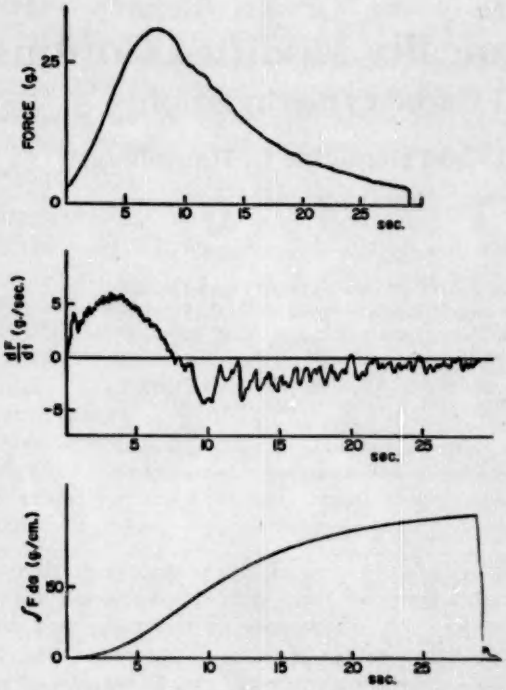

Fig. 9. Worsted roving from the finishing box.

As far as the analysis of the gradient dF/dt or de/dt is concerned, this report is only a first incursion into this field. It will be possible, by using a similar technique, subsequently to analyze the working of other dynamometers, such as the Scott or Instron machine; for each such apparatus it is very easy to obtain dF/dt and de/dt simultaneously.

Moreover, a knowledge of the corresponding gradients provides us with a much better knowledge of the way in which the load is applied. In this connection attention has already been called to (1) the fact that the Hooke's law region is not linear but has a point of inflexion, and (2) that the rate of loading at break is not constant even for forms of apparatus which are supposed to give constant rate of loading. This observation may lead us to revise the idea of an "equivalent time of break."

Finally, there is an evident facility with which we can obtain data on the momentary rate of loading at any point and the work of stretching.

Acknowledgments

The authors are very grateful to Mr. M. Franck for his assistance in the building of the apparatus and in the measurements, to the firm of Fabelta, of Zwynaerde (Mr. Quintelier and Mlle. Warzee), to the firm "La Lys" of Gand (Mr. Goossens and Mr. Van der Stegen), to the firm of "La Textile de Pepinster" (Mr. Lamarche and Mr. Lecocq), to the firm Peltzer and Fils, Verviers (Mr. Rensonnet) for the kind loan of various measuring apparatus, and to Dr. E. G. Carter for the translation of the paper into English.

They also wish to thank the International Wool Secretariat and l'Institut pour l'encouragement de la Recherche Scientifique dans l'Industrie et l'Agriculture (I.R.S.I.A.) of Belgium for their support.

Literature Cited

1. Raymond, P. H., "Calcul Analogique" (Société de la Revue d'Optique, Paris).
2. Monfort, F. and Franck, M., "Essais dynamométriques sur rubans et mèches non-tordus." Report 10, I.W.T.O. Conference in Cannes 1957. To be published in *Annales Scientifiques Belges.*
3. Electronique Industrielle (in the press).
4. Instruction Manual for the Zellweger-Uster Dynamometer.

Manuscript received August 16, 1957.

Physical Properties of Chemically Modified Cottons
Part IV: Effects of Partial Carboxymethylation

James N. Grant, Allan W. McDonald,[1] and Geraldine C. Humphreys[1]

Southern Regional Research Laboratory,[2] New Orleans, Louisiana

Abstract

Yarns from six cottons selected for their widely different inherent fiber characteristics were partially carboxymethylated to a degree of substitution averaging about 0.125 while held at their original length. Moisture regain, linear density, breaking load, and elongation at break, measured on the fibers and/or yarns, were increased by the modification. Fiber cellulose density and length decreased. Samples of the different cotton varieties were found to differ in their response to the treatment with interrelationships existing between the linear density, degree of substitution, and moisture regain. Changes in fiber properties in the caustic treatments of cottons, such as carboxymethylation and mercerization, were found to be similar when the tensional conditions during treatment were essentially equal.

CHEMICAL treatment of cotton cellulose to alter physical properties of the fibers without changing their fibrous form is a common practice in the textile industry. Partially carboxymethylated cotton produced by reacting the cellulose with monochloroacetic acid in the presence of a strong caustic is one of these modified cottons [6, 11]. Certain properties of the carboxymethylated cotton depend upon the final salt or acid form of the product and the degree of substitution [3, 11, 12, 13]. When the reaction progresses beyond a substitution of carboxymethyl units greater than 1 per 2 or 3 glucose units, the sodium salt of carboxymethylated fiber is soluble in water [3, 14]. At lower degrees of substitution, the fiber is insoluble but has a high water swelling capacity. Fabrics of partially carboxymethylated cotton are more impenetrable to water in a spray test, are improved in wrinkle recovery and resistance to microbiological deterioration, and have greater cation exchange characteristics than untreated cotton [2, 5, 11, 16].

In the present investigation, studies of the effects of partial carboxymethylation (CM) on certain physical properties of fibers and yarns were limited principally to those of the sodium salt of carboxymethylated cotton. The degree of substitution was about 0.11–0.14, or an average of about one carboxymethyl group for every eight anhydroglucose units. Fabrics with substitutions in this range had no measurable leakage of water in an orifice test, a very high water absorbency, and, at standard conditions, a strength greater than that of the untreated fabric. Several physical properties of partially carboxymethylated cottons have been reported for the yarns and fabrics [3, 11, 12]. The changes found were composite effects attributable to those of several properites of fibers and also to the effects of the yarn and fabric construction. In the present investigation, measurements on the carboxymethylated cottons have been restricted to certain physical properties of fibers and yarns of the different cottons. Comparisons of changes in certain properties caused by carboxymethylation have been made with those brought about by mercerization with tension, since both modifications use caustic as the swelling agent.

Experimental Procedure

Samples

Six different cottons varying widely in several inherent fiber characteristics, but not necessarily representative of the varieties named, were selected for treatment. The cottons were mechanically processed into low twist yarns, 16/2 construction (73.8 tex), and chemically treated as 60 yd. skeins. The physical properties of the untreated fibers and yarns and the structures of the yarns before partial carboxy-

[1] Resigned.

[2] One of the laboratories of the Southern Utilization Research and Development Division, Agricultural Research Service, United States Department of Agriculture.

methylation were given in Part I of this series [7]. The low twist yarn structures were selected to provide materials which could be uniformly treated and defibered after treatment. Properties of the fibers and yarns of these cottons after partial acetylation [8] and mercerization [9] have been given in other reports.

Treatment

The partial carboxymethylation of the cottons was carried out according to the methods described by Reid and Daul [11, 12, 13]. The skeins of yarns were pressure boiled at 15 psi for 3 hr. in a 2% solution of caustic, washed in hot water, and air-dried. The procedure used to produce carboxymethylated cotton as the sodium salt was as follows. After drying, the yarns were impregnated with a 20% solution of monochloroacetic acid containing a wetting agent and then were centrifuged to about 60% wet pickup. The centrifuged skeins of yarns were placed on a laboratory size mercerizing frame and held at constant length while rotating for 20 min. through a 50% solution of sodium hydroxide. The caustic was withdrawn and the yarns neutralized with 5% acetic acid. After neutralization, the yarns were washed with several changes of alcohol, removed from the frame, and suspended in the laboratory air until they were dry.

Test Methods

Methods of selecting the test specimens and measuring their physical properties were those described in the report on the physical properties of the untreated cottons [7, 10]. In both investigations, the properties were measured on the yarns and on fibers taken from the yarns according to described methods [7].

The degree of substitution of the treated yarns was determined by the copper substitution method of Chowdhury [1] as adapted to the measurement of carboxymethylation by Reid [11].

Results and Discussion

The degree of substitution (DS), cellulose density, and moisture regain are given in Table I for each of the six carboxymethylated cottons. Also given are the length and linear density of fibers and linear density of the yarns, with the percentage changes from values for the corresponding properties of the untreated. While yarns were held at normal length during the treatment and variables were controlled at conditions which in duplicate samples produced equivalent degrees of substitution of the cellulose, the DS ranged from 0.113 to 0.135 in the different cottons. The degree of substitution varied inversely with the linear density of the untreated cotton fibers [7]. The fact that the cotton having the larger fibers reacts more slowly than do those cottons with the finer fibers indicates a physical or chemical effect in modification which is related to the amount of cellulose in a fiber unit. Differences in the rates of reaction were found both when these cottons were partially acetylated [8] and when carboxymethylated in a nonaqueous medium [15]. Differences in the reaction rates during acetylation of other cottons varying through a wide range of fiber properties were reported by Taylor [17].

TABLE I. The Degree of Substitution of Six Carboxymethylated Cottons Together with Cellulose Densities, Moisture Regains, Fiber Lengths, Linear Densities of Fibers and Yarns, and the Changes in These Properties from Those of the Untreated Cottons

Sample identification	Degree of substitution, DS	Density, g./cc.	Moisture regain, %	Fiber length		Linear density			
						Fibers*		Yarns	
				Mean, in.	Decrease, %	Mean, tex	Increase, %	Mean, tex	Increase, %
Acala 1517	0.135	1.536	13.6	0.93	11	.189	12	79.8	9
Coker 100 Wilt	0.123	1.536	13.1	0.86	9	.201	14	76.3	9
Deltapine 14	0.123	1.534	13.3	0.86	9	.207	10	91.9	23
Rowden 41B	0.113	1.534	13.2	0.94	2	.275	8	76.9	1
Stoneville 2B	0.125	1.536	13.4	0.84	13	.207	9	79.6	10
S × P	0.130	1.534	13.4	1.30	2	.149	4	86.9	16
Average	0.125	1.535	13.3		8		10		11

* Linear density (g./1000 m.) for 1 cm. length sections from center of fibers.

Density

Cellulose density of the six partially carboxymethylated cottons averaged 1.535 g./cc. as compared to 1.550 g./cc. for untreated. A difference of only 0.002 g./cc. between the CM cottons with extremes in other values was observed. The average density was slightly greater than that for cotton mercerized at normal length (1.533 g./cc.) [10] and appreciably greater than that of the free acid carboxymethylated cellulose of equivalent degree of substitution (1.527 g./cc.); see Curve A, Figure 1. The difference in densities of the acid form and sodium salt is partially explainable by differences in respective molecular weights. The position of the average density for the six cottons, B, with respect to the curve, A, is indicative of a difference in the relationship between density and degree of substitution in the two types of carboxymethyl celluloses.

Moisture Regain

Moisture regains at 65% R.H. of the partially carboxymethylated cottons (oven dry method), when equilibrium was approached from the dry state, ranged from 13.1 to 13.6%. These values are about twice those on the untreated cottons [7] and above the normal values for these cottons mercerized at normal length [9]. While the ranges in degree of substitution and moisture regain were small, a slight trend for regain to increase with DS was evident in the six cottons. The greater moisture regains and higher absorptions of liquid water by the carboxymethylated than the untreated cottons caused by the hydrophilic nature of the sodium carboxymethyl groups introduced have been reported by others [3, 11]. Moisture regains greater than those of the mercerized or untreated are expected from the hydrophilic groups.

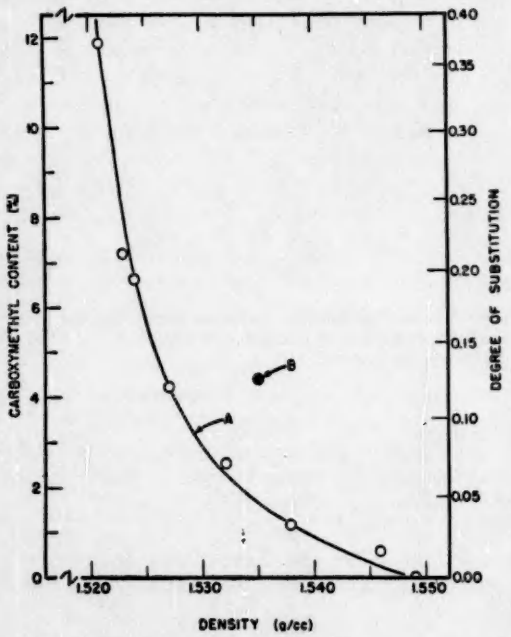

Fig. 1. Relationship between density and carboxymethyl content of partially carboxymethylated cotton. (A) Densities of the free acid form; (B) average density for the sodium salt form for the six cottons.

Fiber Length

When yarns are prevented from contracting in length during chemical treatments with swelling agents, the lengths of the fibers and yarns usually decrease when the stresses from swelling are relieved. The fibers from the carboxymethylated yarns averaged 8% shorter than those of the untreated yarns. Length distribution curves for the six cottons showed increases in the percentages of short fibers, indicating that fiber breakage had occurred. Shifts of the curves on the length axis were evidence of shrinkage in length. The increased cross-sectional areas of carboxymethylated cotton, observed microscopically, are evidence also that fiber shrinkages in length have occurred.

While changes in length of yarns were not determined, increases were observed in cross-sectional areas and moisture regains of the fibers in the yarn structure, as well as the delayed elastic recovery of the tensioned fibers, which would cause shrinkage of the yarns.

Linear Density

Linear densities of both the fibers and yarns were greater than those of the untreated cottons (see Table I). The increases, caused by changes in chemical and physical properties of the cellulose as a result of carboxymethylation, would have been greater if losses in noncellulosic constituents had not occurred during kiering. The increases averaged 10% for fibers and 11% for yarns. When contributions of factors responsible for the changes are estimated, an increase of 6.5% was caused by the higher moisture regain and 6.3% by the addition of

the sodium carboxymethyl groups. The larger cross-sectional areas of the fibers [4] were observed but not measured; however, the cellulose density of the swollen fiber was less than that of the untreated. There is usually about 6% loss in weight attributed to kiering [18], which on the dry cellulose basis leaves an increase in linear density of about 4% in fibers and 5% in yarns to be accounted for by the change in cross-sectional areas. The decrease in fiber length, averaging 8%, was attributed to both the shrinkage in length and the breakage of fibers. If changes in length were caused equally by the two factors, the shrinkage would be equivalent to the 4% increases in linear density attributed to the increase in cross-sectional area of the fibers. The fact that the changes in yarns were greater than those in fibers is consistent with the above considerations.

Experimental errors of measurements and difficulties of securing accurate measures of the changes in individual properties preclude the possibility of an accurate accounting for the percentage contribution of each factor to the change in linear density for the individual cottons. Several cottons departed significantly from the average change in linear density, which indicates that considerable difference in the behavior during carboxymethylation at normal length can be expected of cottons with different fiber characteristics.

Breaking Load

The average increases in breaking loads of fibers and yarns were 24 and 44% respectively (see Table II). These increases were larger than those resulting from mercerization [9]. The pretreatment in carboxymethylation, which included kiering and soaking of yarns while they were relaxed, did not occur in mercerization. However, the reaction with caustic took place while the yarns were held at a fixed length. Differences in the conditions of treatment were sufficient to prevent a strict comparison with mercerization. However, a similarity in response was found in the cottons given the two chemical modifications. Stoneville and S × P, which gave the maximum and minimum changes respectively in mercerization, were the corresponding extremes in carboxymethylation. Differences in the fiber properties of the other cottons were too small to show trends as consistent as those of Stoneville and S × P. The effects of fiber structures, such as crystal alignment, percentage of crystalline cellulose, and the presence of weak points in the fibers as they affect strength were discussed in an earlier report for the process of mercerization [9]. While breaking load is often used to estimate changes in strength for both fibers and yarns, the tenacity calculated from breaking load and linear density is more meaningful if the weight added is small in a chemical modification.

Tenacity

The tenacities of the fibers and yarns and the percentages of change from the corresponding values for the untreated are given for each cotton in Table II. The increases in breaking loads were larger than those of linear densities, which caused the tenacities to increase with treatment. The average percentage

TABLE II. Breaking Loads and Tenacities of Carboxymethylated Cotton Fibers and Yarns and Changes in These Properties from Those of the Untreated

	Breaking load				Tenacity					
	Fibers		Yarns		Fibers		Bundles		Yarns	
Sample identification	Mean, g.	Increase, %	Mean, g.	Increase, %	Mean, g./tex	Increase, %	Zero spacing,* g./tex	Increase, %	Mean, g./tex	Increase, %
Acala 1517	6.4	21	1618	28	34	6	41	5	20.3	18
Coker 100 Wilt	6.4	25	1460	47	32	10	41	8	19.1	36
Deltapine 14	7.1	29	1680	49	24	17	41	2	18.3	20
Rowden 41B	8.7	21	1443	52	32	14	42	0	18.8	46
Stoneville 2B	6.7	40	1715	67	32	23	44	0	21.5	57
S×P	6.7	8	2049	19	45	2	47	2	23.6	4
Average		24		44		12		3		30

* Pressley index = zero spacing tenacity × 0.185.

increases were 12% for the single fibers, 3% for the bundles, and 30% for the yarns. The tenacities of fibers, bundles, and yarns for the carboxymethylated cottons are compared in Figure 2 to the corresponding values for the untreated. Calculated regression curves A (fibers) and B (bundles) have equivalent slopes within experimental error, while the slope for curve C (yarns) is much less. A scatter of points about each of the curves is indicative of an appreciable difference in the response of these cottons. The scatter could be caused in part by uncontrolled stress which occurs during the treatment of a yarn at a fixed length and the experimental errors of the measurements.

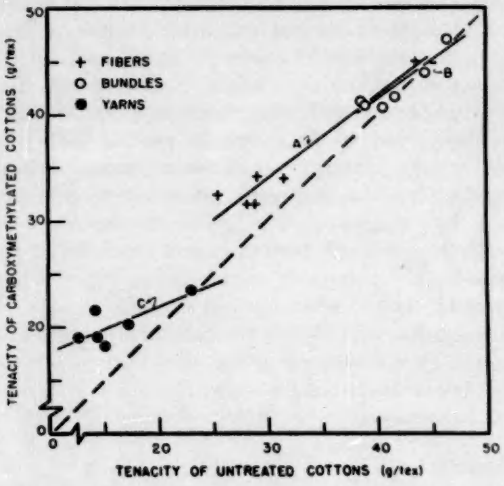

Fig. 2. The relationships of tenacity of partially carboxymethylated to that of the untreated: (A) fibers; (B) bundles; and (C) yarns.

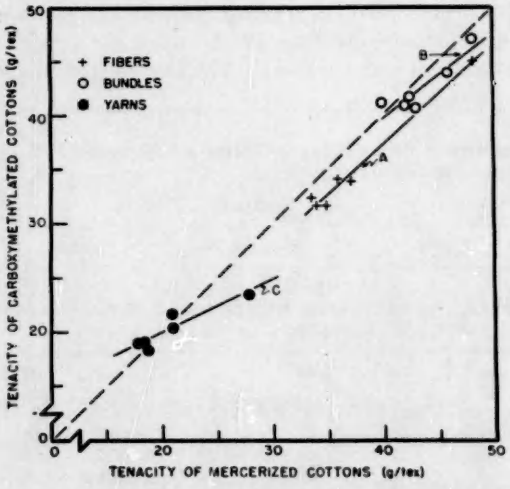

Fig. 3. Relationships of tenacity of the carboxymethylated to the mercerized samples: (A) fibers; (B) bundles; (C) yarns.

Bundle tenacities showed smaller increases with treatment than did those of either the fibers or yarns. For two cottons, bundle tenacities were unchanged even though increases were found for both the fibers and yarns.

In other investigations of the effects of swelling agents on the changes in tenacity, the percentage increases in tenacity are related to the length of the section of fiber under strain. Tenacities determined from the shortest length of section under strain are the least affected by removal of weak points in the fibers. In these cottons, the bundle tenacities (zero jaw spacing) were determined from the shortest length of section, while those of the single fibers were determined from the longest section under strain. The percentage change of tenacities of single fibers was intermediate between that of bundles and yarns. However, in the yarns, the fiber adjustments during swelling, increase in frictional forces, and the removal of noncellulosic constituents from fibers in the helical yarn structure caused the greatest changes to occur in the yarns.

In Figure 3, the tenacities of the fibers, bundles, and yarns are plotted against the corresponding values for the mercerized samples. The fact that the scatter of points about curves A, B, and C is smaller than about the corresponding curves in Figure 2 is indicative of a similarity in response of these cottons to the two modifications. The slopes of the corresponding curves are essentially equivalent in Figures 2 and 3, but those of the latter are shifted in position with reference to the line of unit slope. The shift is to be anticipated, since the increases in linear densities are greater with carboxymethylation than with mercerization.

Elongation at Break

The average elongation at break of the single fibers showed an increase of 2% and that of the yarns of 4% over the corresponding values for the untreated cottons (see Table III). The sample of Stoneville was the only cotton which gave appreciable increases in elongation in both the fibers and yarns—19% and 24% respectively. The sample of S × P showed decreases in both the fibers and yarns of 6% and 13%

respectively. Changes in elongation for the other four cottons were either inconsistent in fibers and yarns or were within the sample errors. Measurements of elongation of cottons in other investigations [9] have shown that the property is sensitive to the strains on the yarn during swelling as well as those applied to fibers or yarns while being prepared for testing. These uncontrolled variables could account for many of the inconsistencies observed.

Secant Modulus

The large increases in tenacities and small average increases in elongation caused an increase in secant moduli for both fiber and yarn. The average increase for fibers of the six cottons was 10%, with a spread of 12% between cottons. Increases for yarns averaged 23%, with a spread of 21%. The observation that the increases in yarns were larger than those in fibers is attributed to the fact that increases in tenacities of yarns were greater than those of the fibers.

The increases in secant moduli are indicative of increases in stiffness of the textile product. The property of stiffness is very important in qualities such as hand, tear strength, and wrinkle resistance. Since secant moduli of cotton fibers and yarns are important in product performance, the property can be controlled to some extent during caustic treatment by adjustment of strains which affect either or both the tenacity and elongation.

Summary

Several significant changes were found in the physical properties of the six cottons which were carboxymethylated and investigated as the sodium salt of carboxymethyl cellulose. Density of the cellulose was decreased. Moisture regain was increased to approximately twice that of the untreated cotton.

Fibers taken from the yarns were shorter than those of the untreated cottons. The decrease in length was attributed to combined effects: (*a*) fiber breakage and (*b*) shrinkage in length during caustic swelling.

Linear densities of the fibers and yarns were increased by the addition of the carboxymethyl groups, as were cross-sectional areas and moisture absorptive capacity.

Breaking loads were increased; the percentage increases were larger for yarns than for fibers. Tenacities of both fibers and yarns were greater than those of the untreated controls, but increases were smaller than those of breaking loads. Bundle tenacities showed smaller increases than those of either the single fibers or the yarns.

The smallest changes in mechanical properties were found in the elongations at break. The elongation of the S × P sample was less in both fibers and yarns than that of the untreated sample.

The secant moduli of both fibers and yarns were increased by carboxymethylation of yarns held at fixed length. The secant modulus changes were caused principally by substantial increases in tenacity in conjunction with very small changes in elongation.

Changes in fiber properties in the caustic treatments of cottons such as carboxymethylation and mercerization were found to be similar when the tensional conditions during treatment were essentially equal. In both treatments, the largest percentage increases in breaking load, tenacity, and elongation at break were found for the Stoneville sample. The smallest increases in breaking load and tenacity and the largest decrease in elongation

TABLE III. The Elongations at Break and Secant Moduli of Carboxymethylated Cotton Fibers and Yarns and Changes in These Properties from Those of the Untreated Cottons

	Elongation at break				Secant modulus			
	Fibers		Yarns		Fibers		Yarns	
Sample identification	Mean, %	Change, %	Mean, %	Change, %	Mean, g./tex	Change, %	Mean, g./tex	Change, %
Acala 1517	8.6	4	8.3	1	394	5	245	14
Coker 100 Wilt	8.2	−5	8.5	6	388	15	225	22
Deltapine 14	8.1	0	8.1	0	423	17	226	21
Rowden 41B	8.4	1	7.1	9	376	9	265	35
Stoneville 2B	6.9	19	8.3	24	470	7	259	24
S×P	9.6	−6	7.7	−13	469	9	306	19
Average		2		4		10		23

at break were found for the S × P sample. Increases in linear density were the principal causes for the fact that increases in tenacity of carboxymethylated samples were smaller than those of mercerized samples.

Acknowledgments

The authors wish to express their appreciation to G. C. Daul and R. M. Reinhardt for treating the yarns, to Annie B. Cooper and Dorothy Legendre for fiber length measurements, and to R. S. Orr for densities of the carboxymethylated cottons.

Literature Cited

1. Chowdhury, J. K., *Biochem. Z.* **148**, 76–97 (1924).
2. Daul, G. C., Reinhardt, R. M., and Reid, J. D., TEXTILE RESEARCH JOURNAL **22**, 787–797 (1952).
3. Daul, G. C., Reinhardt, R. M., and Reid, J. D., TEXTILE RESEARCH JOURNAL **23**, 719–726 (1953).
4. deGruy, Ines V. (private communication).
5. Goldthwait, C. F. (to Secretary of Agriculture of the United States), U. S. Patent 2,352,707 (July 4, 1944).
6. Lilienfeld, L., British Patent 231,803 (April 4, 1924).
7. McDonald, A. W., Humphreys, G. C., Kromhout, O. M., and Grant, J. N., TEXTILE RESEARCH JOURNAL **26**, 641–646 (1956).
8. McDonald, A. W., Humphreys, G. C., Orr, R. S., and Grant, J. N., TEXTILE RESEARCH JOURNAL **26**, 646–652 (1956).
9. McDonald, A. W., Orr, R. S., Humphreys, G. C., and Grant, J. N., TEXTILE RESEARCH JOURNAL **27**, 641–648 (1957).
10. Orr, R. S., Weiss, L. C., Moore, H B., and Grant, J. N., TEXTILE RESEARCH JOURNAL **25**, 592–600 (1955).
11. Reid, J. D. and Daul, G. C., TEXTILE RESEARCH JOURNAL **17**, 554–561 (1947).
12. Reid, J. D. and Daul, G. C., TEXTILE RESEARCH JOURNAL **18**, 551–556 (1948).
13. Reid, J. D. and Daul, G. C. (to Secretary of Agriculture of the United States), U. S. Patent 2,448,153 (Aug. 31, 1948).
14. Reid, J. D., Daul, G. C., and Reinhardt, R. M., TEXTILE RESEARCH JOURNAL **20**, 657–659 (1950).
15. Reinhardt, R. M., Fenner, T. W., and Reid, J. D., TEXTILE RESEARCH JOURNAL **27**, 873–878 (1957).
16. Stallings, J. W. (to Röhm and Haas Co.), U. S. Patent 2,390,032 (Nov. 27, 1945).
17. Taylor, J. L. and Owens, E. D., TEXTILE RESEARCH JOURNAL **24**, 810–819 (1954).
18. Valko, E. I., in "Chemistry and Chemical Technology of Cotton," Kyle Ward, Jr., ed. Chapter 3, Interscience, New York (1955).

Manuscript received September 3, 1957.

Carbonizing Investigations[1]

Part IV: Industrial Carbonizing Trials to Assess the Protection of Wool by Surface Active Agents Added to the Acid

W. G. Crewther and T. A. Pressley

Biochemistry Unit, Wool Textile Research Laboratories, C.S.I.R.O., Parkville, Victoria, Australia

Abstract

In a series of trials in four carbonizing mills, the addition of a nonionic surface active agent to the sulfuric acid bowl resulted, in each experiment, in an increased yield of carbonized wool and, on spinning, increased yarn strength. In a similar trial with combing wool, the addition of nonionic surface active agent to the acid used for carbonizing resulted in improved gilling and combing. The amount of acid taken up by the wool was increased by this addition, whereas the water content was decreased; this facilitated drying of the acidified wool.

Introduction

It has been shown [3] that the loss of tensile strength which normally occurs when wool is moistened with dilute sulfuric acid and baked at about 100° C. is decreased or prevented by the addition of ionic or nonionic surface active agents to the acid. It has also been shown [7] that the addition of surface active agent to the acid does not significantly change the rate of uptake of sulfuric acid by wool and burrs once they are wet by the acid, but the amount of liquor removed from the wool and burrs during centrifuging is increased.

Industrial trials in a number of carbonizing mills have now been made to determine whether surface active agents provide protection for the wool in full scale operation in loose-wool carbonizing and whether they affect retention of acid liquor by the wool passing through the squeeze rollers.

Materials and Methods

Wool

Wool about to be processed in normal mill production at the time of each experiment was used. Lambswool (carding length), Merino crutchings, 64's Merino (carding length), Corriedale 56's, and 64's Merino (combing length) were used in different experiments.

Surface Active Agent

The nonionic surface active agent used throughout these tests was 4-(ω-hydroxy octa-ethyleneoxy) n-octyl benzene (Lissapol NX, I.C.I.). Surface active agents of this class have the advantage that, unlike anionic agents, they are not appreciably adsorbed by the wool and so removed from the acid bowl; they are also less expensive than cationic agents.

Regain

The regain of the wool was determined in a standard Heal condition testing oven.

Acid Content of Wool

The method used to determine acid content of wool was essentially the pyridine extraction method of Barritt [2] as modified by the American Society for Testing Materials [1]. The results are expressed as a percentage of the neutral oven-dry wool.

Water Content of Acid Soaked Wool

After extraction with pyridine reagent to determine acid content, the wool recovered from a known weight of acid soaked wool was thoroughly rinsed

[1] Part I of this series, which is a review of the literature on carbonizing by D. H. Simmonds, was published as Technical Paper No. 2 of the Wool Textile Research Laboratories. Parts II and III are to be found in Vol. E of the Proceedings of the International Wool Textile Research Conference, Australia, 1955. These publications are available from the Commonwealth Scientific and Industrial Research Organization, Melbourne, Australia.

with distilled water, dried to constant weight at 105° C., and weighed. The loss in weight gave an estimate of the total weight of acid and liquor on the wool; the water content was obtained from the acid content by difference.

Control of Acid Liquor

Acid liquors were titrated at intervals of 15 min. during the mill trials and adjusted to maintain the acid concentration at a constant value, which varied from mill to mill.

Concentration of Surface Active Agent in Acid Liquor

In view of the difficulty and time involved in estimating nonionic surface agents, no analytical procedures were adopted. The amount of froth on the surface of the acid liquor was used as an index of changes in concentration of surface active agent in solution. At a concentration of 0.05% in grease-free sulfuric acid, Lissapol NX gives a stable froth when the surface is agitated, as by the rakes in the acid bowl. The amount of froth was kept approximately constant by additions of Lissapol NX at intervals of 15 min.; about half the surface of the acid bowl was covered with froth.

Yarn Strength

Strength and elongation at break of the yarn were tested in a Uster tester.

Alkali Solubility

The modification of the original method of Harris [6], recommended by the Standards Association of Australia [8], was used. The method involves a preliminary treatment of the wool in 0.5% sodium bicarbonate solution followed by water washing. The alkali solubility is expressed as a percentage of the oven-dry neutralized wool.

Experimental and Results

Laboratory Experiments on Yarn

In order to confirm earlier laboratory experiments, in which a manual method was used for testing strength, a procedure using a mechanical strength test was required. Hanks of worsted yarn were steeped in sulfuric acid, and other similar hanks were steeped in acid containing ionic or nonionic surface active agents. More concentrated acid than that employed in carbonizing practice was used to accentuate the effects of damage. Excess acid was removed by centrifuging; the hanks were dried and baked in a laboratory oven at 100° C. for 1 hr. The concentration of acid used in each test was such that before baking the wool contained approximately 11.0% of H_2SO_4 on the neutral oven-dry weight. Control hanks were treated with water in a similar manner. All yarn was washed with distilled water, neutralized with two changes of 0.5% sodium bicarbonate solution, and again water washed prior to drying and testing. Table I shows the reduction in elongation at break and in breaking load resulting from the acid treatment. All types of surface active agents protected the wool against acid attack.

Industrial Trials with the Woolen Process

Mill A. Merino 64's lamb's wool (2 bales) was opened, blended, and divided into two lots which were sampled for regain determination and weighed. One lot was carbonized using 4.3% (wt./vol.) sulfuric acid without added Lissapol NX. The remainder was processed using acid of the same concentration containing 0.05% Lissapol NX, with further additions of Lissapol NX at the rate of 0.5 lb./100 lb. greasy wool processed. Similar conditions of drying and baking were maintained. The products were weighed and sampled for determination of regain. Two bales of Merino crutchings were treated in a similar manner; each of the resulting lots of carbonized wool was blended with the lot of lamb's wool carbonized under the same conditions. The two blends were carded, spun on the mule, and woven. The yields and strengths of yarn are recorded in Table II.

Mill B. Wool from 6 bales of Merino crutchings was blended, divided and carbonized in the absence and in the presence of surface active agent as described above; yield and strength of yarn were measured (Table II). An acid concentration of 7.4% was used. The scouring in this plant (a 3 bowl system) was incomplete, and considerable amounts of grease and dirt were carried on the wool into the acid bowl. With the control run, most of this remained on the wool, but with the addition of Lissapol NX to the acid a considerable amount was emulsified and retained in the acid bowl. Fresh acid was used for this trial and, at the end of the test, it was possible to estimate the amount of dirt in a representative sample of the acid liquor by

centrifuging, washing, and drying. Knowing the total amount of acid, the amount of dirt removed by the action of the Lissapol NX could be calculated; the yield was corrected accordingly. Larger amounts of Lissapol NX were required in this test. The initial concentration was 0.1%; further additions were made at the rate of 0.5 lb./100 lb. of greasy wool processed.

Mill C. Wool from 8 bales of Merino fleece (carding) was blended and divided as above. An acid concentration of 5.3% (wt./vol.) was used. The 4 bowl scouring plant was efficient, and acid penetration was assisted by the use of two consecutive acid bowls separated by squeeze rolls. Lissapol NX was added to both acid bowls to give an initial concentration of 0.05%, and additions of Lissapol were made at the rate of 0.25 lb./100 lb. of greasy wool processed.

Mill D. High yielding fine Crossbred lamb's wool (20 bales) was blended and divided into three lots which were carbonized in 5.1% sulfuric acid (*a*) with no additions to the acid, (*b*) with the addition of 0.1% of an anionic wetting agent (sulfonated castor oil) and further additions to the acid at intervals of about 30 min., and (*c*) with the addition of 0.05% Lissapol NX to the acid and further additions at the rate of 0.25 lb./100 lb. of greasy wool processed. It was apparent from the appearance of the acid bowl that the anionic agent was rapidly removed by the wool, and for a considerable proportion of the processing time the concentration would be insufficient to protect the wool. The yields and strengths of yarn are recorded in Table II.

Industrial Trial with the Worsted Process

A single trial was carried out (Mill E) with heavily burred Merino 64's combing length wool. The wool was blended, divided, and processed by the two methods as with carding wools, using an acid concentration of 5.7% (wt./vol.) and Lissapol NX

TABLE I. Elongation at Break and Breaking Load of Worsted Yarn Carbonized With and Without Addition of Surface Active Agent to the Acid

Surface active agent		H_2SO_4 content, %		Reduction in elongation at break,‡ %	Reduction in breaking load,‡ %
Name and type*	Conc., *M*	Liquor†	On wool†		
No addition	nil	15.0	9.8	36	20
CTAB (cation)	0.01	21.8	11.8	10	5
SLS (anion)	0.01	21.8	11.9	11	4
Teepol (anion)	0.0003 (0.25%)	21.8	11.9	4	1
LNX (nonion)	0.005 (0.25%)	21.8	12.0	2	2

* CTAB = cetyltrimethylammonium bromide, SLS = sodium lauryl sulfate, Teepol = Teepol 610 (Shell Chemicals), LNX = Lissapol NX (I.C.I.).

† Estimated sulfuric acid content expressed as % on oven-dried wool and as wt./vol. % for the liquor.

‡ Based on 60 tensile tests with each sample treated with acid containing surface active agents, 110 tests on samples treated with acid only, and 170 tests on water treated control samples.

TABLE II. Effects of Adding Surface Active Agent (SAA) to the Sulfuric Acid Used in Industrial Carbonizing

		Mill A		Mill B‡		Mill C		Mill D§	
Test	Wool	Control	SAA*	Control	SAA*	Control	SAA*	Control	SAA*
Yield at 16% regain, %	L†	57.0	58.9	45.0	45.3	55.5	58.9	66.4	79.3
	C†	55.5	59.7						
Yarn strength‖ (g.-wt.)		547	602	335	386	689	841	778	989

* Wool processed with the addition of Lissapol NX to the acid.

† L = Lambs' wool, C = Merino crutchings.

‡ The test batch was left in the acid containing SAA during the weekend. This would certainly reduce the yield by increasing losses during neutralizing.

§ In this mill the yield was determined after the wool was spun into yarn. Yield of yarn from the batch processed with anionic agent in the acid was 73.9%; the yarn strength was 768, which is not significantly different from that of the control.

‖ In each test the yarn counts and turns/in. for the control and test samples were not significantly different.

at an initial concentration of 0.1% (wt./vol.), with further additions at a rate of 0.5 lb./100 lb. of greasy wool processed. After carbonizing, the two lots of wool were carded, gilled, and combed, and the tear values were taken as an index of fiber strength.

The plant was unsuited to the processing of combing wools of good staple length. The wool passed through the three scouring bowls and the acid bowl in a total of 4 min.; the rapid rake action caused extensive felting of both the control and test lots of wool. As a result of this and acid damage, the control lot which was carbonized in the absence of Lissapol NX was too badly damaged to permit gilling and combing; the lot carbonized with the addition of Lissapol NX to the acid, despite its greater acid content (Table IV), could be gilled and combed, giving a tear value of 3.2.

Alkali Solubility of Wool at Different Stages of Processing

When wool is moistened with sulfuric acid and heated in a closed vessel at 100–105° C., its alkali solubility increases markedly if water is present, whereas under anhydrous conditions an equivalent amount of acid causes little or no increase [5]. Consequently, any large increase in alkali solubility which occurs during the carbonizing process is almost certainly due to excessive heating before drying is complete. Table III lists the alkali solubilities of a series of wool samples collected at different stages in processing during the trials described above and at other carbonizing mills. There were no major changes in alkali solubility, but in each mill there was a small consistent increase in solubility during the period of immersion in the acid bowl. There was little change during drying and baking, and a small decrease during neutralization and drying. The presence of surface active agent in the acid appears to reduce the damage responsible for increased alkali solubility of the wool.

Retention of Water and Acid by the Wool

Samples of wool leaving the squeeze rolls after acid impregnation were analyzed for sulfuric acid and water content. In each experiment the acid content of the wool was increased by the presence of surface active agent, whereas the water content was decreased (Table IV).

Accumulation of Sodium Sulfate in the Acid Bowl

During certain of the trials the sulfuric acid concentration in the acid bowl was determined both by titration and by the conventional method of hydrometry. Often the values obtained did not agree within reasonable limits; total sulfate was therefore estimated gravimetrically to determine whether salt accumulation was responsible for the discrepancy. Table V lists the sodium sulfate concentrations of a number of acid liquors and the period over which these accumulations occurred. Laboratory carbonizing tests [3] were also carried out to determine the effect of sodium sulfate on loss of strength of the wool during baking with sulfuric acid at 100° C. Table VI shows that even at the concentrations occurring in the acid bowl during industrial carbonizing there is a noticable protection of the wool.

Discussion

The increase in yield of carbonized wool and increase in yarn strength (Table I) which accompany the addition of surface active agent to the acid bowl

TABLE III. Alkali Solubility of Wool at Various Stages in Carbonizing

Mill	Additive to acid	Alkali solubility, %				
		Ex scour	Ex acid	Ex drier	Ex baker	Final
A	nil	12.1	13.9	13.2	13.1	12.5
A	Lissapol NX	11.9	12.7	12.3	12.2	12.9
A	nil	13.6	15.2	14.5	14.9	13.7
A	Lissapol NX	13.0	13.7	14.3	14.2	13.3
E	nil	13.5	15.5	16.2	15.0	13.6
E	nil	11.0	16.3	16.4	15.9	14.6
F	nil	11.1	12.9	—	12.9	12.7
F	nil	11.1	12.4	11.6	13.9	11.9
G	nil	12.3	13.1	13.1	15.6	12.2
G	nil	11.6	16.0	12.4	8.9	12.2
Mean		12.1	14.2	13.8	13.7	13.0

provide definite evidence that the wool has been protected against acid damage by the surface active agent. Probably the increase in yield is due largely to a retention of the tensile strength of the individual wool fibers, which would reduce losses during crushing and willeying, but Table III indicates that it also may be due partly to decreased losses during neutralization. Thus there appears to be a noticeable increase in alkali solubility of the wool after it has passed into the acid bowl (Table III), which may result partly from local heating when the wet wool passes into the sulfuric acid and partly from the tendency for the temperature of the bowl to rise as acid is added. This increase in alkali solubility is reduced when surface active agent is present in the acid.

It should be clearly understood that an improved yield and yarn strength, such as we report in this paper, can be expected only when the conditions of carbonizing—acid on the wool, conditions of drying, baking, and willeying—are comparable to those employed in the mills which cooperated in these trials. Such conditions of high acid concentration and rapid throughput are encountered in most Australian mills,[2] but British and, in particular, Continental mills tend to favor lower acid concentrations and longer periods of treatment. It may well be that with these relatively mild methods the improvement in yield and yarn strength will be within the range of experimental error. We would point out, however, that the more rapid process is sufficiently improved by the use of wetting agents to warrant a reassessment of the two alternatives—short time and high acid concentration or long time and low acid concentration.

The increase in H_2SO_4 uptake by the wool and concomitant decrease in water uptake (Table IV) may be related to differences in liquor retention by the wool, such as were observed in the laboratory [7]. However, this cannot be the only factor involved, since acid uptake is increased. Probably it is related also to the observation that when wool is soaked in sulfuric acid solutions, water initially passes from the wool into the bulk of the solution until the water content of the wool reaches a minimum ([3], Figure 4). The presence of surface active agents hastens this initial removal of water from the wool and the attainment of minimum water content. Since more than 30 min. is required for this condition to be reached and the immersion time in the acid bowl in Australian mills is normally 1–5 min., the incorporation of surface active agent in the acid would be expected to result in a decrease in water within the fibers. The initial removal of water probably is an osmotic effect due to the slow diffusion of sulfate ions into the wool. If this explanation is correct, it is conceivable that an important decrease in the amount of water held by the wool would be achieved by increasing the time of immersion in the acid bowl. Such a prolonged treatment in the acid bowl would also facilitate carbonizing of Noogoora burr, the most refractory variety occurring in Australian wools. Laboratory tests have shown that treatment of Noogoora burrs in acid for 30 min. followed by thorough drying and baking constitutes an adequate treatment for these burrs.

The trial with combing wool was not designed to determine the possibilities of applying the method to wools for worsted manufacture. The speed with which the wool passed through the scour bowls and

[2] The mean acid content of wool leaving the acid squeeze roller is 8.03% of the neutral dry wool.

TABLE IV. Acid and Water Content of Wool Leaving Acid Squeeze Rolls

(Results are based on oven-dry neutral wool. Each value is the mean of 6 to 12 tests.)

Mill	Conditions of carbonizing	H_2SO_4, %	Water, %
E	Without surface active agent	6.6	33.3
E	With surface active agent	7.9	29.3
F	Without surface active agent	7.2	35.4
F	With surface active agent	8.0	30.4

TABLE V. Sodium Sulfate Content of Carbonizing Acid Liquors

Mill	Age of liquor	Na_2SO_4 content, %
A	Not known	2.6
B	2 days	2.0
C (bowl 1)	Infinite	2.8
(bowl 2)	Infinite	2.5
D	3 months	1.8

TABLE VI. Protection of Wool by the Addition of Sodium Sulfate to the Acid Used for Carbonizing

Na_2SO_4 in acid, %	0	0.5	1	2	5	10
Acid on wool, %	10.5	10.4	10.5	10.4	10.2	10.0
Strength rating	1	1	1	2	2	4

acid bowl was too great to give information of this type, because the resulting ropiness and felting would lower the tear value considerably. With the protection against acid damage afforded by surface active agents, and with a gentle harrow motion, it should be possible to obtain a satisfactory tear value from carbonized combing wools. The use of wide, short bowls for scouring and acid treatment may achieve this.

Table VI shows that in laboratory carbonizing experiments, acid damage to wool was reduced by the addition of sodium sulfate to the acid. This is of interest in connection with the protective action of wetting agents during carbonizing, as it has been observed (Crewther, unpublished data) that salts, like ionic surface active agents [4], can decrease the disordering of wool proteins by alkaline buffer solutions. The latter observation suggested the use of surface active agents in carbonizing. It is apparent from Table V that, during industrial carbonizing, sodium sulfate accumulates rapidly in the acid bowl and reaches a more or less constant concentration when the sodium sulfate leaving the acid bowl on the acidified wool is equivalent to the sodium carbonate and soap entering the acid bowl with the scoured wool. The steady state concentration of sodium sulfate would be determined largely by the efficiency with which alkali is removed from the wool in the rinse bowl of the scour. From Tables V and VI it seems probable that the concentration of sodium sulfate would be sufficient to provide some protection to the wool. However, if the acid concentration is checked only by hydrometry, the acid concentration may be unusually high when the acid is replaced by a fresh solution.

From the financial point of view, the increased yield of wool which is obtained when surface active agent is added to the acid far outweighs the additional cost of the surface active agent required. Even with additions at the high rate of 0.5 lb. of surface active agent/100 lb. greasy wool processed, the cost is less than 0.5¢/lb. of greasy wool processed, whereas the average increase in yield is valued at about 3¢/lb. of greasy wool processed. With an efficient scour the cost of surface active agent could be reduced to considerably less than 0.1¢/lb. of greasy wool. It is probable also that the estimated increase in yield is rather low, since no allowance has been made for the higher proportion of grease in the wool carbonized in the absence of surface active agent. Other factors which may affect costs are the increase in acid uptake by the wool (which does not occur also in the burrs) and the saving in fuel due to the lower proportion of water held by the wool. The former effect amounts to about 1% sulfuric acid on the weight of clean wool; i.e., to an increased cost of about 0.03¢/lb. of greasy wool processed. The fuel saving is calculated to be of the order of 0.1¢/lb. of wool processed.

Acknowledgments

The authors appreciate the help rendered by the management and staff of Albion Woollen Mills Co. Pty. Ltd., Collins Bros. Pty. Ltd., Federal Woollen Mills Ltd., Godfrey Hirst Pty. Ltd., Laycock Son & Co. Pty. Ltd., Pacific Wools (Aust.) Pty. Ltd., Patons and Baldwins (Aust.) Ltd., and Tweedside Manufacturing Co. Ltd. Thanks are also due to Mr. L. M. Dowling for technical assistance, to Mr. D. L. C. Jackson for providing and testing the worsted yarn, and to Mr. T. Topham for assistance in arranging and conducting trials in carbonizing mills.

Literature Cited

1. *A. S. T. M. Standards 1955,* Part 7, p. 613, American Society for Testing Materials, Philadelphia (1956).
2. Barritt, J., *J. Textile Inst.* **26**, T87 (1935).
3. Crewther, W. G., *Proc. Int. Wool Text. Res. Conf. Aust. 1955* **E**, 408 (1956).
4. Crewther, W. G., *Proc. Int. Wool Text. Res. Conf. Aust. 1955* **C**, 486 (1956).
5. Crewther, W. G. and Pressley, T. A., TEXTILE RESEARCH JOURNAL **28**, 74 (1958).
6. Harris, M., *J. Research Nat. Bur. Standards* **15**, 63 (1935).
7. Pressley, T. A., *Proc. Int. Wool Text. Res. Conf. Aust. 1955* **E**, 389 (1956).
8. Standards Association of Australia, *Australian Standard Specification for Shrink-Resistance of Plain Knitted Underwear Composed Wholly or Partly of Wool,* A.S. No L.2. Appendix D (1952).

Manuscript received July 15, 1957.

Part V: The Effect of Water Content on the Action of Sulfuric Acid on Wool: The Significance of Tests for Damage

Abstract

The nature of the reaction of sulfuric acid with wool at 105° C. depends on the water content of the acid–wool system. When wool moistened with dilute sulfuric acid is heated in a closed system to prevent loss of the water present (approximately 40% of the dry weight of the wool), there is a slow decrease in tensile strength and a marked increase in alkali solubility and, after pretreatment with alkali or alkaline caprate at 30° C., in digestibility by trypsin. By contrast, when the acid–wool is dehydrated before heating there is a rapid decrease in tensile strength but little change in alkali solubility or trypsin digestibility. The addition of a surface active agent to the acid prevents loss of strength of the wool, particularly under anhydrous conditions, and it also reduces deterioration of color.

It is concluded that sulfuric acid can attack wool by at least two different reactions and that there is little direct relationship between alkali solubility and fiber strength.

Introduction

It has been shown [1] that the brittleness and loss of tensile strength of wool which become apparent when it is moistened with dilute sulfuric acid and baked at 100° C. is decreased or eliminated by the addition of surface active agents to the acid. It was observed, however, that this addition did not produce a comparable decrease in the loss in weight of wool samples when baked with acid, neutralized, washed, and dried. Furthermore, the relationship between loss of weight and loss of strength for wool samples baked with acid differed according to whether or not surface active agents were present. This suggested that loss of weight and strength probably resulted from at least two different reactions of the sulfuric acid with the wool.

In order to investigate these effects further, the alkali solubility test has been chosen because of its possible relationship to the loss of weight during neutralizing in industrial carbonizing practice and because it has been used as a means of testing wool for damage [6, 7, 10, 11]. The extent of digestion with trypsin and manual strength tests have also been used as methods of assessing changes in the wool. These tests have provided information concerning the effects of water and surface active agents on the reaction between wool and sulfuric acid.

Materials and Methods

Wool

Corriedale 56's wool was detipped and cleaned by extraction three times with cold light petroleum (b.p. 40–60° C.), once with cold ethanol, and several times with cold distilled water. The wool was dried in a forced draft at 40° C. and thoroughly mixed and hand carded.

Surface Active Agent

4-(ω-hydroxy octa-ethyleneoxy) n-octyl benzene (Lissapol NX, I.C.I.) was the only surface active agent used in these experiments because of its use in industrial carbonizing trials [4].

Alkali Solubility

The modification of the original method of Harris [6], recommended by the Standards Association of Australia [13], was used.

Trypsin Digestibility

The wool to be tested was conditioned at 70% R.H. and 20° C. If it had been previously acid treated it was neutralized, washed, and dried before conditioning. Samples in the range 0.199–0.201 g. were accurately weighed and soaked for 20 hr. at 30° C. in 10 ml. of one of the following pretreatment liquors [2]: (*a*) 0.1 *M* acetate buffer at pH 4.0, (*b*) 0.1 *M* piperidine buffer at pH 11.0, or (*c*) 0.1 *M* piperidine containing 0.1 *M* sodium caprate at pH 11.0. The pretreated samples were washed with suction on a Buchner funnel for 1 min. in running distilled water and incubated at 40° C. in 5 ml. of a centrifuged 5% solution of trypsin (Pfanstiehl 1:110) in 0.1 *M* sodium borate at pH 8.0. After incubation at this temperature for 4 hr. the wool was

washed with running distilled water for 1 min. on a conditioned, tared filter paper and dried, conditioned, and weighed. A control sample of wool was treated in a similar manner, using 0.1 *M* sodium borate at pH 8.0 to replace the trypsin solution. The difference in loss of weight of the control and test samples was taken as a measure of the amount of protein hydrolyzed by the trypsin.

Miscellaneous

Manual strength tests, the estimation of acid content of wool, and methods for controlling the acid liquor retained during centrifuging have been described previously [1, 12]. Color changes in the wool were assessed by submitting samples to two assessors in random order. Control samples were allotted 10 points, and the points assigned to the test samples were reduced with increasing degrees of yellowing. The mean of the two assessments was taken.

TABLE I. Strength, Color, and Alkali Solubility of Wool Heated with Sulfuric Acid

(Wool samples were moistened with 10% (wt./vol.) H_2SO_4, excess liquor removed, and the wool heated at 105° C. for 1 hr. Before heating, water was removed from anhydrous samples by evaporation at room temperature in vacuo.)

Acid	Surface active agent*	Strength rating	Color rating	Alkali solubility, %
Anhydrous	Absent	1.0	7.5	13.2
Anhydrous	Present	8.0	9.0	16.3
Aqueous	Absent	6.5	4.0	81.4
Aqueous	Present	8.0	5.5	80.1
No acid, anhydrous	Absent	10.0	10.0	9.5
No acid, anhydrous	Present	10.0	10.0	9.1
No acid, aqueous	Absent	10.0	10.0	7.7
No acid, aqueous	Present	10.0	10.0	7.7
Original wool	—	10.0	10.0	8.6

* The acid solution contained 0.1% Lissapol NX.

TABLE II. Trypsin Digestibility of Wool Heated with Sulfuric Acid

Acid	Surface active agent	Trypsin digestibility, %*		
		Pre-treatment pH 4	Pre-treatment pH 11	Pre-treatment caprate
Anhydrous	Absent	0.0 (−0.4)	9.1 (2.5)	13.9 (2.8)
Anhydrous	Present	0.0 (1.0)	10.8 (1.5)	12.8 (2.4)
Aqueous	Absent	0.0 (0.4)	43.9 (13.5)	38.0 (18.5)
Aqueous	Present	0.0 (0.4)	49.8 (7.8)	40.0 (13.4)
No acid	—	0.0 (1.0)	4.4 (0.6)	8.4 (0.4)

* Solutions used for pretreatment were 0.1 *M* acetate at pH 4.0, 0.1 *M* piperidine at pH 11.0, and 0.1 *M* caprate in 0.1 *M* piperidine at pH 11.0; NaOH and HCl were used for pH adjustments. Loss of weight (%) of the control samples for each test is given in parentheses. The percentage loss of weight is based on the original weight of the wool in each case.

Experimental and Results

Effects of Water and Surface Active Agents

Duplicate samples of wool (2 g.) were thoroughly wet out with and immersed in 10% (wt./vol.) H_2SO_4 for 30 min. at room temperature; excess liquor was removed by centrifuging. The speed of centrifuging was reduced to a predetermined value when surface active agent (0.1% Lissapol NX) was present; in this way it was possible to obtain an approximately constant H_2SO_4 content in the wool. Immediately after centrifuging, one sample from each pair was enclosed in a stainless steel bomb of approximately 200 ml. capacity which was immersed in a saline bath at 105° C. for 1 hr. The second sample of each pair was placed in a large test tube attached to a trap and pump by glass joints; the water was removed by evacuation at room temperature overnight. When no further water could be removed in this way, the wool was transferred to the dry bomb and heated at 105° C. for 1 hr. The samples were immersed in the acid solutions at time intervals such that each sample remained for a constant period in the wet acid state during centrifuging before heating in the bomb was commenced. When removed from the bomb, all samples were rinsed in distilled water, neutralized by soaking in two lots of a 0.5% solution of $NaHCO_3$ with a wool/liquor ratio of 1/100, and again rinsed in distilled water, dried, and conditioned.

Each sample of conditioned wool was subdivided and tested for alkali solubility and trypsin digestibility using each of the three methods of pretreatment; color changes and strength were also assessed. Table I shows that loss of strength occurred chiefly when water was absent; under these conditions there was about 100% increase in the alkali solubility of the wool. When water was present during heating with the acid, there was a small loss of strength but a 900% increase in alkali solubility. Considerable improvement in strength and color of acid treated wool was obtained by the addition of surface active agent to the acid.

The trypsin digestibility gives the same general pattern as the alkali solubility (Table II); the loss

in weight of the control samples for the trypsin digestibility test, which were soaked in alkaline buffer or alkaline caprate solution, showed similar relative changes. In each test the control sample treated with caprate lost more protein than the corresponding control sample treated in piperidine buffer. Pretreatment of wool at pH 4 reduced tryptic digestibility to insignificant proportions regardless of the acid treatment applied to the wool. The presence of surface active agent in the acid used in the baking treatment had little effect on the result of the alkali solubility or tryptic digestibility tests, but in general the values obtained by both tests were increased slightly when the wool had been treated with acid containing surface active agents.[1]

Rates of Reaction

The rates of the reactions responsible for loss of strength, increase of alkali solubility, and increase in tryptic digestibility were investigated by heating two series of acidified wool samples in the bomb at 105° C. for varying time intervals. In one series the wool samples were dehydrated before heating. As in the previous experiment, the wool samples were washed, neutralized, rinsed, dried, conditioned, and tested for alkali solubility, trypsin digestibility, and strength (Figures 1 and 2). In this series of tests the acid content of the wool samples after centrifuging was less than in the previous experiment; the results after heating for 1 hr. at 105° C. are correspondingly lower. In this and confirmatory experiments the values obtained for alkali solubility and trypsin digestibility of the samples which were dried before heating remained practically constant at the value for untreated wool, whereas the corresponding values for wool heated with acid in the presence of water increased continuously. The values for the strength rating decreased continuously for both types of treatment over the total time employed, but the initial rate at which the strength decreased was much greater when the conditions were anhydrous during heating. It was characteristic of the time curves for both alkali solubility and trypsin digestibility that, when water was present during heating with the acid, the values obtained after short periods of heating were less than the corresponding values for untreated wool. This reduction did not occur with the samples treated with anhydrous acid.

Interrelationship of Various Tests

The results for all the experiments have been combined to show the relationship between strength ratings, alkali solubility, and trypsin digestibility (Figures 3 and 4). There is no obvious relationship between strength rating and either trypsin digestibility or alkali solubility when all the results are pooled. It is only when the effects of aqueous acid without the addition of surface active agent are considered apart from results obtained under other conditions that alkali solubility shows a tendency to increase as strength rating decreases (Figure 4). There is an obvious close relationship between tryp-

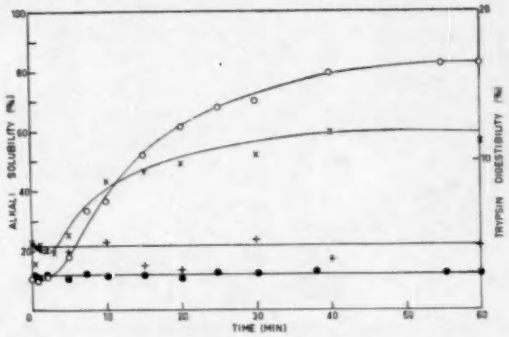

Fig. 1. Relation between the alkali solubility and trypsin digestibility of wool and the time of heating at 105° C. in the presence of sulfuric acid under aqueous and anhydrous conditions. ○ = alkali solubility, aqueous acid, ● = alkali solubility, anhydrous acid, × = trypsin digestibility, aqueous acid, and + = trypsin digestibility, anhydrous acid.

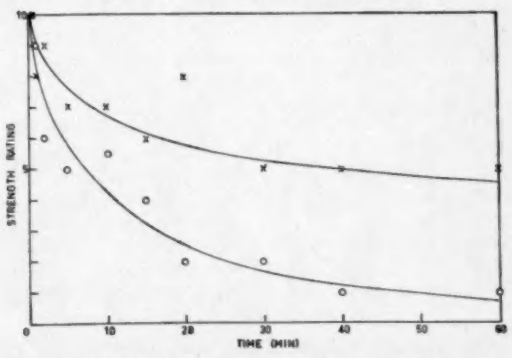

Fig. 2. Relation between the loss of strength of wool and the time of heating in the presence of sulfuric acid under anhydrous and aqueous conditions. ○ = anhydrous acid, × = aqueous acid.

[1] In industrial carbonizing trials, however, the presence of surface active agents in the acid caused a decrease in alkali solubility of the wool at various stages in processing [4]. A similar decrease occurred in the loss of weight of controls for the trypsin digestibility tests (Table II).

sin digestibility and alkali solubility, even though the results are derived from two experiments in which different samples of trypsin were used (Figure 3). A similar relationship holds between alkali solubility and the loss of weight of control samples in the trypsin solubility test (Figure 5).

Discussion

These experiments provide definite confirmation of the hypothesis that the nature of the reaction of sulfuric acid with wool depends on the amount of water present [1]. When water is present in considerable amount, catalytic hydrolysis of amide and peptide bonds by hydrogen ions occurs [8, 9]; breakage of these covalent linkages may be chiefly responsible for the increase in the amount of degraded protein extracted by alkali. Breakage of the covalent disulfide bonds of cystine residues is known to have a similar effect [6, 7].

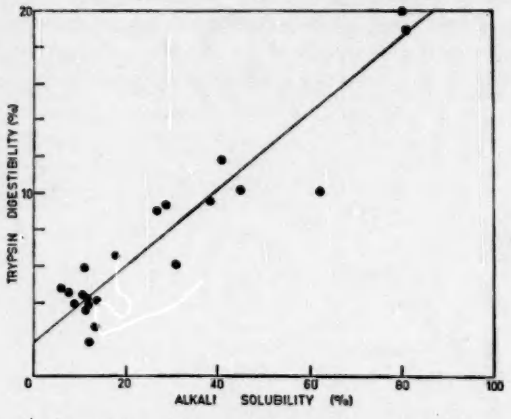

Fig. 3. Relation between the trypsin digestibility and the alkali solubility of wool heated with sulfuric acid under various conditions.

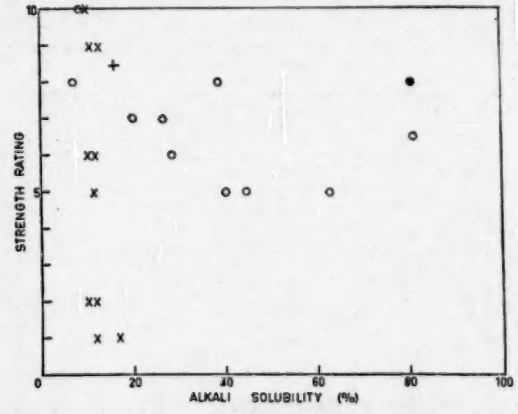

Fig. 4. Relation between the alkali solubility and the strength of wool samples heated in the presence of sulfuric acid under various conditions. ○ = aqueous acid, ● = aqueous acid containing surface active agent, × = anhydrous acid, and + = anhydrous acid containing surface active agent.

There is an increase in serine and theonine end groups in wool dried and baked with sulfuric acid [1], but it was suggested that this may be due to a mechanism other than catalysis by hydrogen ions. It was thought that a quantitative sulfation of seryl and threonyl alcoholic groups may occur during desiccation of the wool moistened with acid followed by selective rupture of the peptide bonds adjacent to the sulfated residues during baking. Though the strength ratings indicate loss of strength for at least the first 20 min. of heating at 105° C., they do not show whether the reaction responsible for loss of strength continues over the whole time range or reaches an equilibrium. The trypsin digestibility and alkali solubility tests give no information concerning this second type of reaction. Another chemical method of assessing the extent and nature of the reaction of anhydrous sulfuric acid with wool is therefore required before the catalytic or non-catalytic nature of this reaction can be determined.

The demonstration [3] that wool fibers from the bulk sample used in the present study supercontract during hydrolysis with dilute sulfuric acid at 100° C. may have some bearing on this investigation. Wool fibers which have been supercontracted by heating with solutions of either phenol or electrolytes such

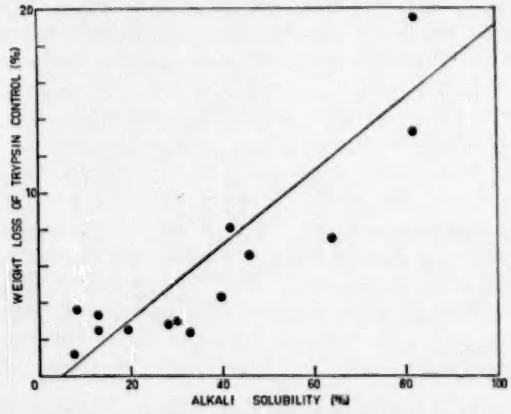

Fig. 5. Relation between the alkali solubility of wool heated in the presence of sulfuric acid and the loss in weight of the control samples for the estimation of trypsin digestibility.

as lithium bromide, lithium iodide, sodium iodide, or sodium thiocyanate are characterized by brittleness and low tensile strength after washing and drying. Microscopic examination of acid treated wool recovered from the trypsin digestibility tests showed that whereas the wool heated with anhydrous acid was degraded into cortical cells with little further breakdown, the cortical cells derived from fibers treated with aqueous acid were themselves breaking up into rod-like structures. Since wool supercontracted with other reagents is readily attacked by trypsin with extensive damage to the cortical cells, it seems unlikely that supercontraction is responsible for the loss of tensile strength of fibers heated with anhydrous sulfuric acid. However, the marked increase in trypsin digestibility of wool heated with aqueous sulfuric acid may be due partly to supercontraction of the fibers.

Dusenbury, Mercer, and Wakelin [5] have studied the increase in alkali solubility of wool during boiling in dilute acid at pH 1.6 (0.12% wt./vol.) They conclude that the *ortho*cortex is sensitised by the acid at a specific rate about 11 times that for the *para*cortex. With the higher acid concentration used in the present study, there is no indication of a similar two stage reaction (Figure 1). This may be due to the fact that the *para*cortex itself supercontracts when heated at 105° C. in 2 *N* sulfuric acid [3]. In the supercontracted condition many of the differences between the two cortical segments are minimized, so that even with partial supercontraction the whole of the wool fiber may become readily accessible to the acid.

These experiments give a more precise meaning to the alkali solubility test as applied to carbonized wools. It has been found by Lees and Elsworth [11] that the results of the alkali solubility test show good correlation with the resistance to abrasion of wool boiled in dilute sulfuric acid at concentrations in the range 3–22.5%; they suggest that this test gives a good indication of the performance of wool in wear after a particular type of treatment. They point out, however, that the history of the wool must be known if the alkali solubility test is to have any significance. It is now apparent that when dealing with carbonized wool, the reaction chiefly responsible for causing loss of strength and brittleness has no appreciable effect on the alkali solubility; the test indicates mainly whether the wool has been in contact with dilute acid for long periods or at high temperatures. It is conceivable that a carbonized wool could have a satisfactory alkali solubility and yet have greatly decreased resistance to wear. Although useful for detecting changes in wool due to treatment in alkali or alkaline detergent solutions, the slower and more cumbersome trypsin digestibility test is unlikely to prove more useful than the alkali solubility test for detecting damage to wool due to the action of aqueous acid. The good correlation between the two methods suggests that they assess the same modification in the wool structure. If the trypsin digestibility were being tested, the loss in weight of the control wool sample used for the trypsin digestibility test would give an adequate indication of alkali solubility.

It is also of interest to note from the control values for the trypsin digestibility (Table II) that the solubility of acid damaged wool in an alkaline medium is increased by the incorporation of a soap in the alkaline solution. Woolen garments which have suffered damage due to treatment with dilute acid may therefore lose considerable weight during washing in alkaline soap solutions both in the mill and in the home.

Literature Cited

1. Crewther, W. G., *Proc. Int. Wool Text. Res. Conf. Aust. 1955* **E**, 408 (1956).
2. Crewther, W. G., *Proc. Int. Wool Text. Res. Conf. Aust. 1955* **C**, 227 (1956).
3. Crewther, W. G. and Dowling, L. M., unpublished results.
4. Crewther, W. G. and Pressley, T. A., TEXTILE RESEARCH JOURNAL **28**, 67 (1958).
5. Dusenbury, J. H., Mercer, E. H., and Wakelin, J. H., TEXTILE RESEARCH JOURNAL **24**, 890 (1954).
6. Harris, M., *J. Research Nat. Bur. Standards* **15**, 63 (1935).
7. Harris, M. and Smith, A. L., *J. Research Nat. Bur. Standards* **17**, 577 (1936).
8. Leach, S. J., *Proc. Int. Wool Text. Res. Conf. Aust. 1955* **C**, 181 (1956).
9. Leach, S. J. and Parkhill, E. M. J., *Proc. Int. Wool Text. Res. Conf. Aust. 1955* **C**, 92 (1956).
10. Lees, K. and Elsworth, F. F., *J. Soc. Dyers Colourists* **68**, 207 (1952).
11. Lees, K. and Elsworth, F. F., *Proc. Int. Wool Text. Res. Conf. Aust. 1955* **E**, 425 (1956).
12. Pressley, T. A., *Proc. Int. Wool Text. Res. Conf. Aust. 1955* **E**, 389 (1956).
13. Standards Association of Australia, *Australian Standard Specification for Shrink-Resistance of Plain Knitted Underwear Composed Wholly or Partly of Wool.* A.S. No L.2. Appendix D.

Manuscript received July 15, 1957.

Rhovyl—Polyvinyl Chloride Fibers

L. Hochstaedter[1]

Rhodia, Inc., 60 East 56th Street, New York, N. Y.

POLYVINYL chloride (PVC) for the use of synthetic fibers became commercially important in 1913, at which time a patent [2] was issued for producing a polymerized vinyl chloride using gaseous hydrogen chloride, acetylene, and catalysts. In order to spin the PVC into a textile fiber, however, it was necessary to find a suitable solvent. This proved to be a difficult problem due to the inherent insolubility of PVC in most solvents. It was solved partially by I. G. Farben [1] when the PVC was postchlorinated and spun from an acetone solution.

The Rhodiaceta Company of France, one of the pioneers in acetate and producers of polyester, polyamide, and polyacrylic fibers, is credited with the major discoveries and advances in the manufacture of PVC into a textile fiber. Through their research, Rhovyl, a nonpostchlorinated PVC, was first spun in France in 1941. It is also manufactured under licensee agreements in Italy and Germany.

The reactions in the commercial manufacture of the polymer from which Rhovyl fiber is spun are based upon acetylene and hydrogen chloride.

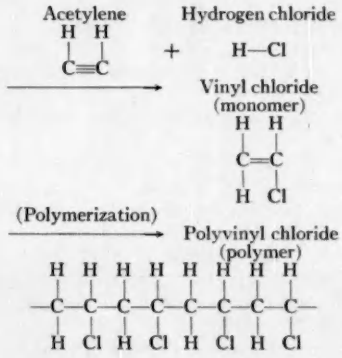

A dry spinning process, in which the solvent is evaporated from the filaments as they are extruded, is used in the manufacture of Rhovyl fibers. After the polyvinyl chloride solvent mixture has been heated and filtered, it is passed through the conventional spinnerets and down a hot air column that evaporates the solvent. The solvent-laden air enters a cold chamber where the solvent is recovered by condensation; the air is reheated for use in the evaporating column again. By this process, up to 90% of the solvent is recovered for re-use.

As the filaments leave the spinnerets, they must first be stretched to give them the characteristic crystallinity and molecular orientation of Rhovyl. Figure 1 illustrates the process diagrammatically.

Four types of Rhovyl fiber—Rhovyl 55, Rhovyl 30, Rhovyl 15, and Rhovyl T [2]—are produced by varying the molecular orientation to give these fibers residual shrinkages of 55%, 30%, 15%, and 0% respectively. The denier sizes of these are shown in Table I.

The general properties common to all of these PVC fibers are noninflammability, high resistance to atmospheric and destructive biological destructive agents, resistance to a wide range of chemicals, and thermoplasticity (see Table V).

The noninflammability of the PVC fibers is a permanent natural property. However high the temperature to which it is subjected, Rhovyl will not flame nor release molten incandescent drops which may ignite a combustible material.

TABLE I. Shrinkage Properties and Deniers of Rhovyl Types

	Shrinkage fibers			Non-shrinkage fiber
	Rhovyl 55	Rhovyl 30	Rhovyl 15	Rhovyl T
Possible shrinkage, % at 212° F.	55	30	15	0
Denier sizes	1.5	3.0	4.0	2.5
	1.8	6.0	7.5	3.5
	3.0			5.0
	6.4			8.0
				15.0

[1] Technical Sales and Service Representative.
[2] Trademarks of the Societe Rhovyl Company.

Tests were performed with 10 g. of blended yarns placed on a ceramic tile and subjected to a flame. The time from ignition to the total extinction of the yarns was measured, as shown in Table II.

We have said in the preceding paragraphs that Rhovyl shrinks up to 55% at a temperature of 212° F., and that Rhovyl was noninflammable to a high degree. These two statements may seem somewhat confusing at first, but may be explained as follows:

Although Rhovyl is noninflammable and will not release molten incandescent drops, this does not mean that a wearer is protected against heat of a high temperature. In fact, Rhovyl PVC fibers have a lower melting point than some of the other synthetics, but at the same time, the PVC will not emit flames or burn, nor release molten drops.

The resistance of the PVC fibers to atmospheric and biological destructive agents is excellent. During scientific expeditions, such as the Dragonfly Mission in Africa and the Tumuc-Humac Mountain Mission through the jungles of French Guiana, clothes, socks, tenting, mosquito netting, and many other forms of apparel and military equipment were subjected to rigorous testing. Under the extreme conditions such as desert heat, mountain cold, jungle humidity, and intentional exposures to termite, roach, and fungus attacks, no destruction, weakening, or rotting of the materials was reported. Controlled laboratory tests repeatedly confirm the properties found during these missions.

TABLE II. Results of Flame Tests

	Time required for total extinction, sec.	Residue, g.	Unburnt percentage
100% cellulose fibers	310	0.9	9
Blend of 75% cellulose fibers 25% PVC fibers	42	6.04	60.5
Blend of 50% cellulose fibers 50% PVC fibers	35	7.3	73
Blend of 25% cellulose fibers 75% PVC fibers	It is not possible to light this blend		

TABLE III. Comparison of Regain Values

Fiber	Increase in weight, %
Cotton	8.5
Spun viscose	13
Wool	17
Rhovyl	0

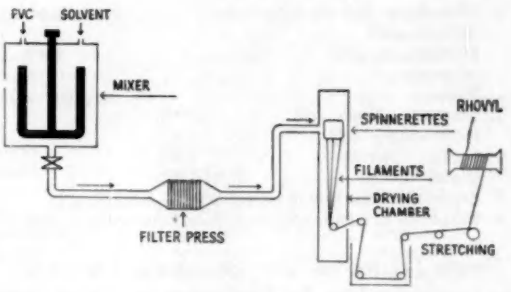

Fig. 1. Schematic diagram of Rhovyl manufacturing process.

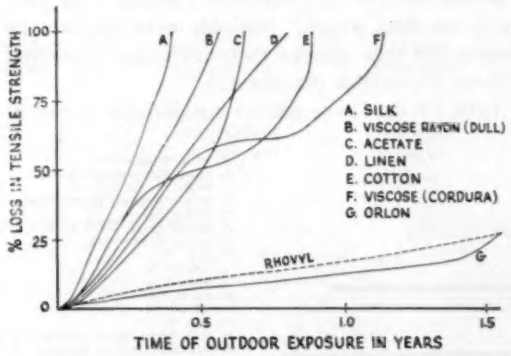

Fig. 2. Comparative losses in tensile strength—sunlight exposure.

Prolonged exposure to sunlight has little effect on the tensile strength of PVC. Figure 2 plots the loss in tensile strength of Rhovyl and seven other fibers under controlled exposure to Southern light. Only Orlon has a comparable resistance, with a 25% loss in strength after 1½ yr. [3].

The dynamometric properties of PVC are exactly the same wet and dry (Table V), and since PVC is also inert to mineral salts, it is completely unaffected by salt water.

PVC yarns will absorb water only by capillary action. The relative weight gains of Rhovyl vs. cotton, wool, and spun viscose at 68° F. and 65% relative humidity are shown in Table III.

The chemical resistance of PVC is the highest in the vinyl group. For example, Rhovyl fabrics are in use commercially to filter solutions such as those below where other filter materials have failed or are impractical.

1. Phosphoric acid (as anhydride)		40–60.0%
Sulfuric acid		3.5%
Hydrofluoric acid		1.0%
Alumina		0.3%
Water		to 100.0%
2. Methene sulfonic acid	21.0%	
Hydrochloric acid	31.0%	
Sodium chloride	3.0%	
Water	to 100.0%	

3. Separation filtration of adipic acid from nitric acid.
4. Filtration of acetic acid 30% containing sulfuric acid.

Froger [4] reports that "Samples of Rhovyl fabrics have been kept for four years in concentrated nitric acid, sulfuric acid (66° Bé.), potassium chloride solution (47° chlorometric), caustic soda (36° Bé.), and 50% potash. Not only were they not destroyed, but they retained their mechanical properties without appreciable deterioration."

Table IV lists some relative comparisons of chemical resistance of PVC and other fibers to acids, alkalies, and oxidizing agents.

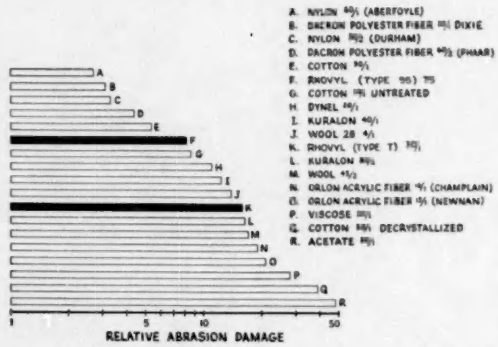

Fig. 3. Resistance to abrasion of various textile fibers. The average values of relative abrasion damage are demonstrated graphically on a logarithmic scale to show the small differences in yarns with low abrasion damage and also the great differences among the textile fibers.

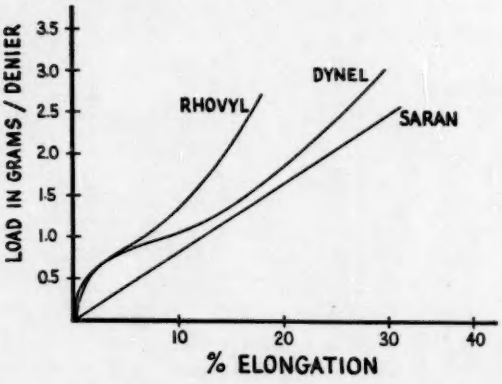

Fig. 4. Stress–strain curves.

Application of Blends

Today, Rhovyl 55 and Rhovyl T yarns are made commercially in a wide range of sizes for the different spinning systems. Table VI lists sizes of PVC fibers and blends on the cotton, woolen and worsted systems.

Table VII shows the general applications of the Rhovyl types for pure and blended fibers on the cotton, woolen, and worsted systems.

All of the above yarns have been manufactured for the cited applications for up to 10 years, and the engineering and handling problems that confront a new synthetic have been resolved. For example, in the spinning of Rhovyl T, control of tension and roll settings avoids undesired stretching. For fabrics with Rhovyl 55, special techniques to assure uniform shrinkage have been developed and are recommended.

Shrinkage fibers may be employed in a multitude of different unusual applications, such as novel three-dimensional fabrics. A background in the mechanics of these fibers is helpful for a realization of their potential applications.

Muchiroud (6) reported in "The Journal of the Textile Institute":

> In the Woolen industry, the phenomenon of milling; i.e., shrinkage of the cloth with moisture, heat and mechanical action, is employed extensively, where the wool fibers turn the network or raw woven or knitted goods into a compact and homogeneous cloth or felt.
>
> Rhovyl 55 also is able to bring about the "shrinkage" of a fabric of which it forms an integral part, by a phenomenon which is without doubt different from that of milling, but which can often be associated with it. It is, moreover, a strong textile material which will enable the manufacturer to produce various effects among which the following four are mention in particular:
>
> (1) To maintain the quality of the blend and increase the strength of the final cloth.
> (2) To use Rhovyl 55 in order to compensate for the loss of firmness in a fabric resulting from a lowering of the quality of the raw materials and to shorten the milling time and increase the yield.
> (3) The elimination of the milling process and its substitution by a heat treatment, thus allowing advantageous modifications in the appearance of the cloth.

TABLE IV. Chemical Resistance Properties

Chemical agent	Acrylic fibers	Polyamide fibers	Polyvinyl chloride fibers
Acids at 20° C.			
Formic acid, conc.	resistant	dissolved	resistant
Chromic acid, 50%	resistant	attacked	resistant
Acetic acid, conc.	resistant	attacked	resistant
Hydrofluoric acid, 70%	resistant	attacked	resistant
Aqua regia	deteriorated	destroyed	resistant
Nitric acid, 50%	attacked	destroyed	resistant
Hydrochloric acid, 30%	attacked	dissolved	resistant
Sulfuric acid, 50%	attacked	destroyed	resistant
Sulfuric acid, 96%	dissolved	destroyed	resistant
Alkalies at 20° C.			
Potassium hydroxide sol., conc.	not resistant	resistant	resistant
Sodium hydroxide	not resistant	resistant	resistant
Ammonia hydroxide	resistant	resistant	resistant
Oxydizing agents at 20° C.			
Sol. of bleach with 15% chlorine	resistant	not resistant	resistant
Sol. of potassium permanganate, conc.	resistant	not resistant	resistant

TABLE V. General Properties of Rhovyl Staple

	Fibravyl staple	Thermovyl staple
Tensile strength, g./d.		
Std.	1.6–2.4	0.7–1.3
Wet	1.6–2.4	0.7–1.3
Std. loop	83% of yarn-stretch	87% of yarn-stretch
Std. knot	75% of yarn-stretch	83% of yarn-stretch
Tensile strength (lbs./sq. in.)	28,700–43,000	12,000–22,400
Elongation, %		
Std.	16–40	120–180
Wet	16–40	120–180
Elastic recovery, % of breaking elongation	50 at 80% 57 at 33% 100 at 11%	0 at 20% 100 at 2%
Resistance to abrasion	Excellent (see Figure 3)	
Average stiffness, g./d.	10	0.6
Average toughness	0.25	1.35
Specific gravity	1.4	1.35
Moisture regain	0% at 70° F., 65% RH	
Moisture absorbency	0% at 70° F., 85% RH	0.35% at 70° F., 97% RH
Effect of heat	Starts to shrink at about 168° F. Decomposes at 350° F. Does not burn	Starts to shrink at 212° F. Decomposes at 350° F. Does not burn
Effect of age	None	None
Effect of sunlight	Very little	Very little
Chemical resistance	Excellent (see Table IV)	
Effect of organic solvents	Soluble in mixture of carbon disulfide and acetone. Affected by some phenolic compounds, chloroform, trichlorethylene, nitrobenzene.	
Dyes used	Selected dispersed (acetate) and developed (azoic). Pigment dyeing.	
Resistance to moths	Not attacked	Not attacked
Resistance to mildew	Not attacked	Not attacked
Electrical properties	Low conductance. Developes high negative charge	
Identification	Does not support combustion. Soluble in a mixture of carbon disulfide and acetone.	

TABLE VI. Deniers and Yarn Numbers of Rhovyl and Rhovyl Blends

Composition	Denier	Yarn numbers
Cotton System		
Rhovyl 55		
100% Rhovyl 55	3.0	6–12
	1.8	17–24
30% Rhovyl 55 70% Nylon	1.8	36 29–17
30% Rhovyl 55 70% Viscose	1.8	36–29–17
25%–30% Rhovyl 55 70%–75% Rhovyl T	1.8	36–29–17
25%–30% Rhovyl 55 70 –75% Cotton	1.8	17
Rhovyl T		
100% Rhovyl T	3.5	6–12–17
82% Rhovyl T	3.5	16.5–23.5–28.5–30 33.5
30% Rhovyl T 70% Viscose	5 or 3.5	17.7–21–23.5–30 28.5
Woolen System		
Rhovyl 55		
100% Rhovyl 55	3	3.4–5.0
80% Rhovyl 55 20% Wool	3	Various
Rhovyl T		
100% or blends of 2 denier sizes	3.5	8.0–9.0
100% or in blend with 20% wool, viscose, Nylon, or Orlon	Same	8.0–9.0
100% or blends of both denier sizes	5 and 8	2.0–6.0
100%	8	2.0–3.4
Blend with 25% of viscose or Rhovyl 15 or 30	Various	Various
Blend with 8–12% wool	3.5 and 5	Various
Rhovyl 30 and 15		
Blend with different denier sizes of Rhovyl T	3 and 6	Various
Blend with wool or wool-Rhovyl T		
Worsted System		
Rhovyl 55	(Worsted Count)	
100% Rhovyl 55	3 or 1.8	Up to 88.5
70% Rhovyl 55 30% natural or synthetic fibers	1.8	71.5 54–42.5–26.6
Rhovyl T		
100% Rhovyl T	8	8.8
100% Rhovyl T	8 or 5	21–26.5
100% Rhovyl T	5–3.5	35.5
100% Rhovyl T	3.5	44–50
82% Rhovyl T 18% Nylon	3.5	25–35–42 44–53
75% Rhovyl T 25% Nylon	3.5	72
60% Rhovyl T 40% Nylon	3.5	88.5
33% Rhovyl T 67% Wool	5 or 3.5	25–35
49% Rhovyl T 51% Wool	5 or 3.5	25–35–60–53

(4) A very great improvement in the resistance to abrasion of the fabric.

In order to bring out the finer points of the above effects, Muchiroud cites examples of each, substantially as follows:

Effects 1 and 4. A fabric with 12% Rhovyl 55 was manufactured similar in respect to an acetate–wool or 100% wool fabric. Processing such as spinning, weaving, and wet finishing was also handled in the usual manner.

Rhovyl 55 behaved as an inert material during milling, working its way towards the center of the fabric together with the acetate staple. The heat treatments (calendering, decatizing, and tentering) during dry finishing, however, caused Rhovyl 55 to shrink, following the shortest possible route. The resultant fabric, due to shrinkage, had a strength far in excess of that usually required for this type of cloth—see Table VIII.

> It is interesting to note the way in which the Rhovyl 55 moves into the center of the yarns in the cloth during finishing. The sample of the above cloth is a solid shade and shows no flecks, despite the fact that the 12% of Rhovyl 55 was undyed. The dissolving of the wool in caustic soda exposes the skeleton of Rhovyl 55.

Effect 2. The effect of quality compensation is illustrated in a case where a government specification would normally require that 80% virgin wool be used. A new blend (where a high percentage of the wool was of poor felting qualities) was made of 20% pulled rags (mungo) and only 20% virgin wool, and met all specifications. Any such blend without Rhovyl 55, of course, does not "mill" properly with respect to rate or amount of contraction, and after prolonged "milling" actually loses strength and deteriorates. The author [5] continues "despite its inferior materials, the new blend will be comparable to that of a fabric containing a higher proportion new wool."

Effect 3. Here a heat process is substituted for milling to make a worsted "appearing" fabric on the woolen system. Normally, on the worsted system overcoating material is made of plied yarns with fairly fine counts in the singles, both in warp and filling, in order to have a close set warp. The contraction of this type of cloth is slight during finishing.

With only 15% Rhovyl 55 in the blend, however, the woolen manufacturer may imitate the worsted type of cloth on his woolen spinning equipment, and,

TABLE VII. Application of Rhovyl and Rhovyl Blends

	Rhovyl 55	Rhovyl T	Rhovyl 15 and 30
Spinning on the Cotton System			
Pure	Filtration fabrics Underwear Mosquite netting Cloque and 3-D effect fabrics Fish nets Cable coverings	Underwear Shirt fabrics	
Blends of			
Cotton or viscose	Shrinkage yarns Imitation fulling	Dress material	
Acetate	Suede or deer-skin effect	Shirting material	
Other synthetics	Suede effect Shrinkage yarns Fancy yarns	Underwear Pleated skirt material Men's hose	
Spinning on the Woolen System			
Pure		Diapers Carpet yarns Mosquito netting Upholstery goods Filtration fabrics Underwear	
Blends of			
Wool	Cloque or 3-D Carpet yarns Upholstery Material for: suits, coats, blankets	Underwear Jackets, sweaters, suits	Cloque or 3-D Bulk yarns for hand knitting
Cotton or viscose	Blankets	Underwear	
Acetate	Blankets		
Synthetics	Suede or deer-skin imitation	Blankets	Imitation fulling Blankets Diapers—all PVC
Spinning on the Worsted System			
Pure	Filter fabrics Fish nets Cable coverings	Filter fabrics Upholstery material Underwear Shirting fabrics	
Blends of			
Wool	Shrinkage yarns Suede or deer-skin	Underwear Sweaters Dress fabrics Men's hose Hand knitting wools	Shrinkage yarns Hand knitting wools
Cotton or rayon	Imitation suede	Wrinkle-proof fabrics	
Synthetics	Chemical-resistant work fabrics	Underwear Shirting fabrics Work clothes Table cloths	

instead of using a plied yarn, he may employ a single yarn. In this case, Rhovyl 55 shrinks in such a manner to close up the ends and picks without felting or losing the clear finish associated with worsted fabrics.

Finishing

When working with the shrinkable Rhovyl 55 fiber, finishing treatment will vary for the different textiles according to whether Fibravyl is used as a 100% yarn in making cloques or 3-D fabrics, in blends with either natural or synthetic fibers, or in bulk yarns. Yarns may be shrunk before or after dyeing, in hot water baths, or on heated rolls or loop dryers. Precautions must be taken against any undue tensions and temperature variations to obtain even shrinkage rates. In the shrinking of an all PVC cloth, such as for filtration of very fine particles, the cloth is mounted on a jig. The let-off wind roll must be completely tensionless so as to permit free passage through the bath and allow free, unrestricted shrinkage. Even shrinkage is obtained by passing the fabric back and forth through the jig into progressively hotter baths. An example of the temperatures and handling used commercially would be:

Temperature, °C.	No. of passages
85	2 (once backwards, once forward)
90	2
95	4
100	6

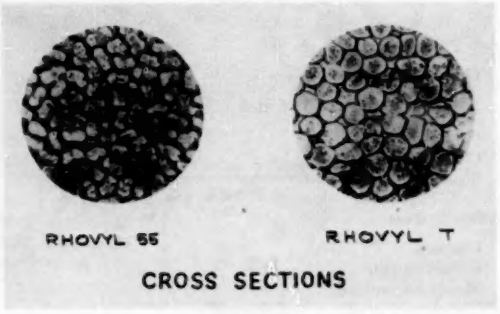

Fig. 5. Cross sections of PVC fibers.

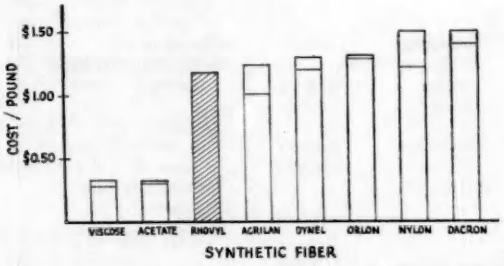

Fig. 6. Comparative cost of white or whitened synthetic textile fibers (October 1, 1957).

TABLE VIII. Results of Tests on Samples Containing 12% Rhovyl 55*

	Warp, kg.	Filling, kg.	Abrasion
Strength specifications for an all-wool cloth	34.0	30.0	1,500
Strength of samples containing 12% Rhovyl 55, same weight as above	56.7	43.1	14,500

* Figures from [8].

Dyeing

PVC fibers may be dyed with acetate colors, naphthols, and indigosols, the choice depending on properties desired, such as light fastness, wash fastness, crocking, etc. The Rhovyl Co. also has perfected a range of twenty shades of dope-dyed colors for their staple fibers.

Stains and antistatic oils from looms may be removed by scouring for 1 hr. at 50–60° C. in a bath containing 2 cc. of liquid caustic soda 36° Bé. and 1 cc. of a fatty sulfonated amide or alcohol/l. of water. If the cloth is very heavily stained, an auxiliary bath of 1 g. of trisodium phosphate and 1 g. of ammonia/l. of water may be used.

With Rhovyl 55, dyeing is carried out either before or after shrinkage. If it is dyed before shrinkage, a carrier such as Dacronol is used to obtain dark shades with the acetate dyes. After shrinkage, Rhovyl 55, like Rhovyl T either in blends or alone, may be dyed without a carrier.

With Dowicide A as the carrier, the following procedure is used to dye Rhovyl 55 before shrinkage at 140° F. in a bath containing the following:

0.25–0.5 g./l. Duponol RA at 120° F.
5.0 g./l. Dowicide A
5.0 g./l. diammonium phosphate

Dispersed dye pasted with 2.0% Avitone T. Dye 1–½ hr.—rinse and scour with 2% Duponol RA surface active agent N.

A few of the Latyl, Acetamine, and Celanthrene (Du Pont) dyes are:

"Latyl" Yellow 3G
"Latyl" Orange R
"Latyl" Cerise B
"Latyl" Scarlet FS
"Latyl" Violet 2R
"Latyl" Blue RB
"Latyl" Blue 4R
"Latyl" Yellow YL
"Latyl" Orange 3R
"Latyl" Red B
"Latyl" Violet BN
"Latyl" Blue FL
"Latyl" Blue RL
"Latyl" Brilliant Blue 2G
"Latyl" Brilliant Blue BG
"Acetamine" Fast Yellow 4RL
"Acetamine" Yellow CG
"Acetamine" Orange GR Conc. 175%
"Celanthrene" Fast Yellow GL Conc. 300%
"Celanthrene" Fast Pink 3B
"Celanthrene" Violet BGF
"Celanthrene" Brilliant Blue FRN Conc.

Summary

The properties of nonpostchlorinated PVC fibers, such as noninflammability, extreme resistance to chemical attack, and, in Rhovyl 55, high shrinkage, place these Rhovyl fibers in a unique position among synthetics.

Rhovyl 55, which shrinks up to 55%, is most often used in industrial filters, bulk yarns for novelty effects (suede, three-dimensional fabrics, etc.), and wherever high resistance to abrasion is necessary.

Rhovyl 15 and Rhovyl 30 are intermediate partially shrunk PVC fibers with residual shrinkage of 15% and 30% respectively, and are used in bulk knitting yarns, for imitation fulling, and special novelty effects.

Rhovyl T is Rhovyl that is preshrunk so as to be applicable to apparel fabrics and is used where softness, crease resistance, and compatability in blends are desired.

Literature Cited

1. Froger, C., *Fibres, Engineering and Chemistry* **17**, 289 (1956).
2. German patent 281,877 (July 4, 1913).
3. McFarlane, S. B., "Technology of Synthetic Fibers," Fairchild Publication, New York, 177 (1953).
4. McFarlane, S. B., "Technology of Synthetic Fibers," Fairchild Publication, New York, 431, 445, 447 (1953).
5. Machiroud, G., *J. Textile Inst.* **43**, P469 (1952).
6. Susich, G., TEXTILE RESEARCH JOURNAL **24**, 225 (1954).

Manuscript received August 28, 1957.

Letters to the Editor

Short communications in the form of Letters to the Editor are intended to provide prompt publication of significant new research results and to permit an exchange of views on papers previously published in the JOURNAL. These communications are not submitted to formal review as are research papers, and the editors do not assume any share of the author's responsibility for the information given or the opinions expressed. When work previously published in the JOURNAL is the subject of critical comment, the authors of the original paper are given an opportunity to submit a reply, which will be published concurrently when possible.

Activation Analysis of Fibrous Materials

North Carolina State College
School of Textiles
Raleigh, North Carolina
October 24, 1957

To the Editor
TEXTILE RESEARCH JOURNAL

Dear Sir:

In connection with the work in this Laboratory dealing with the effect of nuclear radiation on fibrous materials, it has been found that many fibers become radioactive when subjected to a high flux of neutrons. This behavior has been observed in wool, cotton, rayon, and acetate, as well as a few synthetic fibers. Radioactivities induced in the samples may be identified by appropriate nuclear techniques; a method is therefore provided for determining in trace quantities chemical elements (generally impurities) present in the sample.

TABLE I

Fiber	Radiation type	Energy, Mev	Half life, days	Isotope
Cotton	beta	1.70	14.1	P^{32}
Rayon	beta	1.64	14.3	P^{32}
	gamma	0.511; 1.105	long	(?)
Acetate	beta	0.100	46.7 (?)	Hg^{203} (?)*
	beta	1.31	12.8	I^{126} (?) / Ba^{140} (?)

Table I is an example of preliminary work in this connection dealing with three fibers.

The type of radiation emitted by the radioactive samples after exposure is shown in Column 2, and the energies and half lives associated with the radiation are given in Columns 3 and 4. Phosphorus^{32} has been positively identified in cotton and rayon. The elements responsible for the remaining radiation types shown as yet are not definitely identifiable, but Mercury^{203}, Barium^{140}, and Iodine^{126} are suspected.

It is planned to continue this work in greater detail, and it is anticipated that many more elements may be found, particularly when the activation analysis is conducted upon these fibers immediately upon removal from the neutron bombarding source. This method is very practical for the analysis of fibers for trace materials, and can be conducted in a short period of time. Exposure of the sample for a maximum of 500 min. at a neutron flux rate of 1.5×10^{12}/cm.^{2}/sec. is required to induce the necessary radioactivity for analysis. The basic data for the analysis may be obtained within 2 hr.

OTTO TESZLER
HENRY A. RUTHERFORD

IP-4 Chart Computer

American Enka Corporation
Research and Engineering Division
Enka, North Carolina
September 16, 1957

To the Editor
TEXTILE RESEARCH JOURNAL

Dear Sir:

In testing cord strengths by means of the Scott IP-4 Tester, it is frequently the practice to make a standard number of breaks from each sample and to use the average strength and elongation of these breaks as the best estimate of the sample properties. This information is usually obtained from the chart by reading visually and writing down the value of the strength and elongation of each break, adding up these values, and dividing by the number of breaks to find an average. In this process considerable time is consumed, and there are several opportunities for errors to creep in. As a means for speeding up this calculation and avoiding the possible errors, a small plastic analog computer was designed.

Since the IP-4 chart presents its data as distances, one must be able to feed in these distances to the computer, and it must then present the average of these distances. If the number of breaks is always constant, the process of addition and division can be accomplished by a proper choice of scales, so that it is only necessary to provide means for accumulating successive displacements and reading the final average result. The instrument used to do this is shown in Figure 1.

Essentially, it consists of a frame containing a base line (1) and having a slide (2) free to move perpendicularly to this base line. The slide carries an anvil (2a) which coincides with the base line when the slide is in its lowest position. The slide also normally carries with it a movable scale (3), but this scale may be locked with reference to the frame by the small button (4). In calculating the average strength in five IP-4 breaks, for instance, the frame is placed and held with the base line along some arbitrary strength level slightly less than the lowest break indicated, and preferably at some value which is a multiple of 10. A pencil or steel pointer is then placed at the break in the first IP-4 curve, and the slide, carrying the scale with it, is pushed upward until the anvil is stopped by the pencil. At this point the scale is locked in position and the slide returned to its zero position. The pencil or marker is then placed at the break of the second IP-4 curve, and the slide moved upward again, carrying the scale, until stopped by the pencil. As before, the scale is locked, the slide returned to its original position, and the process repeated for the rest of the breaks. In this way the scale is moved upward with reference to the frame a distance equal to the sum of the heights of the breaks above the base line. If a standard number of breaks is always used, the scale may then be designed to read the average distance; when this is added to the arbitrarily chosen reference line, the average breaking point is obtained. To calibrate the scale, multiply the length of a unit division of the IP-4 chart by the number of breaks to be averaged, and make the length thus obtained a unit division of the sliding scale.

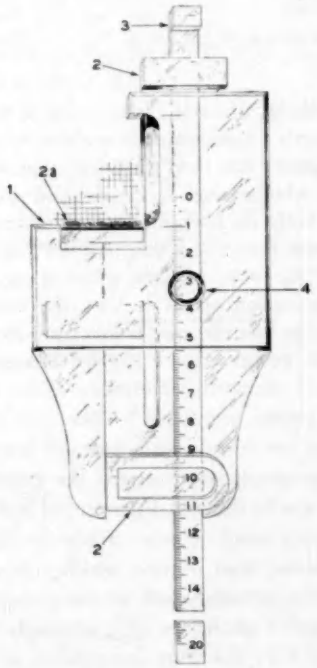

Fig. 1.

In the same way, by turning the chart sideways, the total elongation and the elongation at 10 lb. may be averaged. If, as is the case in this laboratory, the IP-4 chart is displaced by 0.2 in. along the extension axis between each break, proper compensation for this shift must be made. To do this it is only necessary to subtract a fixed value from the average obtained, or if desired, to read the sliding scale at a different index point.

This instrument has been in use in our laboratories for more than two years and has proven quite satisfactory. The manipulation, while difficult to describe, is quickly and easily learned. The major drawback is, of course, that this computer provides only an average value with no indication of the variability or spread in the breaking point values. For some types of work, however, the average values are quite sufficient, and in these cases it has been found that this instrument can provide a greater speed in obtaining the results and can also be of help in avoiding computational errors.

C. M. RICE
J. P. PARKER

Some Historical Evidence Relative to the Assessment of Wool Fiber Diameter

Department of History
and Philosophy of Science
University of Melbourne
Carlton, N. 3, Australia
August 14, 1957

To the Editor
TEXTILE RESEARCH JOURNAL

Dear Sir:

In the classing of wool, the question of the validity of the classer's counts estimation given by visual and tactile judgment has been a subject of much controversy as to whether such a classification is based partially or wholly on fiber diameter and/or crimp.

It has been found [6] that only for diameter differences of the order of three microns was "reasonable discrimination" possible with the unaided eye. Thus, with no intereference from crimp shape, fibers singly or in groups should not be differentiable on the basis of diameter differences alone when the equivalent counts are above 44/46s.

The literature reveals many cases of investigations which have attempted to assess the capabilities of the human eye in the visual perception and discrimination of very small objects. Early in this century it was reported that objects which subtend visual angles of five seconds could be recognized as separate by trained observers [5], although the more recent wool fiber diameter assessments of both experts and laymen were found to be very similar [6]. It has generally been accepted that bright line sources required subtended visual angles of the order of the Helmholtz figure of 60 seconds, but many much smaller values have been recorded in special cases, e.g., 3–4 seconds [1, 10], 1.0 second [11], and even as low as 0.5 second [4].

In defining visual acuity as the inverse of the visual angle in minutes, it has been shown repeatedly that acuity can vary considerably with such factors as the illumination of the object [2, 3, 8, 11], the shape of the object [8], the wave length of the incident light [8, 11], and the object distance [7].

The application of any of the above results or others of similar nature to the practical problem of wool classing must be made very cautiously and only on the basis of further optical and tactile research. Further quantitative evidence will be necessary on the vernier acuity of the eye and also on the degree of applicability of the Weber-Fechner law. For example, it is known that the vernier acuity of the eye (the power of recognition of variations in the width of a line) is many times higher than the traditionally defined resolving power. On the basis of the Weber-Fechner law an exceptionally low stimulus change seems able to produce perceptible differences in optical sensation [9].

The purpose of this note is to draw attention to previous investigations which may suggest lines of inquiry into the wool classing problem and which have certainly shown the human eye to be capable of discriminations quite beyond that thought possible

on the basis of the traditionally accepted resolving power.

Literature Cited

1. Hartridge, H., *J. Physiol.* **57**, 22 (1923).
2. Hecht, S., *J. Gen. Physiol.* **11**, 255 (1928).
3. Hecht, S., *Bulletin No. 4*, Howe Lab. Ophthalmology, Harvard (1931).
4. Hecht, S. and Mintz, E. U., *J. Gen. Physiol.* **22**, 593 (1939).
5. Hill, A., *The Body at Work*, Arnold, London (1908).
6. Lang, W. R., *J. Aust. Inst. Agr. Sc.* **12**, 108 (1946).
7. Luckiesch, M. and Moss, F. K., *J. Opt. Soc. Amer.* **31**, 594 (1941).
8. Macleod, J. J. R., *Physiology and Biochemistry in Modern Medicine*, Mosley, St. Louis (1926).
9. Moncrieff, R. W., *The Chemical Senses*, Wiley, New York (1946).
10. Reese, H. M., *J. Opt. Soc. Amer.* **29**, 519 (1939).
11. Wells, G. L., *Ibid.* **33**, 487 (1943).

F. BRYANT

Modified Vibrascope Technique

G. F. Bush Associates
Box 175
Princeton, N. J.

October 4, 1957

To the Editor
TEXTILE RESEARCH JOURNAL
Dear Sir:

Perhaps the following might be useful as an aid to Vibrascope users.

A modification of the vibrascope technique previously described [1, 2, 3] has been developed. This method of fiber linear density determination obviates the necessity of employing a delicate microbalance or variable precision oscillator. A fiber of ½ to 3 in. in length is vibrated at constant frequency and variable load until it resonates for a given preset length. While two such lengths are theoretically sufficient to determine the linear density, three lengths will check the straight line given by

$$w = k_3(R_2 - R_1) \tag{1}$$

where

$$k_3 = k_c/(2f)^2(L_2^2 - L_1^2)$$

For example, if k_c is 2.79 dynes/dial div., L_2 and L_1 are 2.54 and 1.91 cm., and f is 1000 cps, then $w = 0.247(R_2 - R_1)10^{-6}$ g./cm. If R_2 and R_1 are 50.3 and 9.5, then w, the linear density, is 10.1 (10^{-6}) g./cm.

The derivation of Equation 1 is as follows:

$$w = P/(2fl)^2 = (P_0 + k_cR)/(2fL)^2$$

where

$$P = P_0 + k_cR$$

or

$$R = [(2fL)^2w - P_0]/k_c$$

$$k_c = \frac{\Delta P}{\Delta R} \tag{2}$$

Then

$$dR/dL^2 = \text{slope of Figure 1} = (2f)^2w/k_c$$

from which

$$w = [k_c/(2f)^2]\,dR/dL^2$$
$$= [k_c/(2f)^2](R_2 - R_1)/(L_2^2 - L_1^2)$$
$$= k_3(R_2 - R_1)$$

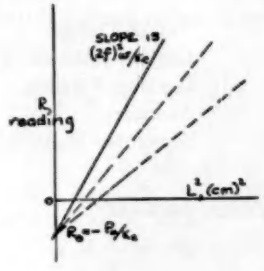

Fig. 1.

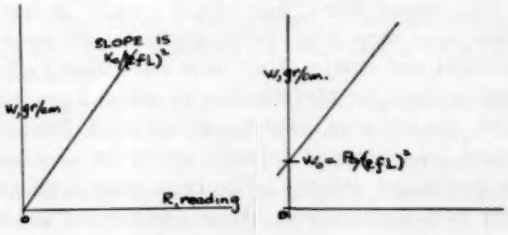

Fig. 2.

The term k_3 is defined in the following equation as

$$k_3 = k_c/(2f)^2(L_2^2 - L_1^2)$$

w = linear density, g./cm., R_2 and R_1 are readings of the vibrascope dial, $k_3 = k_c/(2f)^2(L_2^2 - L_1^2)$, L = fiber specimen gauge length, cm., f = fiber frequency, k_c = fiber load/dial division, P = fiber load, and P_0 = fiber load when R is zero.

Precision gauges or a graduated adjustable fret expedite an accurate setting of the various lengths so that a "vibraweigh," as this method of weighing might be called, can usually be made in less than five minutes.

A typical plot of Equation 2 is given by Figure 1, in which it should be noted that

1. The R intercept value $R_0 = -P_0/k_c$ can be calculated from k_c and P_0, the number of fiber-loading links when R is zero, and the load per link.
2. All graphs of any linear density pass through R_0, as shown by the dotted lines.
3. The plot of Figure 1 in this "vibraweigh" method may reveal instrument or operator errors, since the points should all be on a straight line passing through R_0.

A calibration curve such as either Figure 2a or Figure 2b for a given Vibrascope may be obtained by using two, preferably three, linear density values obtained by the Vibraweigh Method. While the slope in each is $k_c/(2fL)^2$ and can be readily calculated as the "instrument characteristic," the intercept in Figure 2b is now $w_0 = P_0/(2fL)^2$. That the graph does not pass through the origin is not serious, as long as the vibrascope operates within the desired range.

G. F. BUSH
Director

Literature Cited

1. Dart, S. L. and Peterson, L. E., TEXTILE RESEARCH JOURNAL **22**, 819–822 (1952).
2. Gonsalves, W. E., TEXTILE RESEARCH JOURNAL **17**, 369–385 (1947).
3. Montgomery, D. J. and Milloway, W. T., TEXTILE RESEARCH JOURNAL **22**, 729–735 (1952).

Cortical Differentiation in Burmese Wool

Textile College
Gordon Institute of Technology
Geelong, Victoria
Australia
September 26, 1957

To the Editor
TEXTILE RESEARCH JOURNAL

Dear Sir:

During a recent visit to the Union of Burma (July–August 1956), four typical samples of Burmese wool were submitted to the writer for measurement and study. They were understood to be derived from the Meiktila District, where a grazing flock was observed. The breed was small, Roman-nosed, lop-eared, and definitely not of the fat-tailed or fat-rumped varieties. The fleece showed brown and black pigmentation. Mean fineness and staple length measurements revealed the following:

Sample	Mean fiber thickness, μ	Standard deviation of fiber thickness	Coefficient of variation of fiber thickness, %	Range, μ	Staple length, cm.
1	49.2	30.6	62.1	128	6.0
2	69:3	37.0	53.4	128	7.0
3	62.1	34.1	54.9	126	8.0
4	40.9	28.4	69.5	120	8.5

The medulla in the coarser fibers was so large that the cortex and cuticle together formed an annulus of only 10–20μ thickness. Since Ahmad and Lang [1] had noted that in a variety of Pakistani carpet wools, which with one exception had mean finenesses in the 30–40μ region, the coarser fiber cross sections showed a typical orthocortical annulus around the medulla and the finer fibers showed bilateral segmentation, it was thought useful to examine all fibers in the Burmese wool for cortical segmentation. When these latter were stained with either Methylene Blue or Coomassie Violet RS, the

finer fibers showed some cortical differentiation; fiber thickness increased and a central orthocortex became more common, both in the presence and in the absence of a medulla. In the coarsest fibers—60–140μ—there was no indication of any cortical differentiation. This latter was in contrast to the Pakistani carpet wool results and accorded with the observations of Dusenbury and Jeffries as reported by Dusenbury and Menkart [2], who, in characterizing B.A. fleece wool of mean diameter 50μ, noted that there was no indication of cortical asymmetry and suggested that the two components, if present, may be randomly distributed.

Literature Cited

1. Ahmad, N. and Lang, W. R., TEXTILE RESEARCH JOURNAL **26**, 954 (1956).
2. Dusenbury, J. H. and Menkart, J., *Proc. International Wool Textile Research Conference, Australia* **F142** (1955).

W. R. LANG

A Rapid Approximation for Standard Deviation and Coefficient of Variation

Courtaulds, Inc.
Research Lab.
Mobile, Alabama
October 7, 1957

To the Editor
TEXTILE RESEARCH JOURNAL
Dear Sir:

The routine computation of standard deviations, or standard deviations expressed as a percentage of the averages (i.e., the coefficients of variation) from groups of test data is at best an onerous talk. It seems, however, that many laboratories find this quantity useful, particularly in single fiber work. In most cases, the reason for obtaining this statistic is the fact that it gives an indication of the spread of the data. More precisely, for large samples of a normal distribution, approximately 68% of the universe from which the sample was drawn lie within plus or minus one standard deviation of the average.

The question presents itself, that since one is primarily interested in the spread of data, why compute a laborious statistic which approximates it, instead of measuring it directly? We have found the following technique very useful for approximating standard deviations, and consider the result more indicative of the true spread of data than the true standard deviation σ.

$$\sigma = \left[\frac{1}{n-1}\sum_{i=1}^{n}(\chi_i - \bar{\chi})^2\right]^{\frac{1}{2}} = \left[\frac{1}{n-1}\left\{\sum_{i=1}^{n}\chi_i^2 - \frac{1}{n}\left(\sum_{i=1}^{n}\chi_i\right)^2\right\}\right]^{\frac{1}{2}} \quad (1)$$

where χ_i = the ith value, $\bar{\chi}$ = the average value $\left(\frac{1}{n}\sum_{i=1}^{n}\chi_i\right)$, n = number of values, and σ = standard deviation.

For convenience, we refer to the statistic obtained by our method as σ', and the corresponding "average" as $\bar{\chi}'$. We desire to find σ' such that 68% of the χ_i lie within $\bar{\chi}' \pm \sigma'$. Assuming a non-skewed distribution, of the 32% of the values outside this range, 16% will lie above and 16% below. We then merely count in from both extremes a number of values equal to 16% n (i.e., approximately $\frac{1}{6}n$) to obtain two values, χ_a and χ_b, $\chi_b > \chi_a$.

We then define

$$\sigma' = \frac{\chi_b - \chi_a}{2}$$

$$\chi = \frac{\chi_a + \chi_b}{2}$$

and

$$\delta' = \frac{\sigma'}{\bar{\chi}'} \times 100\%$$

σ' is approximately the standard deviation and $\bar{\chi}'$ is approximately the average. δ' is the approximate C.O.V. Note that the individual χ_i's are not used at all.

To obtain the χ_a and χ_b values, one frequently has to estimate. Thus if $n = 40$, $n/6$ is slightly less than 7. Let the seventh highest and seventh lowest values themselves be χ_b and χ_a respectively. For $n = 42$, $n/6 = 7$. Take the average of the seventh and eighth values for χ_a and χ_b. In prac-

tice these approximations are minor compared to the approximate nature of σ or σ' as a spread statistic.

As an illustration of the method, the following three sets of data were taken at random from our files, and the true averages, standard deviations, and C.O.V.'s compared with those derived by this method. The true C.O.V. is represented by δ; other notations are as above.

Set #1

1.20	1.57	1.30	1.43	1.28
1.37	1.33	1.45	1.42	1.43
1.33	1.39	1.48	1.49	
1.35	1.45	1.46	1.42	
1.30	1.27	1.45	1.34	
1.22	1.28	1.48	1.47	
1.47	1.42	1.49	1.23	
1.33	1.32	1.50	1.22	
1.28	1.35	1.24	1.42	
1.22	1.22	1.32	1.50	

$n = 42$ values, $n/6 = 7$

7th lowest value = 1.24 7th highest value = 1.48
8th lowest value = 1.27 8th highest value = 1.47

$\chi_a = 1.255$ $\chi_b = 1.475$

$$\bar{\chi}' = \frac{1.255 + 1.475}{2} = 1.365 \qquad \bar{\chi} = 1.370$$

$$\sigma' = \frac{1.475 - 1.255}{2} = 0.11 \qquad \sigma = 0.10$$

$$\delta' = \frac{0.11 \times 100\%}{1.365} = 8.1\% \qquad \delta = 7.2\%$$

Set #2

21	20	17	11	16
23	18	21	22	18
22	21	21	17	
22	18	20	19	
20	19	20	14	
19	23	20	14	
18	17	19	16	
19	21	15	12	
17	20	15	17	
13	17	20	18	

$\bar{\chi}' = 18.3$ $\bar{\chi} = 18.3$
$\sigma' = 2.8$ $\sigma = 2.87$
$\delta' = 15.6\%$ $\delta = 15.8\%$

Set #3

1.29	1.20	1.32	1.07	1.25
1.38	1.32	1.28	1.18	1.38
1.33	1.49	1.38	1.20	
1.15	1.21	1.68	1.79	
1.57	1.41	1.52	1.50	
1.20	1.35	1.65	1.52	
1.27	1.25	1.43	1.69	
1.21	1.23	1.19	1.53	
1.20	1.28	1.23	1.49	
1.35	1.45	1.11	1.28	

$\bar{\chi}' = 1.360$ $\bar{\chi} = 1.350$
$\sigma' = 0.16$ $\sigma = 0.165$
$\delta' = 11.8\%$ $\delta = 12.2\%$

JAMES H. BURKHALTER

Book Reviews

Biological Treatment of Sewage and Industrial Wastes. Vol. 1, Aerobic Oxidation, Edited by Brother Joseph McCabe and W. W. Eckenfelder, Jr. Reinhold Publishing Corp., New York, 1956. 393 pages. Price $9.50.

Reviewed by Edward Abrams, Chemical Preservative Dept., National Cylinder Gas Co., Chicago, Ill.

This book is the first in a series that will cover the field of biological waste treatment. This volume is a record of the proceedings of the first conference on Biological Waste Treatment held at Manhattan College. It contains 33 papers on the subject of Aerobic Oxidation arranged in logical sequence. The authors are recognized authorities in the field.

The 33 papers have been arranged in four parts. Part 1 is a review of the basic biochemical principles of bio-oxidation and a discussion of their application to waste treatment processes. Part 2 is concerned with the basic mechanism of oxygen transfer and its application to the design of aeration equipment. Parts 3 and 4 discuss the design and operation of typical biological processes for the treatment of municipal and industrial waste waters.

While no reference is made to textile wastes on an industry-wide basis there is an interesting discussion of cotton kiering wastes. Moreover, much of the information given for other industries is, in some measure, applicable to the varied wastes of the textile industry.

This book is indispensable to those who are interested in stream pollution abatement. It is expected that a future conference on anerobic decomposition will be the basis for Volume 2 in this fine series.

Statistical Methods in Research and Production. 3rd ed. Owen L. Davies. London, Oliver and Boyd, 1957. 396 pages. Price 45 s.

Reviewed by H. Mack Truax, Atlas Power Company, Wilmington, Delaware

This edition has been revised and enlarged compared with earlier editions. The new third edition, edited by Davies, represents a great improvement. In the reviewer's opinion, the modifications make the third edition currently the most outstanding book in its classification, whereas the earlier editions were considered of average value.

The book is now divided into eleven chapters. Some concept of the extent of revision is gained from the fact that only four chapters remain substantially the same as in the earlier editions. New topics include the economics of testing and experimentation, sequential sampling, the estimation of variance components and their confidence limits, and the analysis of covariance. An extra chapter on relationships between variables has been added to permit a fuller treatment of multiple curvilinear relationships, with particular reference to difficulties in interpretation.

Statistical Methods makes special reference to the chemical industry; it is recommended for technical personnel in any allied field, such as textiles. The analogues are easily seen from the examples presented. The book was actually written by a team of chemists, statisticians, engineers, and physicists who have had considerable experience in research and process work in the chemical industry.

The consequences are emphasis on the practical aspect of the statistical analysis of experimental data, on the basic conditions to be satisfied, and on the interpretation of the final result.

Methods are explained step by step in detail and illustrated by actual examples.

The Encyclopedia of Chemistry. George L. Clark and Gessner G. Hawley, Editors. New York, Reinhold Publishing Corp., 1957. 1037 pages. Price $19.50.

Reviewed by L. Rebenfeld, Textile Research Institute, Princeton, New Jersey

In these days of ultraspecialization it is heartening to find all the facets and ramifications of chemistry clearly summarized in a one-volume encyclopedia. The editors have brought together the experience and knowledge of over 500 contributing authors, each of whom is an authority in his field of specialization. The many topics within chemistry are treated by these authors in brief and concise chapters intended to give the reader an over-all view of the topic. Both the fundamental and applied topics of chemistry are covered in this reference book. Thus,

it is not surprising to find the section on Gas Analysis preceded by a section on Galvanizing and the section on Stripping Agents to be followed by a section on Strontium and its Compounds. A system of cross references following each topic makes it easy to find additional information in the field under consideration. Most topics occupy less than one page of this treatise; the breadth of the coverage necessitates a limit on depth.

In addition to the discussions of the chemical sciences, there are to be found in proper alphabetic sequence brief descriptions of the several associations, research institutes, and societies which are concerned with chemical topics. Of particular interest to students will be the brief biographic sketches of eminent scientists who have contributed to our knowledge of chemistry since the chemical revolution was sparked by Lavoisier.

This reference book constitutes a distinct contribution to the chemical literature and it will be found useful in all libraries.

The Mathematics of Diffusion. J. Crank. New York, Oxford University Press, 1956. vi + 347 pages. Price $8.00.

Reviewed by Howard J. White, Jr.,
Textile Research Institute,
Princeton, New Jersey

As the author states in the preface, a more precise title for this book would be "Mathematical Solutions of the Diffusion Equation." After a short development of the diffusion equations from Fick's Laws, the author discusses the methods of solution of the diffusion equation and gives a series of results. The results include solutions for the case when the diffusion coefficient is constant and boundaries are fixed and various geometrical shapes and boundary conditions are involved. Also included are chapters on moving boundaries, simultaneous diffusion and chemical reaction, variable diffusion coefficients, finite difference methods, simultaneous diffusion of heat and moisture, and the definition and measurement of diffusion coefficients. The treatment is uniformly mathematical and physical matters only enter implicitly in determining which equations and boundary conditions are important.

The author has performed an important service for a large variety of research workers. In the textile field his book will be useful to anyone interested in such important rate processes as those involved in absorption of water, drying, and dyeing. In fact, in keeping with the author's personal interest in textile problems, the literature in the textile field, which is usually slighted in such books, is given full coverage.

The reviewer has only one regret—that the author has not spent a little more time on the physics of the diffusion process. However, he is forced to agree that 347 pages are enough for any one book and that perhaps it is best to leave the physics for another time.